3

Dynamics of chemically confined water near lipid bilayers

3.1 INTRODUCTION

Hydration water near biological membranes have been studied extensively both via experiments and computer simulations. However, several questions regarding the origin of slow relaxation rates of hydration layers of membranes are unresolved to date. It is not clear whether different chemical moieties of lipid heads or chemical influence on hydrogen bond networks significantly slow down the relaxation rates. Whether the degree of slowing down of the relaxation is dependent on the chemical nature of the confinement is not investigated. The relation between slow rotational and translational relaxation rates of chemically confined water near bilayer and dynamic heterogeneity is not thoroughly established yet. Whether the nature of the hydrogen bond relaxation rate is thermodynamics or kinetic is not known for the hydration layer of bilayers. The present chapter attempts to answer these questions and unravels their implications on membrane associations and other biomolecules.

Vibrational anisotropic experiments are used to probe the anisotropy of water in a multi-bilayer as a function of lipid hydration level since the water stretching mode is dependent on the local environment [Gruenbaum and Skinner, 2013]. Polarization-resolved 2D-IR experiments are successful in measuring the reorientation associated with the hydrogen bond exchange [Ji *et al.*, 2010]. Although linear or 2D infrared spectroscopy [Woutersen *et al.*, 1997; Nienhuys *et al.*, 2000; Gallot *et al.*, 2002] provides information on the hydrogen bond dynamics and pump-probe spectroscopy provides data on vibrational relaxation and reorientational motion, limited spatial resolution, intermolecular coupling, energy transfer, non-Condon effects, and distributions in vibrational lifetime are few sources of ambiguous results [Laage *et al.*, 2011]. Other experimental techniques such as quasi-elastic neutron scattering (QENS), terahertz spectroscopy, optical Kerr-effect spectroscopy, nuclear magnetic resonance (NMR), ultrafast IR spectroscopy, and di-electric relaxation have been used to study water dynamics. A major limitation of the experimental techniques is the coupling of contributions from hydration layer and bulk and limited to the individual reorientation mechanism [Teixeira *et al.*, 1985; Cola *et al.*, 1996; Faraone *et al.*, 2003; Russo *et al.*, 2005]. NMR can also provide information on weighted average of reorientational relaxation time, [Jonas *et al.*, 1976; Ropp *et al.*, 2001; Qvist and Halle, 2008] but not on different individual mechanisms. The other drawback of the experimental techniques is sensitivity issues on their concentration dependency [Russo *et al.*, 2005].

Molecular dynamics studies have been carried out to study several properties of lipid bilayers. A fully hydrated dimyristoylphosphatidylcholine (DMPC) bilayer has been studied using the SPC water model showing two types of lateral diffusive behavior: cage hopping and two-dimensional liquid [Moore *et al.*, 2001]. Between two groups of DMPC molecules, stable charge associations are formed between positively and negatively charged groups of DMPC [Pasenkiewicz-Gierula *et al.*, 1999] Diffusion of protons near DMPC is inhibited at a membrane surface [Smondyrev and Voth, 2002a]. Molecular dynamics simulations are carried out to model the creation of bilayer gaps, a common process in bilayer patterning [Kasson and Pande, 2004]. Thermodynamic properties of a hydrogen bond can be obtained from the probability distribution of donor-acceptor pair in the first hydration shell of an electronegative atom [Sapir and Harries, 2017]. The Gibbs free energy of hydrogen bonding at equilibrium is found to be independent of the environment in alcohol solutions with an entropic barrier [van der Spoel *et al.*, 2006]. Molecular dynamics of hydration layers of the membrane protein reveal additive contributions from the membrane and the proteins to the

activation energies of water diffusion [Fisette *et al.*, 2016]. However, the surface of DNA duplex intrinsically weakly interacts with water and translationally more mobile in nature [Franck *et al.*, 2015].The 2D-IR study of hydration layers confined in reverse micelles shows the correspondence between spectral decomposition performed in experiments and spatial decomposition in simulations [Biswas *et al.*, 2013]. A mosaic water orientation has been found near zwitterionic lipids using vibrational sum frequency generation (VSFG) spectra [Re *et al.*, 2014]. Molecular dynamics of water near DMPC lipids show that 70% of DMPC molecules are linked via bridging water and the average geometry of hydrogen bonding to oxygens of lipid heads is planar trigonal instead of steric tetragonal [Pasenkiewicz-Gierula *et al.*, 1999].The vibrational dynamics of water in the vicinity of anionic and cationic head groups of multibilayers reveal the difference in vibrational lifetime for different charge groups [Kundu *et al.*, 2016b]. The sum-frequency generation spectroscopy study shows that lipid carbonyl groups stabilize the hydrogen bond networks with its up-oriented O-H groups [Ohto *et al.*, 2015].

Here in this chapter, we emphasize on the dynamics of water in the locale of DMPC lipid bilayers hydrated with TIP4P/2005 water using an all atom molecular dynamics simulation. Although previous studies have found the influence of chemical environment near lipid heads [Pasenkiewicz-Gierula *et al.*, 1999; Lopez *et al.*, 2004; Biswas *et al.*, 2013; Re *et al.*, 2014; Ohto *et al.*, 2015; Franck *et al.*, 2015; Kundu *et al.*, 2016b], none of the investigations (a) decouple the contribution of bulk and interface water (IW) towards hydrogen bonding, (b) report the mechanism which interface water molecules follow to form hydrogen bonds and their implications on lipid aggregations, and (c) investigate the dynamics of hydrogen bond networks. Unlike the previous approaches, the water molecules are characterized in terms of hydrogen bonding to the lipid heads when confined to the interface. This can clearly de-construct the contribution of bulk and interface as well as the influence of different chemical environments. Further the interface water molecules are classified into four categories in terms of hydrogen bonds among themselves and concertedly to either another set of hydrogen bonded water or to lipid head groups. Thus, the present analysis can probe the dynamics of hydrogen bond networks instead of the dynamics of a single hydrogen bond shown in earlier approaches [Lopez *et al.*, 2004]. Radial distribution functions (RDFs), mean square displacements (MSDs), reorientational correlation functions, and hydrogen bond autocorrelation functions (HBACFs) are calculated for the concerted hydrogen bond networks to show the influence of chemical confinements on their dynamics. The calculations demonstrate that chemical confinements play a crucial role on the relaxation rates of hydrogen bond networks and suggest that the networks influence the water mediated lipid-lipid associations.

3.2 SIMULATION DETAILS

Molecular dynamics simulations are carried out with 128 DMPC molecules in the presence of 5743 TIP4P/2005 water molecules. Since the TIP4P/2005 water model correctly reproduces the water phase diagram and the dynamics of water [Abascal and Vega, 2005; Srivastava *et al.*, 2019b], it is used in our simulations. Force field parameters for DMPC lipids are obtained from Berger united atom force fields [Berger *et al.*, 1997; Cordomí *et al.*, 2012].

An NPT run is carried out for 100 ns with 2 fs time step. The system is equilibrated at 308 K using velocity rescaling method [Bussi *et al.*, 2007] with a coupling constant of 0.50 ps. The pressure is maintained at 1 bar using semi-isotropic pressure coupling scheme by Berendsen pressure coupling [Berendsen *et al.*, 1984b] with a coupling constant of 0.10 ps. Coulombic and van der Waals interactions are cut off at 1 nm and long range interactions are corrected using Particle Mesh Ewald (PME) method [Darden *et al.*, 1993; Essmann *et al.*, 1995b] with a 4 nm grid size. Periodic boundary conditions are applied in all three directions. Nest, an NVT simulation is carried out for 1 ns with 0.40 fs time step where the last 100 ps is analyzed for water dynamics. Parameters for temperature coupling, cutoff distances and long range interactions are same as in the previous NPT run. Trajectories are collected at every 10 fs. The simulation box length for the hydrated DMPC lipid is 6.24 nm along x and y directions and 7.95 nm along the z direction.

To compare the dynamics of interfacial water with bulk water, a box of 851 TIP4P/2005 water molecules is simulated for 2 ns with 2 fs time step in an NPT ensemble with the same set of parameters as in the hydrated DMPC. Next a NVT run is carried out for 100 ps with 0.40 fs time step. The box length for BW is 3.69 nm along the x and y directions and 1.84 nm along the z direction. Trajectories are collected at every 10 fs. All simulations are carried out using GROMACS-4.6.5 [Bekker *et al.*, 1993; Berendsen *et al.*, 1995; Lindahl *et al.*, 2001; Spoel *et al.*, 2005; Hess *et al.*, 2008; D. van der Spoel and the GROMACS development team., 2013].

3.3 CATEGORIZATION OF WATER REGIMES

Water molecules are classified based on their proximity from the bilayer head-groups along the bilayer normal. The Z coordinate of oxygen atoms of water molecules which continuously reside within ±3 Å from the peak position of the nitrogen density of the lipid head for the entire production run is classified as interface waters (IWs) and shown in figure 2.1 b). A molecule residing in a specific layer at a given time step is labeled as 1 and if it is outside the layer, it is labeled as 0 [Debnath *et al.*, 2010, 2013]. Thus, the molecules which continuously reside in a specific layer are classified as interface water, and in our simulation there are such 104 interface water. The interface water molecules are associated with oxygen atoms of carbonyl (CO), glycerol (Glyc.), and phosphate (PO) groups of lipids via hydrogen bonds. Since the interface water molecules are hydrogen bonded to different moieties of DMPC head-group, they are mentioned as chemically confined interface water (IW) for the remaining sections. To find out the presence of hydrogen bonds, the widely accepted geometric criteria [A.Luzar and Chandler, 1996; Rey *et al.*, 2002; Lawrence and Skinner, 2003; Eaves *et al.*, 2005] are used: $R_{OO} < 3.5$ Å and $\theta_{HOO} < 30^o$, where R_{OO} is the distance between donor and acceptor oxygen atoms and θ_{HOO} is the angle between $\vec{OO}$ and $\vec{OH}$ bond vectors. No water molecules are found which form hydrogen bonds with the choline group of lipid heads. Based on the formation of hydrogen bonds among themselves and with the three head groups of DMPC lipids (CO, Glyc., and PO), interfacial waters are further classified among four categories. If an IW molecule is solely hydrogen bonded with any other IW, it is termed as IW-IW. If these IW are hydrogen bonded to the oxygen atom of CO, Glyc., or PO of the DMPC head at any single time step during the production run, they are termed as IW-CO, IW-Glyc., and IW-PO, respectively. This makes the molecules diffusive in nature since they are not hydrogen bonded for the entire simulation period. Among the hydrogen bonded interfacial waters, there are total 70 IW-IW, 80 IW-CO, 55 IW-Glyc., and 98 IW-PO water molecules which form hydrogen bonds at least once for the 100 ps production run. Radial distribution functions (RDFs) between oxygen atoms of respective bound interfacial water are calculated by normalizing volume and density. The RDF in figure 3.1 shows that the peaks for all interfacial water are higher than bulk water (termed as BW). The RDF between oxygen atoms of bound interfacial water and three head groups shown in figure 3.2 demonstrates the ordered behaviors of the IW-CO, the IW-Glyc., and the IW-PO water molecules for the second hydration shells in addition to the first hydration shells. The enhanced amplitudes of the RDF for different classes of IW compared to the BW (figure 3.1) indicate their higher tendency to be in the first and second hydration shells of each other. The presence of more oxygens in the nearest neighbors of each other for the interface water consequently disrupts the tetrahedral structure of the hydrogen bond network in bulk and results in defects in the hydrogen bonding networks in the presence of lipid heads [Bosio *et al.*, 1983].

3.4 TRANSLATIONAL MEAN SQUARE DISPLACEMENT

To quantify dynamical properties of water in different regimes, we computed the translational mean square displacement (MSD) for all classes of water discussed above using the equation 2.1. The translational MSD for different classes of water regimes is shown in figure 3.3.

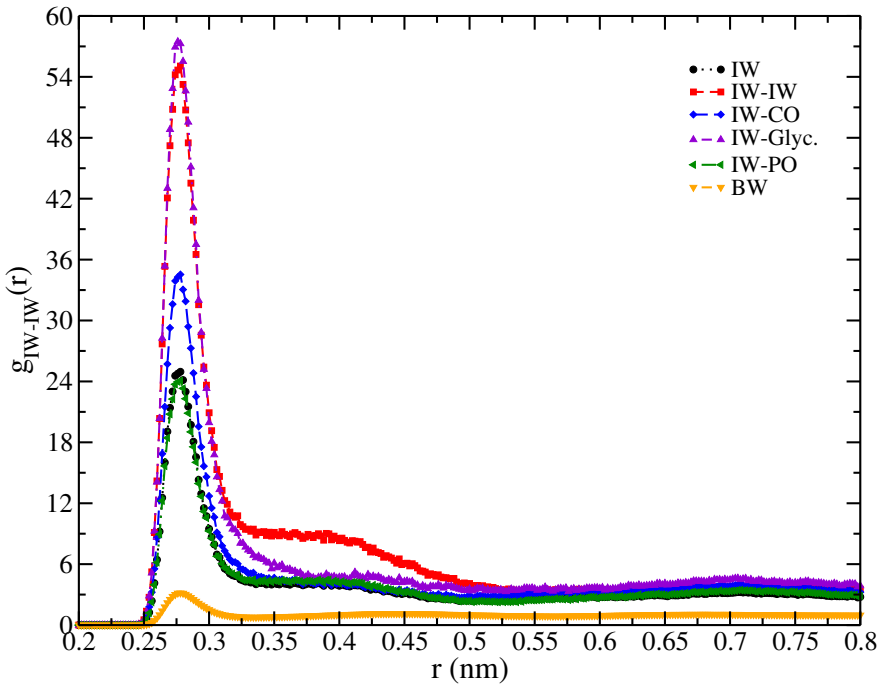

Figure 3.1: Oxygen-oxygen RDF for different classes of water hydrogen bonded to another water. For the sake of clarity in the differences in amplitudes, the RDF of the interface water is not shown until they reach the values of bulk water.

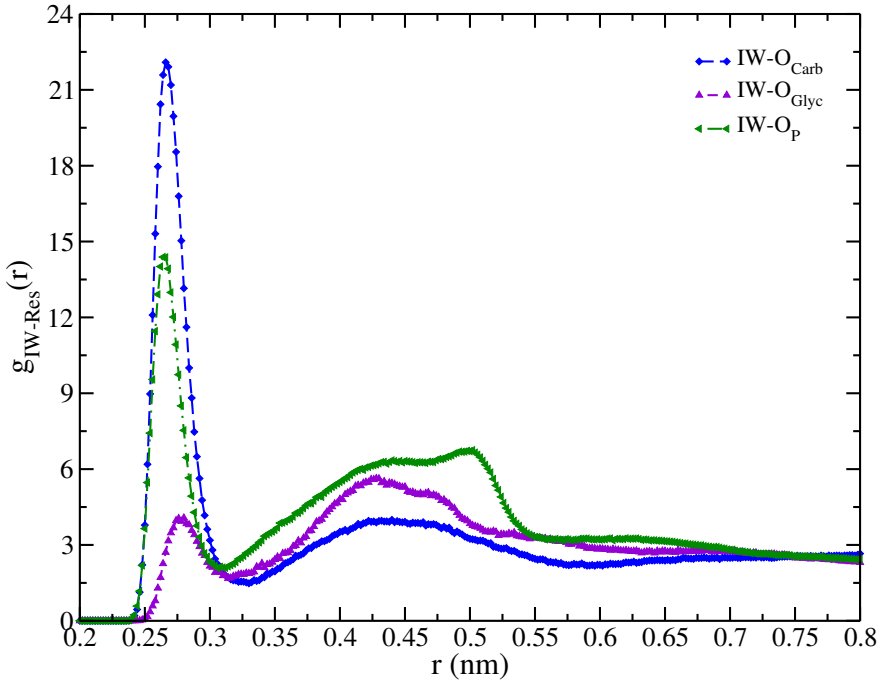

Figure 3.2: Oxygen-oxygen RDF for different classes of water hydrogen bonded to lipid head groups (IW-Res).

All classes of IW show a glass-like behavior from 0.2 to 1 ps after the ballistic region. At longer time, they obey power law function where α depicts the type of diffusion. The values of α for all classes of IW are presented in table 3.1. All interfacial water molecules follow a sub-diffusive behaviour due to the geometric and chemical confinement at the interface forming hydrogen bonds among themselves or with the lipid heads. Interestingly, the MSD of the IW-CO or the IW-Glyc. is slower [Swenson *et al.*, 2008] than that of the IW-PO which is again slower than that of the IW-IW hydrogen bonded only among themselves (shown in the inset of figure 3.3). The slow translational diffusion of IW-CO/Glyc. are buried in the deeper region of lipid chains and translational motion are more restricted. The BW follows a diffusive behavior ($\alpha \approx 1$) for $60 - 90$ ps. The value of the diffusion coefficient (D) for the BW is 2.49×10^{-5} cm^2 s^{-1} (table 3.1) which agrees well with the reported diffusion constant of 2.60×10^{-5} cm^2 s^{-1} for TIP4P/2005 water at 308 K [Vega *et al.*, 2009].

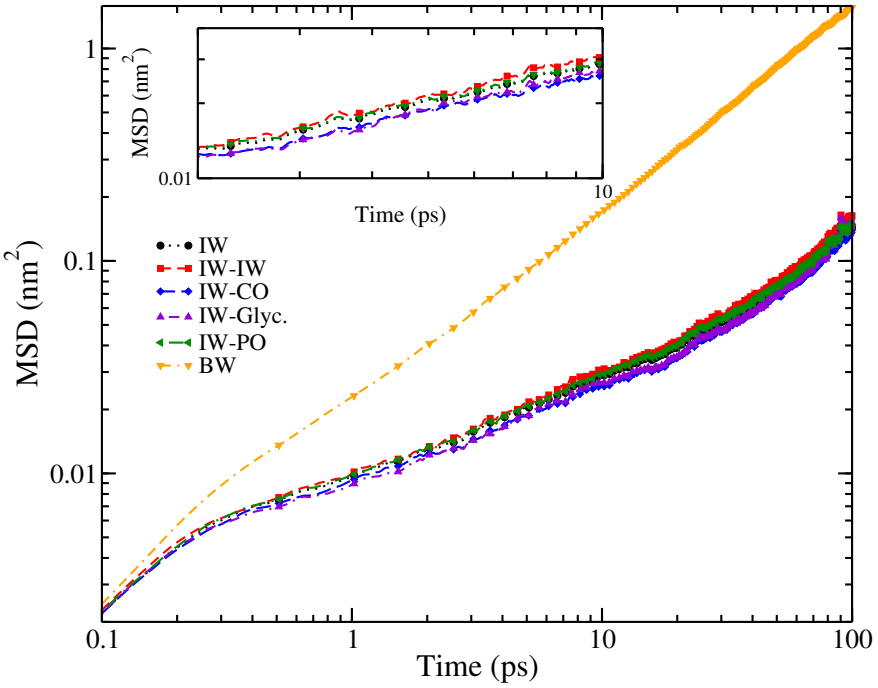

Figure 3.3: Translational MSD for interfacial and bulk water where the BW has a diffusive regime and others follow a sub-diffusive behavior. **Inset**: MSD for interfacial waters showing slowest motion for IW-CO and the fastest motion for IW-IW.

Table 3.1: Values of α and diffusion coefficient (D_{trans}) for translational MSD fitted with function At^{α}. Correlation coefficients for all classes are >0.99

	Type of IW	α	D_{trans} $(10^9 m^2 s^{-1})$
a)	IW	0.51	
b)	IW-IW	0.53	
c)	IW-CO	0.45	
d)	IW-Glyc.	0.53	
e)	IW-PO	0.51	
f)	BW	0.94	2.49 ± 0.31

3.5 REORIENTATIONAL AUTO-CORRELATION FUNCTION

To characterize rotational dynamics of water, reorientational auto-correlation function (RACF) for all classes of water is computed. The l^{th} order Legendre polynomial of water reorientation is given by the following equation:

$$C_{vl}(t) = \frac{< \sum_{i=1}^{N} P_l[e_i{}^v(t).e_i{}^v(0)] >}{< \sum_{i=1}^{N} P_l[e_i{}^v(0).e_i{}^v(0)] >} \tag{3.1}$$

where $e_i{}^v(t)$ is the vector for which the RACF is calculated and P_l is the l^{th}th order Legendre polynomial. We computed $C_{vl}(t)$ for the first and second order Legendre polynomial for vector normal to the plane of OHH ($\hat{n}$), OH bond vector ($\vec{OH}$), HH bond vector ($\vec{HH}$), and dipole moment $\vec{\mu}$. Figures 3.4 and 3.5 show the RACF for the interface and the bulk water for the first and second order Legendre polynomials (l= 1 and l= 2), respectively. Figures 3.4 and 3.5 (a)-3.5(d) represent the RACF of $\hat{n}$, $\vec{OH}$, $\vec{HH}$, and $\vec{\mu}$, respectively. The RACF of the bulk water of all cases decays much rapidly to zero than all classes of IW showing no preferences in orientations. The RACF for the IW-IW and all IW overlaps with each other showing no differences in orientations when they are hydrogen bonded among themselves or not. For all the cases, the second order reorientation relaxations are more rapid than the first order relaxations. We fitted the RACF using bi-exponential or tri-exponential functions given by the following equation,

$$y = \sum_{i=2or3} A_i exp(-\frac{t}{\tau_i}). \tag{3.2}$$

Table 3.2 shows the fitting parameters for the RACF of $\hat{n}$ with a bi-exponential fitting. For l= 1, the slowest time scale (τ_s) is between 50 and 90 ps and the fastest time scale (τ_f) is in the range of $2-9$ ps for all the bound interfacial water. For the BW, τ_s is within $1-4$ ps and τ_f is in the range of $0.2-0.4$ ps. For l= 2, τ_s and τ_f are in between $55-78$ ps and $2-3$ ps, respectively, for the interfacial water, whereas these are 0.2 ps and 1.87 ps for the BW. Comparing all time scales of RACF of l= 1 and l= 2, it has been found that IW-CO obeys slower reorientation relaxation than the rest of the IW. The ratio of τ_s^1 to τ_s^2 is ≈ 1 for all cases indicating non-diffusive reorientation for $\hat{n}$ as found for other complex fluids [Fogarty and Laage, 2014; Das *et al.*, 2015].

Table 3.3 shows the fitting parameters for the RACF of $\vec{OH}$ with a bi-exponential or tri exponential fitting from equation 3.2. For l= 1, τ_s and τ_f are in the range of $35-60$ ps and $0.1-4$ ps for the bound interfacial water and 2.4 ps and 0.2 ps, respectively, for BW. For l= 2, τ_s and τ_f are between $27-35$ ps and $0.8-2$ ps for all bound interfacial water and 1.16 ps and 0.14 ps for the BW. This again demonstrates the slower relaxations in the RACF for the IW-CO. The value of τ_1/τ_2 is in between 1.3 and 2 for all cases, confirming non-diffusive water reorientation for $\vec{OH}$.
Table 3.4 shows the fitting parameters for the RACF of $\vec{HH}$ with a bi-exponential or tri-exponential function. For l= 1, the values of τ_s and τ_f are in the range of $35-48$ ps and $0.20-4$ ps, respectively, for the bound interfacial water and 2.45 ps and 0.29 ps for the BW. For l= 2, τ_s and τ_f are in the range of $34-48$ ps and $0.3-2.8$ ps, respectively, for the interfacial water and 1.29 ps and 0.27 ps for the BW. The time scales of the RACF for l= 1 and l= 2 show slower relaxations for the IW-CO among all IWs. The value of τ_1/τ_2 is $\approx 1-2$ for all cases demonstrating a non-diffusive behavior of $\vec{HH}$.
Table 3.5 shows the fitting parameters for the RACF of $\vec{\mu}$ with a bi-exponential or tri-exponential function. For l= 1, the values of τ_s and τ_f are in the range of $71-159$ ps and $0.9-4$ ps, respectively, for bound interfacial water and $0.18-2.24$ ps for BW. For l= 2, τ_s and τ_f are in the range of $34-44$ ps and $0.13-2.2$ ps, respectively, for bound interfacial water and 0.12 ps and 1 ps for BW. Interestingly, unlike all previous cases, the time scales of the RACF for l= 1 and l= 2 show slower relaxations for the IW-IW among all IW. The values of τ_1/τ_2 are $\approx 1-2$ for all cases except the IW-IW. This indicates a diffusive behavior of the RACF of $\vec{\mu}$ for IW-IW and non-diffusive behaviors for the rest of the cases.

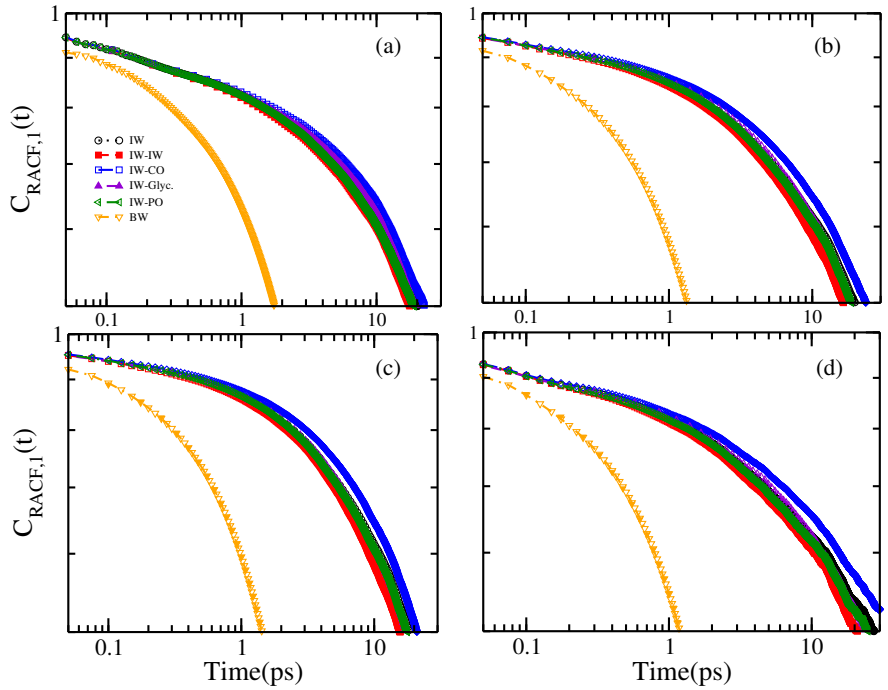

Figure 3.4: RACF for interface and bulk water for l= 1 for a) $\hat{n}$, b) $\vec{OH}$, c) $\vec{HH}$ and d) $\vec{\mu}$.

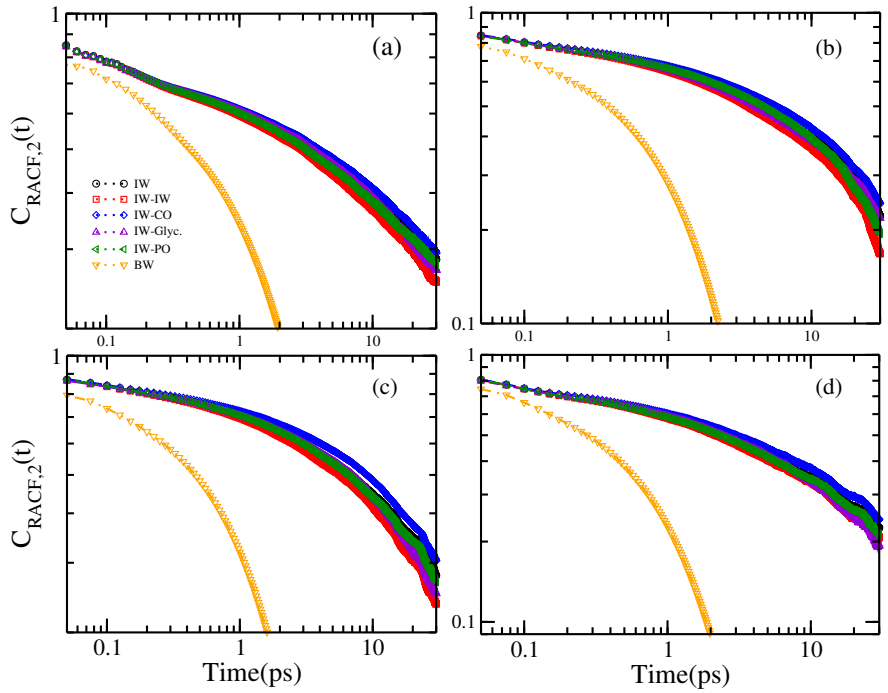

Figure 3.5: RACF for interface and bulk water for l= 2 for a) $\hat{n}$, b) $\vec{OH}$, c) $\vec{HH}$ and d) $\vec{\mu}$.

Table 3.2: Reorientational relaxation time scales for $\hat{n}$ for all classes of water. Correlation coefficients are >0.99. Slow relaxation time scale (τ_s) for second order rotational auto-correlation function for $\hat{n}$ of the IW and the BW are compared with experimental and simulation data showing the applicability of Berger force fields in combination with TIP4P/2005 water model.

	Classification of IW	A_f	τ_f (ps)	A_s	τ_s (ps)	$\frac{\tau_1}{\tau_2}$
l=1	IW	0.25	6.51	0.62	83.26	1.07
l=2		0.29	3.05	0.42	77.83	
l=1	IW-IW	0.22	5.73	0.64	65.05	1.11
l=2		0.29	2.64	0.42	58.56	
l=1	IW-CO	0.26	8.82	0.61	97.28	1.36
l=2		0.26	3.85	0.45	71.67	
l=1	IW-Glyc.	0.19	6.13	0.68	63.55	1.14
l=2		0.26	2.67	0.46	55.92	
l=1	IW-PO	0.26	6.58	0.61	83.74	1.09
l=2		0.29	3.02	0.41	76.33	
l=1	BW	0.10	0.36	0.83	3.44	1.84
l=2		0.26	0.23	0.57	1.87	
Reported literature (τ_s of $\hat{n}$)						
	IW	Simulations	≈ 66.00 ps [Zhang and Berkowitz, 2009]			
l=2						
	BW	Experiments	1.70 ps [Rezus and Bakker, 2006]			

From the analysis, it is found that that the RACF of the IW-CO and the IW-PO water has the most preferred orientations for most of the cases, thereby relaxing at the slowest rate among all interfacial water. In comparison to that, the orientations of the IW-IW or the IW-Glyc. have lower relaxation rates with less preferences for orientations. This is probably due to the strong electrostatic interactions between the interfacial waters and oxygen atoms of CO or PO. The trend of preferences in orientations around different chemical environments is consistent with the mosaic structure of water orientations reported earlier [Re *et al.*, 2014].

3.6 HYDROGEN BOND DYNAMICS

To investigate the hydrogen bond dynamics of the IW and the BW, we first identify four classes of interfacial water as described in above section. Any two IW can form hydrogen bond to

Table 3.3: Reorientational relaxation time scales for $\vec{OH}$ for all classes of water. Correlation coefficients are >0.99.

	Classification of IW	A_f	τ_f (ps)	A_i	τ_i (ps)	A_s	τ_i (ps)	$\frac{\tau_1}{\tau_2}$
l=1	IW	0.19	3.34			0.73	54.43	1.59
l=2		0.26	1.90			0.53	34.13	
l=1	IW-IW	0.07	2.52	0.09	2.80	0.78	35.28	1.30
l=2		0.16	0.08	0.24	1.79	0.53	27.03	
l=1	IW-CO	0.17	4.22			0.74	60.16	1.72
l=2		0.22	2.03			0.57	34.89	
l=1	IW-Glyc.	0.06	0.17	0.14	3.38	0.76	45.33	1.57
l=2		0.15	0.12	0.20	2.19	0.55	28.90	
l=1	IW-PO	0.06	0.32	0.19	4.20	0.70	56.37	1.58
l=2		0.15	0.14	0.24	2.45	0.51	35.71	
l=1	BW	0.06	0.26			0.87	2.41	2.07
l=2		0.18	0.14			0.76	1.16	

each other which may not be hydrogen bonded to a third group and do not form a network. If any one of the two hydrogen bonded interface water is concertedly hydrogen bonded to another pair of hydrogen bonded interface water or to a lipid head, this can form a network structure such as IW-IW-IW-IW or lipid head-IW-IW-lipid head. The dynamics of such a hydrogen bond network between two waters are studied in this section. Since the number of water molecules in different classes of IW is different, we calculated the distribution of hydrogen bonds per water molecule for all cases. Figure 3.6 shows the distribution of hydrogen bonds for the interfacial water and figure 3.7 shows the distribution for the BW. Figure 3.7 clearly demonstrates that the BW has nearly four hydrogen bonds per water. The numbers of hydrogen bonds are reduced in the presence of the lipid head groups in the interface. Among different classes of interfacial water molecules, the distribution of the IW-Glyc. is maximum in comparison with other classes of water. The number of hydrogen bonds per water for the IW-IW is greater than the IW-CO or the IW-Glyc. which is again greater than the IW-PO. Although, the amplitude of the distribution of hydrogen bonds in concerted networks of lipid heads-IW-IW-lipid heads is higher than that of IW-IW-IW-IW, they form a less number of hydrogen bonds compared to water in the absence of network. This is due to the annihilation of network created by hydrogen bonds in the BW due to the presence of foreign elements like DMPC head groups [Pasenkiewicz-Gierula *et al.*, 1999]. Thus, these networks are referred to as defected networks.

A hydrogen bond formed between one pair of donor-acceptor atoms at any time instant may not be intact at other instant. To study the dynamical behavior, we investigated mean lifetime of hydrogen bonds for all cases of waters by computing hydrogen bond auto-correlation functions (HBACFs)

Table 3.4: Reorientational relaxation time scales for $\vec{HH}$ for all classes of water. Correlation coefficients are >0.99.

	Classification of IW	A_f	τ_f (ps)	A_i	τ_i (ps)	A_s	τ_i (ps)	$\frac{\tau_1}{\tau_2}$
l=1	IW	0.17	3.14			0.76	43.79	1.00
l=2		0.26	2.71			0.55	43.95	
l=1	IW-IW	0.07	2.52	0.09	2.80	0.78	35.28	0.86
l=2		0.15	0.61	0.22	5.01	0.49	40.92	
l=1	IW-CO	0.15	3.94			0.78	47.11	1.07
l=2		0.22	3.02			0.58	43.90	
l=1	IW-Glyc.	0.13	2.49			0.80	36.16	1.05
l=2		0.22	2.58			0.58	34.23	
l=1	IW-PO	0.04	0.20	0.18	3.72	0.74	45.39	0.95
l=2		0.13	0.34	0.24	4.06	0.51	47.40	
l=1	BW	0.05	0.29			0.88	2.50	1.94
l=2		0.17	0.17			0.69	1.29	

[Luzar and Chandler, 1996; Chandra, 2000; Balasubramanian *et al.*, 2002] defined by the following equation:

$$C_{HB}(t) = \frac{< h_{IW-HG}(0) h_{IW-HG}(t) >}{< h_{IW-HG} >}, \tag{3.3}$$

where the variable $h_{IW-HG}(t)$ represents the hydrogen bonds between interfacial water molecules (IW) and head-groups (HG) of the lipids. $h_{IW-HG}(t)$ is 1 when the water molecule forms a hydrogen bond with lipid head-groups at time t following the geometric definition mentioned above and is 0 otherwise. Note that the hydrogen bonds are allowed to break and thus we calculated the interrupted hydrogen bond correlation functions. Similarly, we computed the time correlation function for the BWs as well. Figure 3.8 shows $C_{HB}(t)$ for the BW and all classes of IW. The HBACF for the BW decays much rapidly than the HBACF for all IW depicting a bound nature of IW as found earlier [Luzar and Chandler, 1996; Chandra, 2000]. The hydrogen bond correlation functions of the IW-Glyc. exhibit slower decay than that of the IWCO which is slower than the IW-IW which is again slower than that of the IW-PO. The bound water hydrogen bonded to the oxygen atoms of Glyc. is more buried in nature compared to that to the oxygen atoms of PO and thus more restricted in nature among all IW. Thus, the hydrogen bonds to Glyc. persist for a longer time span. The BW, on the other hand, has no head group influence, implying the rapid exchange of hydrogen bonds among neighbouring water molecules.

Interestingly, the hydrogen bond auto-correlation functions ($C_{HB}(t)$, in figure 3.8) of the interface water develop a hump at ~ 10 ps which is not observed in the BW. The humps are not found for

Table 3.5: Reorientational relaxation time scales for $\vec{\mu}$ for all classes of water. Correlation coefficients are >0.99.

	Classification of IW	A_f	τ_f (ps)	A_i	τ_i (ps)	A_s	τ_i (ps)	$\frac{\tau_1}{\tau_2}$
l=1	IW	0.20	3.31			0.69	84.42	1.88
l=2		0.29	2.09			0.43	44.54	
l=1	IW-IW	0.13	1.22	0.28	13.51	0.50	158.74	3.82
l=2		0.19	0.22	0.24	2.94	0.41	41.55	
l=1	IW-CO	0.18	3.96			0.70	96.57	2.14
l=2		0.26	2.16			0.46	45.13	
l=1	IW-Glyc.	0.18	3.67			0.70	71.03	2.04
l=2		0.27	2.08			0.45	34.79	
l=1	IW-PO	0.10	0.98	0.19	7.52	0.61	108.32	2.44
l=2		0.21	0.13	0.26	2.66	0.41	44.37	
l=1	BW	0.09	0.18			0.85	2.24	2.24
l=2		0.22	0.12			0.59	1.00	

water forming hydrogen bonds to lipid heads until the contribution of the bulk is de-constructed. Thus, the humps are consequences of the nature of chemical confinements. However, the humps disappear after $\sim$ 20 ps and then all waters are found to follow a $t^{-1.5}$ asymptotic behavior. Data at longer time is not reported due to the statistical errors. The humps of the interface water are found between 12 and 20 ps which is after the onset of cage-like behavior in the MSD (figure 3.3) and before the diffusive regime of hydrogen bond break dictated by power law behavior. After the ballistic regime (> 0.25 ps), chemically confined hydrogen bond networks start rattling in the cage formed by the crowded networks, and after 20 ps, water molecules succeed to leave the cage undergoing translational diffusion dictated relaxation indicated by $t^{-1.5}$ asymptotic power law irrespective of the chemical confinement. The humps of the interface water within the intermediate time scale of $\sim 12-20$ ps are possibly the signatures of a transition from motion in a cage created by chemically confined hydrogen bond networks to translational diffusions of hydrogen bonds. At longer time, the effect of chemical confinements is no longer significant and thus all classes of water irrespective of their chemical nature follow the same asymptotic behavior. The scaling parameters are clear indications that $C_{HB}(t)$ obeys the following equation:

$$C_{HB}(t) \approx \frac{1}{4\pi D t^{1.5}} \tag{3.4}$$

where D is the diffusion constant at longer time. Thus, irrespective of the nature of the chemical confinement of IW and BW, the hydrogen bond breaking and formation mechanism is found to be dictated by the translational diffusion in three dimensions [Markovitch and Agmon, 2008].
Kinetics of hydrogen bonding formation and breaking are studied using the reactive flux analysis

[A.Luzar and Chandler, 1996; Luzar, 2000; van der Spoel *et al.*, 2006] where the forward rate constant (k) and backward rate constant (k) are considered for the hydrogen bond breaking and formation, respectively,

$$K(t) = -\frac{dC_{HB}(t)}{dt} \tag{3.5}$$

and,

$$K(t) = kC_{HB}(t) - k'n(t) \tag{3.6}$$

Here, n(t) represents the probability that a hydrogen bond existed at time t= 0 but the two atoms which are forming hydrogen bonds are still within the distance cutoff. The lifetime for hydrogen bonding can be computed using the forward rate constant as

$$\tau = \frac{1}{k} \tag{3.7}$$

Assuming the process of hydrogen bond breaking as the Eyring process, one can find the Gibbs energy $\Delta G^{\ddagger}$ of the hydrogen bond breaking activation using the following relation:

$$\tau = \frac{h}{k_B T} e^{\frac{\Delta G^{\ddagger}}{k_B T}} \tag{3.8}$$

where k_B is Boltzmann's constant, T is the temperature, and h is Planck's constant. The bulk water has no influence of lipids; thus two water molecules hydrogen bonded tend to break at a shorter period of time and have shorter lifetime than the IW. Thus the BW has lower $\Delta G^{\ddagger}$ than all IW. The value of $\Delta G^{\ddagger}$ for TIP4P/2005 bulk water is found to be 8.29 kJ mol^{-1} which is somewhat higher than the values reported for bulk water of TIP4P or SPC/E [van der Spoel *et al.*, 2006]. The difference is attributed to the slower diffusion of the TIP4P/2005 water model than that of TIP4P or SPC/E [Abascal and Vega, 2005] bulk water leading to an energy cost in the hydrogen bond exchange mechanism. Bound water hydrogen bonded to lipid head groups stays bonded for a longer period of time. Interestingly, the values of $\Delta G^{\ddagger}$ decrease from IW-Glyc. to IW-CO, to IW-IW, to IW-PO (Table 3.6). The trend of lowering in $\Delta G^{\ddagger}$ indicates the importance of location of DMPC head groups on the activation energy of hydrogen bond breakage. Since the IW-Glyc. is more buried into the hydrophobic region of the bilayer due to the location of Glyc. oxygen along the alkyl chains, diffusion of IW-Glyc. while hydrogen bond exchange or reshuffling through the water depleted hydrophobic environment requires more energy of activation cost. Thus, the interfacial water hydrogen bonded to Glyc. oxygen shows more trapped behavior compared to the ones for the CO or the PO. The confined and buried Glyc. head groups may disrupt the necessary pathways for hydrogen bond exchange. This information indicates that the contribution of hydrogen bond networks on the changes in Gibbs free energy and on the thermodynamic stability of lipid bilayers needs further attention which can be investigated by calculating changes in enthalpy and entropy on breaking of hydrogen bonds in future. Thus the present calculations explain the role of chemical confinement on breaking of defected networks as well as lay a foundation for future work which further may shed light on the connection of thermodynamics of hydrogen bonds to their dynamics and enhance our understanding on the stability of other biomolecules like proteins [Dill, 1990; Efimov and Brazhnikov, 2003].

3.7 HYDROGEN BOND NETWORKS AND LIPID-LIPID ASSOCIATIONS

In order to find the influence of the hydrogen bond dynamics on the membrane structure, the IW-IW, the IW-CO, the IW-PO, and the IW-Glyc. water molecules which remain continuously hydrogen bonded among themselves during simulation time are identified. These hydrogen bonds remain *intact* without allowing changes in their respective donor acceptor partners. However, the

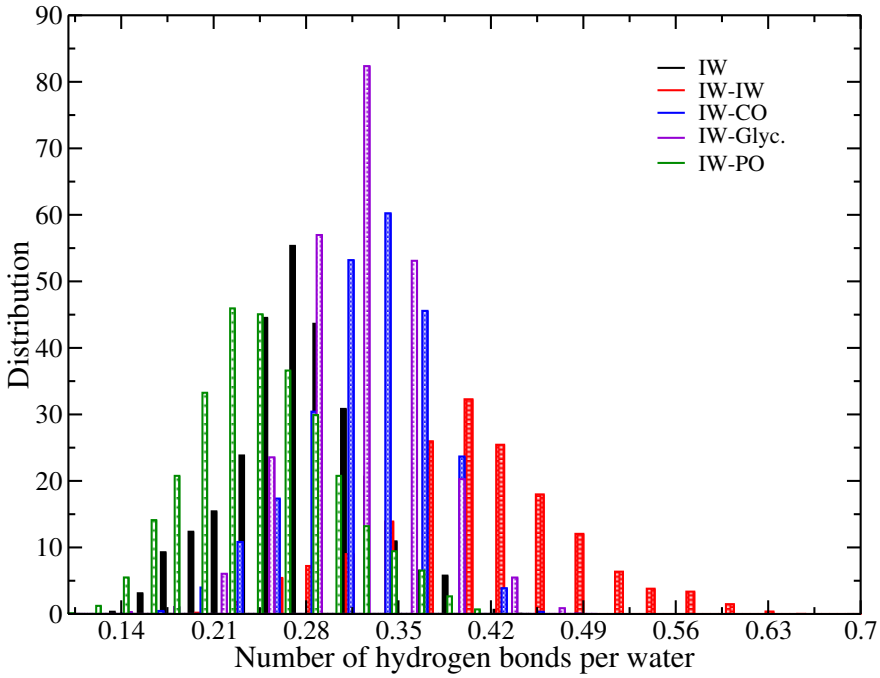

Figure 3.6: Distribution of number of hydrogen bonds per water molecule for all classes of IW.

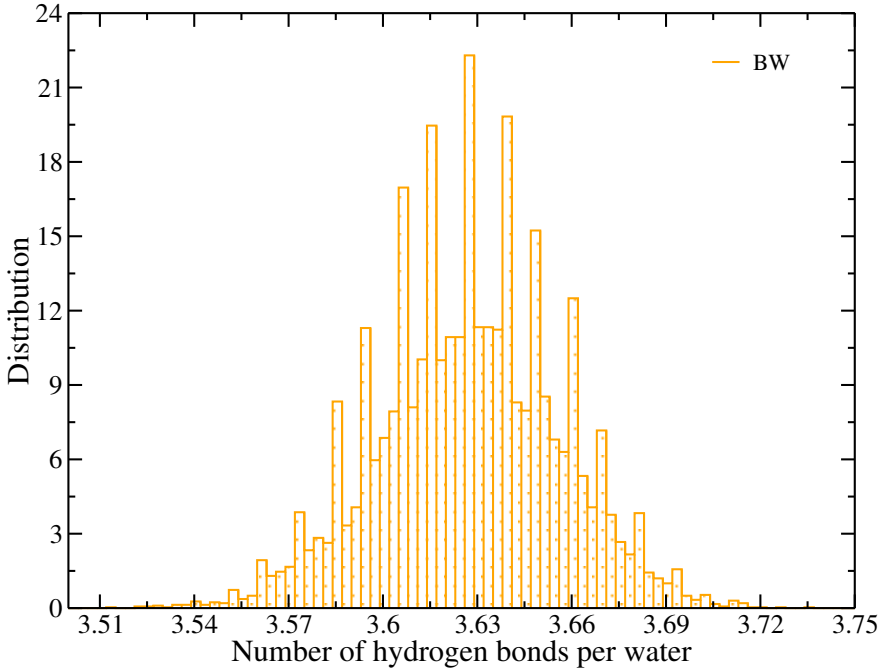

Figure 3.7: Distribution of number of hydrogen bonds per water molecule for BW.

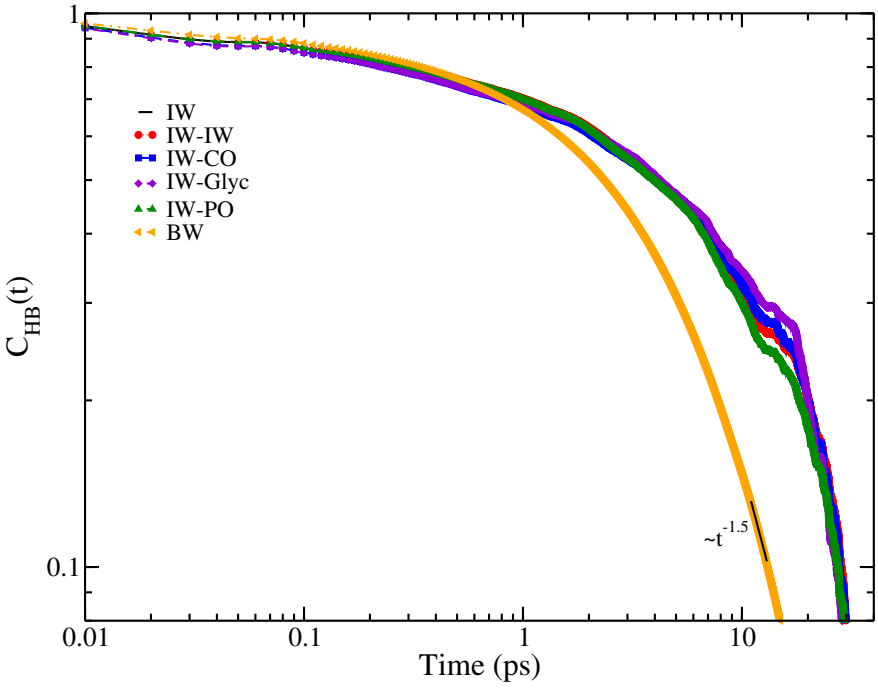

Figure 3.8: Hydrogen bond auto-correlation function for interface and bulk water.

Table 3.6: Hydrogen bond lifetime and Gibbs energy of activation for interface and bulk waters. Hydrogen bond lifetime (τ_{HB}) of the IW and the BW are compared with the previous simulation and experimental data to show the suitability of the Berger force fields in combination with TIP4P/2005 water model.

Region	τ_{HB} (ps)	$\Delta G^{\ddagger}$ (kJ mol^{-1})
IW	14.96	11.69
IW-IW	14.96	11.69
IW-CO	16.74	11.98
IW-Glyc	18.96	12.30
IW-PO	13.00	11.33
BW	3.98	8.29
Reported literature (τ_{HB})		
Simulations	IW	24.00 ps [Chanda *et al.*, 2006] 9.00 ps [Balasubramanian *et al.*, 2002]
Experiments	IW	≈ 20.00 ps [Borle and Seelig, 1983] <10.00 ps [Costard *et al.*, 2014]
Simulations	BW	5.11 ps [Liu *et al.*, 2018] 2.15 ps [Chakraborty and Chandra, 2011]
Experiments	BW	≈ 1.20 ps [Fecko *et al.*, 2003] ≈ 1.60 ps [Paolantoni *et al.*, 2007]

other hydrogen bonds to the lipid heads in the network are allowed to diffuse. Figure 3.9 shows the number of hydrogen bonds per water which are intact during simulation time. The inset shows the

number of *intact* hydrogen bonds per water for the BW. The numbers of the BW are higher than the remaining classes of water which is in agreement with the distribution of number of hydrogen bonds per water molecule shown in the figure 3.7. Interestingly, the number of intact hydrogen bonds for the BW decreases sharply and faster than that for any IW. The number of hydrogen bonds for the IW-PO decreases faster than the rest of the IW. The time evolution of all intact hydrogen bonds indicates toward their lifetime without the information of pair diffusion. They follow similar trends as the lifetime of hydrogen bonds when pair diffusion is allowed (see table 3.6). Importantly, the time evolution of intact hydrogen bonds refer to the lifetime of defected hydrogen bond networks formed between lipid head groups and interfacial water. The defected network by the IW-PO breaks faster than that by the IW-CO or the IW- Glyc. since the IW-CO or the IW-Glyc. is more buried in the core hydrophobic region of lipids. So the hydrogen bonds near lipid tails remain intact for longer time due to the association of dense lipid tails. Figure 3.10 shows a snapshot of hydrogen bond networks where IW is hydrogen bonded to IW and concertedly hydrogen bonded to CO, Glyc., or PO of lipids resulting in water mediated associations of lipids. Experimentally, it is found that IW are hydrogen bond donors forming strong hydrogen bond with the phosphate and the carbonyl head-group moeities of the DPPC lipid using Phase-Sensitive VSFG spectroscopy. The electrostatic potential across the interface region is due to the charged moeities resulting in formation of hydrogen bond between water and lipid heads. Also, IW forming hydrogen bonds with charged moeities simultaneously form hydrogen bonds with neigbouring water [Chen *et al.*, 2010]. The lipid-water interface as observed from SFG spectroscopy and all atom MD simulations for DMPC (CHARMM force field) lipids hydrated with water (Martini flexible water model) reveals three distinct spectral peaks corresponding to different environments at the lipid-water interface [Nagata and Mukamel, 2010; Mondal *et al.*, 2012]. The emergence of three distinct peaks in the SFG spectra for bilayer-water interface can be accounted for the hydrogen bonds between IW and carbonyl, glycerol and phosphate moeities. Two dimensional heterodyne detected vibrational sum frequency generation (2D-HD-VSFG) spectroscopy reveal that the hydrogen bond dynamics of IW is not only because of the individual contribution from the head-group moeities but also from neighbouring IW molecules [Inoue *et al.*, 2017]. Our calculations show similar hydrogen bond networks. The hydrogen bonds between lipid-IW-IW-lipid result in a concerted network leading to lipid aggregation where IW acts as a bridge between two lipids. The concerted hydrogen bond networks of IW with carbonyl, glycerol and phosphate moeities of lipids and simultaneously among themselves are shown in figure 3.10. The formation of hydrogen bonds between the IW and thee lipids is due to electrostatic potential developed across the bilayer interface facilitating preferential orientations of the IW molecules. Due to the dynamic hydrogen bonding, a mosaic of water reorientation is seen on the bilayer-water interface [Re *et al.*, 2014]. The preferential orientation of the IW molecules leads to the formation of an extended hydrogen bond network where the IW are hydrogen bonded among themselves and concertedly with lipid moeities.

3.8 SUMMARY

Continuously residing interfacial water molecules in hydrated DMPC lipid bilayer are identified to form hydrogen bonds among themselves and to the oxygens of CO, PO, or Glyc. of DMPC heads. Radial distribution functions of interface water oxygens are found to have higher amplitudes compared to that of the bulk due to the more tendency of oxygens to be in the nearest neighbors of each other in the presence of lipid heads. This consequently disrupts the tetrahedral network in bulk water and leads to defects in the networks of interface water. Mean square displacements of all classes of interface water show signatures of cage-like and glass-like regions for a short duration of time after the ballistic regions followed by sub-diffusive regions. The nature of chemical confinement is found to be important to translational dynamics since the MSD of the IW-CO is slower than the IW-Glyc. which is slower than the IW-PO or the IW-IW.
The first and second order RACFs are computed for $\vec{n}$ ($\vec{OH} \times \vec{HH}$), $\vec{OH}$, $\vec{HH}$, and $\hat{\mu}$. In all cases, the RACF of the BW decays faster compared to all classes of IW. The IW-CO and the

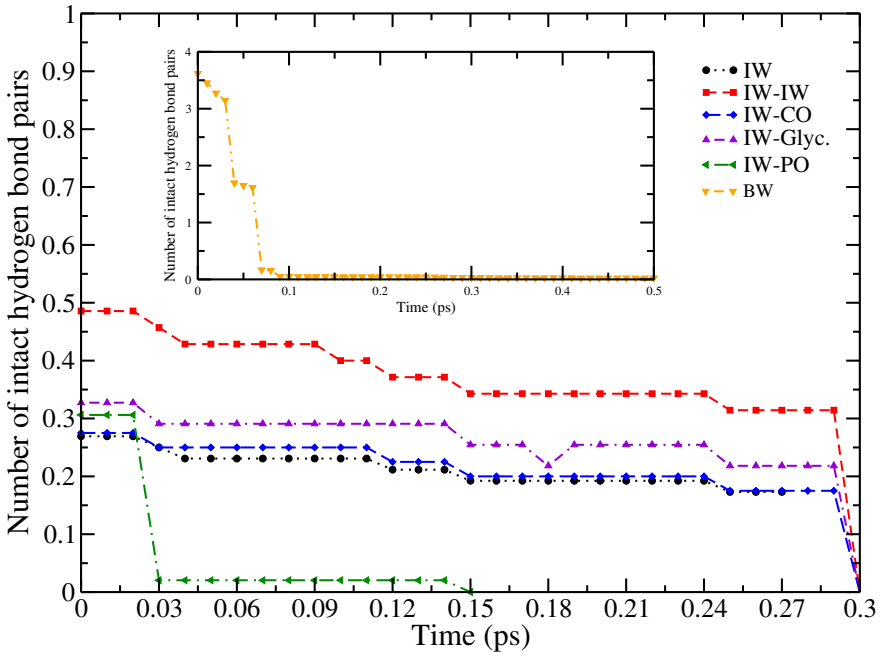

Figure 3.9: Number of hydrogen bonds per water molecule which remain *intact* for simulation time t are shown for interfacial water. **Inset**: bulk water

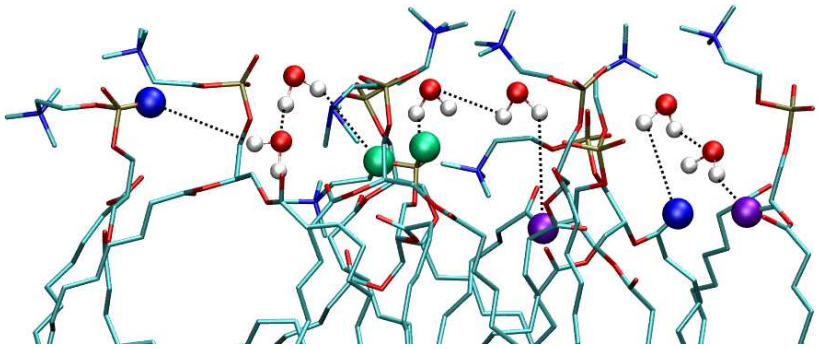

Figure 3.10: Snapshot of DMPC molecules hydrogen bonded to interfacial TIP4P/2005 water. DMPC and water are shown in licorice and Corey, Pauling and Koltun representations respectively. Hydrogen bonded oxygens of DMPC are shown in VDW representations. Color code: green-PO oxygen, violet-Glyc. oxygen, blue-CO oxygen, red-water oxygen.

IW-PO are found to have higher preferences in orientations, whereas the IW-Glyc. or the IW-IW has lower preferences. This is consistent with the mosaic structure in the orientation of IW near DMPC reported earlier [Re *et al.*, 2014]. The ratio of the first and the second order Legendre polynomial of the RACF for all water hydrogen bonded to lipid heads indicates the presence of the jump reorientation mechanism during hydrogen bond switching events.

Although the number of hydrogen bonds for the IW is lower than that for the BW due to the defected hydrogen bond network in the presence of the lipid heads, the amplitude of distribution of hydrogen bonds is higher for the IW than that for the BW. Hydrogen bond correlation functions for the BW decay much faster than all IW. The IW-PO exhibits faster decay in hydrogen bond correlation than the IW-IW which decays faster than the IW-CO or the IW-Glyc. This is due to their locations along the alkyl chains in membranes. Interestingly, hydrogen bond auto-correlation functions for interface water develop humps at ~ 12 ps after the onset of glass-like behavior which is neither present in bulk nor in water hydrogen bonded to lipid heads. The humps disappear at longer time due to the escape of water molecules from the cage of the crowded networks when the effect of confinement is no longer significant and thus all classes of water follow a $t^{-1.5}$ behavior delineating the translational diffusion dictated hydrogen bond dynamics irrespective of the nature of the chemical confinement of water. In the intermediate time scale of $\sim 12 - 20$ ps, the interface water undergoes a transition from the glass-like behavior to the diffusion dictated hydrogen bond breakage mechanism leading to humps in the correlation functions.

Using the reactive flux analysis, the Gibbs energy of activation of hydrogen bond breakage is calculated. The BW has the smallest lifetime with the lowest Gibbs energy of activation, whereas the IW-Glyc. has the longest lifetime with the highest Gibbs energy of activation among all water. Since IW-Glyc. is buried in the core lipid regime, diffusion through the water depleted hydrophobic environment is not favourable leading to a high Gibbs energy of activation. However, the relation of thermodynamics to the dynamics of hydrogen bond can only be found once the changes in entropy and enthalpy are calculated. This can establish the contribution of hydrogen bonding relaxation to thermodynamic or kinetic stability of lipid aggregations in the future.

The calculations show that the hydrogen bond networks which remain intact during the simulation time decay much rapidly for the BW than all defected hydrogen bond networks in the interface. The defected hydrogen bond networks dynamically result in the water mediated lipid-lipid associations. Thus, the present work enhances the understanding on slower hydration dynamics of membranes due to the chemical nature of hydrogen bond networks. This can be useful for further investigations on the dynamics of proton migrations from the hydration layer of membranes to the bulk phase or toward the stability of membranes or other biomolecules like proteins [Dill, 1990; Gabriel and Teissié, 1996; Tuckerman *et al.*, 1997; Smondyrev and Voth, 2002b; Efimov and Brazhnikov, 2003; Tepper and Voth, 2005].

4

Quantification of dynamical heterogeneities of hydration water in lipid membrane above supercooling

4.1 INTRODUCTION

In biological systems, water is confined between molecular assemblies where water dynamics is relevant in membrane functioning and cytoskeletal organizations [Munro, 2003; Lingwood and Simons, 2010; Jungwirth, 2015]. In the last decade, with a major advancement in computer simulation and experimental techniques, water near soft interfaces are found to have very slow relaxation times [Pal *et al.*, 2002; Balasubramanian *et al.*, 2002; Ji *et al.*, 2010; Biswas *et al.*, 2013; Das *et al.*, 2015]. Recently, protein displacements in live cell membranes are found to have robust exponential tails due to the underlying dynamical heterogeneities [Gowrishankar *et al.*, 2012; He *et al.*, 2016].

The nano scale heterogeneity in membrane dynamics is believed to play the dominant role in various cellular processes such as signal transduction, matter transport and enzymatic activities in cells [Mouritsen and Jørgensen, 1992]. Dynamical heterogeneities in fluid membranes are observed on the scale of $80 - 150$ nm with super-resolution stimulated emission depletion microscopic and fluorescence correlation spectroscopic techniques, even in absence of cholesterol [Roobala and K., 2017]. Hydration dynamics has been identified as a sensitive ruler to determine membrane associated protein structure, topology, immersion depth and so on using $1H$ Overhauser dynamic nuclear polarization (ODNP)-enhanced NMR relaxometry [Cheng *et al.*, 2013]. However, time dependent Stoke shift experiments are found not to be suitable for measuring hydration dynamics near proteins due to excess contributions from protein motions [Heid and Braun, 2019]. Large signal acquisition time is required for signal detections below single monolayer coverage by conventional vibrational sum frequency generation (VSFG) spectroscopy. To overcome these limitations, heterodyning is used to shift one frequency range into another [Stiopkin *et al.*, 2008] and thus it has revealed that that hydrogen bond dynamics near a membrane is highly dependent on the water dynamics through a hydrogen bond network rather than hydrogen bonding near a specific interaction site [Inoue *et al.*, 2017]. Combining 2D HD-VSFG spectroscopy and molecular dynamics simulations, it has been found that water dynamics has a transition from interface like to bulk-like behavior at ~ 7 Å away from phosphatidylcholine monolayer interface [Roy *et al.*, 2014]. Structural heterogeneity of interfacial water has been reported near negatively, positively and charged lipid/surfactant interfaces using time-resolved sum-frequency generation spectroscopy [Cyran *et al.*, 2018].

Experimental method to extract length scale of spatial correlations in colloidal system is still inconclusive since the exact relation between correlations and length scale is unknown [Hagamanasa *et al.*, 2015; Zhang and Cheng, 2016]. The influence of hydration layers on global dynamics of proteins is debated [Chen *et al.*, 2006; Persson and Halle, 2008; Schiró *et al.*, 2015; Nandi *et al.*, 2017].

Complementary to experiments, simulation data provide accessibility to atomic trajectories which can be directly used to extract relaxation time scales of water near soft interfaces. Water confined near silica hydrophilic pores at room temperature reveals two different dynamical regimes similar to supercooled bulk water [Gallo *et al.*, 2000a,b]. Confined diffusion of nano-particles is found to follow non-Gaussian statistics even at the long time Brownian stage [Xue *et al.*, 2016]. Intermittency in solute motion has been identified as the source of non-Gaussian behavior where solute solvent dynamics are decoupled [Acharya *et al.*, 2017]. Distinct heterogeneous water dynamics have been found for four dynamically connected water layers [Das *et al.*, 2013]. Dynamics and thermodynamics

of interface water near a bilayer are found to be correlated with the phases of the bilayers [Debnath *et al.*, 2013]. Chemical heterogeneity in a lipid bilayer does not immediately imply dynamic heterogeneity. Different mobility groups are found for lipid membranes in an L_β phase where characteristics time and length scales are identified to be $1-2$ μs and $1-10$ nm which can couple to biomolecules in the membrane [Shafique *et al.*, 2016]. Simple polydisperse systems with continuously varying diameters of particles show dynamic heterogeneity only at low temperatures and not at high temperatures [Russo and Tanaka, 2015; Tah *et al.*, 2018]. Recently it has been shown that such small scale fluctuations of membranes originating from the longitudinal component of lipid orientations can be used in deriving the bending modulus or curvature of the membrane where the tilt moduli can be obtained from transverse components of lipid orientations [Watson *et al.*, 2012; Terzi and Deserno, 2017; Chaurasia *et al.*, 2018]. Increased viscosity at the interface is found to be the source of slowed diffusion of proteins than in bulk [Pronk *et al.*, 2014]. $20-50\%$ faster water diffusion is obtained for disordered surfactant membranes compared to the ordered ones [McDaniel and Yethiraj, 2017]. Long term correlation and sub-diffusion of lipid recognition protein with the membrane are the contributing factors in enhancing the probability of encountering the target complex on the membrane surface [Yamamoto *et al.*, 2015]. The pertinent question remains, (i) what are the sources of distinct dynamics of confined water at room temperature? [Sciortino *et al.*, 1996; Gallo *et al.*, 1996; Bellissent-Funel, 1998; Mazza *et al.*, 2006; Jana and Bagchi, 2009; Youssef *et al.*, 2011] (ii) Can the dynamical heterogeneity length scale be predicted for confined water near membranes? This leads an open question: can the length scale be tunable from the membrane phase?

In this chapter, we use all atom molecular dynamics simulations for a fully hydrated lipid bilayer to identify chemically confined interface water molecules which form hydrogen bonds to lipid heads. Translational mean square displacements, non-Gaussian parameters and van Hove auto-correlation functions are calculated to understand if chemically confined water near DMPC lipid head-groups exhibits dynamical heterogeneity at temperature (308 K) well above supercooling. Wave-length dependence of self intermediate scattering functions of interface and bulk water are calculated. Heterogeneous relaxation time scales present in the interface water are quantified and their dependence on chemical confinement is examined. Block analysis is employed on the interface and van Hove correlation functions are calculated for interface water by varying the block sizes. The dynamical heterogeneity length-scale of interface water is quantified from the block analysis and its relation with the membrane curvature is examined by calculating the Fourier transform of tilt angle fluctuations of lipid molecules. The influence of chemical nature of lipid chains and physical properties of the lipid bilayer on the heterogeneous dynamics of interface water is systematically analyzed to find out the origin of the slow relaxation rates of interface water molecules. Our calculations provide the microscopic mechanism responsible for such a behavior at room temperature with their implications and potential applications. We attempt to predict the dynamical heterogeneity length scale of confined water and its relation to the properties of the membranes.

4.2 SIMULATION DETAILS

An all atom molecular dynamics simulation is carried out for 128 DMPC molecules in the presence of 5743 TIP4P/2005 water molecules at its fully hydrated state [Lopez *et al.*, 2004; Zhao *et al.*, 2008; Trapp *et al.*, 2010] using a previously equilibrated DMPC system at 308 K [Srivastava and Debnath, 2018]. Force field parameters for DMPC are obtained using Berger united atom force field [Berger *et al.*, 1997; Cordomí *et al.*, 2012] which are used in conjunction with a TIP4P/2005 [Abascal and Vega, 2005] water model. The specific combination of the force-fields of water and the bilayer is found to reproduce the experimental dynamical properties of water keeping the membrane fluid phase intact [Srivastava *et al.*, 2019b]. Moreover, force-fields will not alter the underlying mechanism of dynamical heterogeneity of confined water near membranes compared to that of the bulk water as seen for many glass-former liquids [Wong and Faller, 2007; Srivastava and Voth,

2013; He and Maibaum, 2017]. Area per head-group, bilayer thickness and order parameter for the DMPC bilayer using the force-fields match well with the experimental data [Petrache *et al.*, 2000; Aussenac *et al.*, 2003; Gurtovenko *et al.*, 2004; Kučerka *et al.*, 2011; Srivastava *et al.*, 2019b] implying suitability of the TIP4P/2005 force field with the Berger united atom force field.
An NPT run is carried out for 100 ns with a 2 fs time step. The system is equilibrated at 308 K using a velocity rescaling method [Bussi *et al.*, 2007] with a coupling constant of 0.5 ps. The pressure is maintained at 1 bar using semi-isotropic pressure coupling by the Berendsen pressure coupling method [Berendsen *et al.*, 1984b] with a coupling constant of 0.1 ps. Coulombic and van der Waals interactions are cutoff at 1 nm. Long range interactions are corrected using the particle mesh Ewald [Darden *et al.*, 1993; Essmann *et al.*, 1995b; Allen and Tildesley, 1987] method with a 0.12 nm grid size. All bonds are constrained using the LINCS [Hess *et al.*, 1997] algorithm. Periodic boundary conditions are applied in all three directions. Next an NVT simulation is performed for 1.9 ns with a 0.4 fs time step where the last 1 ns run is analyzed for water dynamics. 1 ns run-length is found to be long enough to obtain adequate sampling to calculate the relaxations discussed in the study. Parameters for temperature coupling, cutoff distances and long range interactions are kept the same as in the previous run. Trajectories are collected at every 10 fs. The simulation box-length for the hydrated DMPC lipid is 6.24 nm along the x and y directions and 7.95 nm along the z direction.
For investigating the length-scale associated with dynamical heterogeneities, the hydrated DMPC water system is replicated 4 times using the same set of parameters as for the smaller system. Thus a bilayer of 512 DMPC lipids is simulated, which is known to be large enough to calculate lipid small length scale fluctuations from their tilt [Watson *et al.*, 2012]. An NPT equilibration run is carried out for 100 ns followed by a 2 ns NVT run with the same time step and saving frequency as for smaller systems. All other parameters are kept the same as the smaller system. Simulation box length for the larger system is 12.63 nm^2 both along the x and y directions and 7.76 nm along the z direction. Since the 12.63 nm^2 all atom DMPC-water system is computationally very expensive and the long time relaxation of the interface water molecules in the 6.24 nm^2 bilayer is 1 ns, the last 1 ns trajectory of the 12.63 nm^2 membrane is used for the production run. For the analysis of spectral intensity from lipid tilts, the same trajectory is used. To compare the dynamics of interfacial water with bulk water molecules (BW), a 2 ns NPT run followed by a 400 ps NVT run is carried out for a box of only 851 TIP4P/2005 water molecules using the same parameters as in a DMPC-water system. Equilibration of the system is checked and the last 100 ps data are analyzed for BW since BW relax much faster than the interface water. The box length of BW is 3.69 nm along the x and y directions and 1.84 nm along the z direction. All simulations are carried out using GROMACS 4.6.5 [Bekker *et al.*, 1993; Berendsen *et al.*, 1995; Lindahl *et al.*, 2001; Spoel *et al.*, 2005; Hess *et al.*, 2008; D. van der Spoel and the GROMACS development team., 2013]. All analyses are performed using in-house fortran codes.

4.3 DEFINITION OF DIFFERENT CLASSES OF INTERFACE WATER

Figure 2.1 in the previous chapter show the bilayer and a single DMPC molecule present in the bilayer respectively. To decouple the contribution of bulk water molecules (BW) to the dynamical properties of hydration layers, interface water is classified based on geometric definitions. If a water molecule continuously resides in a layer which is ±3 Å (the first hydration layer obtained from g(r) of O_{water}-N_{lipid} and O-O of water in figure 2.6) away from the location of the nitrogen head group density of DMPC for a 100 ps time window, the molecule is identified as an interface water molecule (IW) [Srivastava and Debnath, 2018]. The definition of IW considers most of the IW molecules forming hydrogen bonds to oxygen atoms of glycerol, carbonyl, and phosphate head groups of DMPC [Srivastava and Debnath, 2018; Srivastava *et al.*, 2019b]. The 100 ps time window is chosen from the residence time of interface water molecules for a 1 ns time window (figure 2.7 and table 2.4). Similar residence time was found earlier for interface water near a DPPC bilayer using an SPC water model [Debnath *et al.*, 2010]. Since IW molecules reside in the hydration

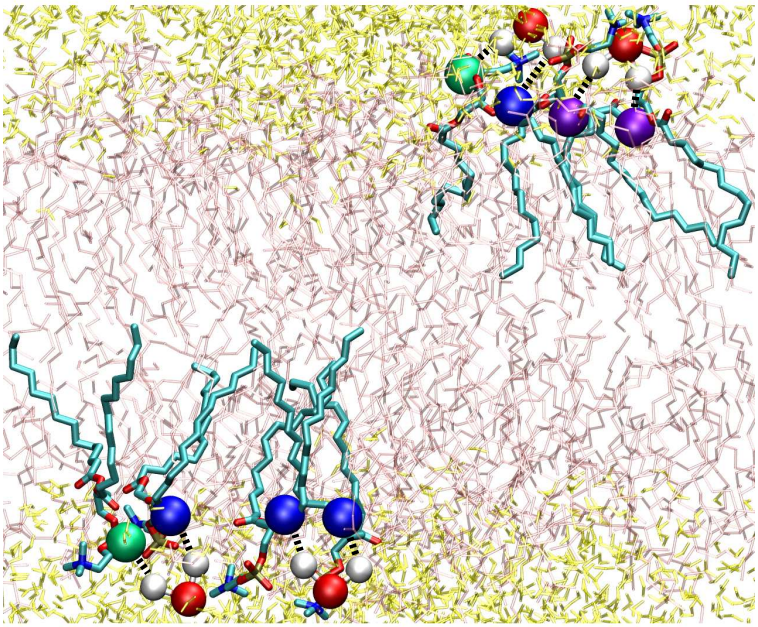

Figure 4.1: Interface water continuously residing for 400 ps (IW_{CR400}) in the first hydration layer of DMPC. Color code: Blue vdw - carbonyl oxygen; Violet vdw - glycerol oxygen; water molecules were shown in CPK. DMPC bilayer shown in transparent in pink licorice representation.

layer continuously for the 100 ps time window, the time window is referred to as their confinement lifetime for further discussion. To check the effect of confinement lifetime on IW molecule relaxation, another class of IW molecules is chosen which stay continuously in the hydration layer for 400 ps and is referred to as IW_{CR400}. Figure 4.1 show the location of IW_{CR400} hydrogen bonded to carbonyl, glycerol and phosphate oxygens for the entire 400 ps. Furthermore, to check the influence of lipid head moieties on the relaxation time-scales of IW, different classes of IW molecules are identified. If one IW molecule of 100 ps confinement lifetime is hydrogen bonded ($r_{O-O} < 0.35$ nm and $\theta_{HOO} < 30^o$) to another IW molecule of the same lifetime, it is referred to as IW-IW. Additionally, if an IW molecule is hydrogen bonded to the carbonyl (CO), phosphate (PO) or glycerol (Glyc) moiety of lipid heads (shown in different colors in figure 2.1 a)), the IW molecule is referred to as IW-CO, IW-PO or IW-Glyc respectively [Srivastava and Debnath, 2018]. Note, these different classes of IW molecules are hydrogen bonded for at least a single time frame during the 100 ps confinement lifetime and thus are allowed to exchange their partners within the observation period.

4.4 TRANSLATIONAL MEAN SQUARE DISPLACEMENT

To analyze the dynamical nature of bound waters, translational mean square displacement (MSD) is calculated in 3 dimensions for all classes of water using the equation 2.1. Figure 4.2 shows that the BW molecules follow diffusive behavior at longer time where all classes of IW remain sub-diffusive due to the trapping in a cage formed by the neighboring hydrogen bond networks. MSD_z is slower than MSD_{xy} (figure 4.4). The nature of the MSD of IW molecules does not coincide with the one followed by the lipid head groups, so the translational displacements of lipid heads are not straight forwardly coupled to that of the IW molecules. IW_{CR400} exhibits the slowest MSD due to longer confinement lifetime compared to the other classes of IW revealing that the confinement lifetime has an influence on the slowest translational dynamics of IW.

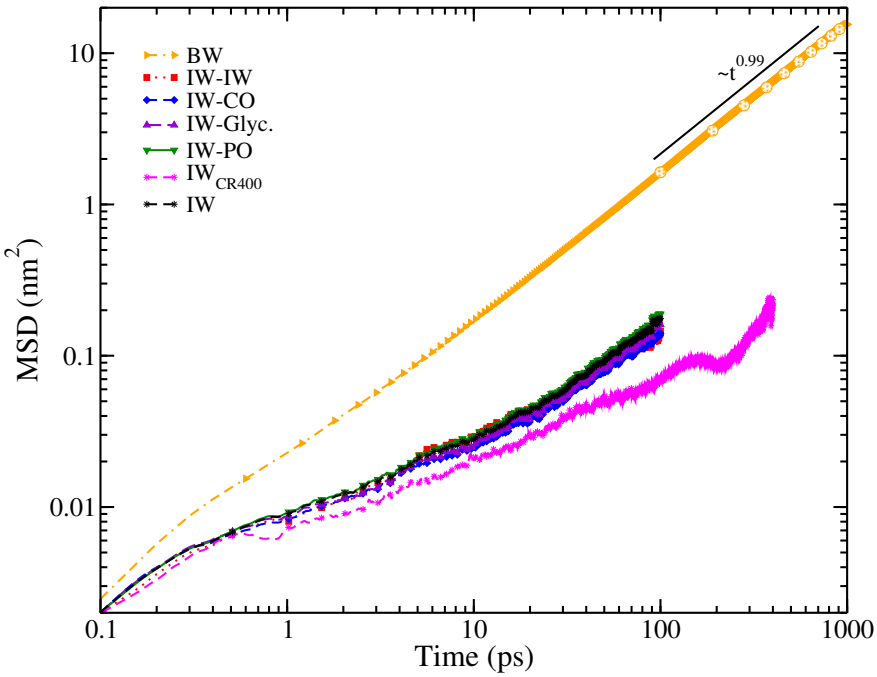

Figure 4.2: Translational mean square displacement for all classes of IW and BW. All classes of IW follow sub-diffusive regime while BW obeys diffusive regime with diffusion exponent as $\alpha = 0.99$.

4.5 NON-GAUSSIAN PARAMETER

To understand the origin of the subdiffusive nature of the IW, a non-Gaussian parameter (NGP, α_2(t)) [Shell *et al.*, 2005; Hansen and McDonald, 2006] is calculated in three dimensions using the equation 2.10. The NGP for the BW decays asymptotically to zero through a maximum confirming the Gaussian diffusion (figure 4.3). The values of NGP for different classes of IW start increasing to much higher amplitudes than that for the BW and reach a maximum between β and α-relaxation time scales. Respective relaxation time-scales, τ_{α_2}, are mentioned in table 4.1. The slow decays of the NGP for IW molecules are due to the release of the IW molecules from the respective cages via diffusion. Earlier it has been found that τ_{α_2} characterizes the correlation timescale of spatially heterogeneous motion for polymer melts and can feature diffusive time-scale [Starr *et al.*, 2013]. The peak of NGP along z appears at a longer time-scale than that along xy. The peak locations of NGP (τ_{α_2}) are consistent with the confinement lifetime of 100 ps (figure 4.4 c) and d)).

Similar cross-over from cage to translational diffusive regime at the time scale of τ_{α_2} are found for Brownian particles in a periodic effective field [Vorselaars *et al.*, 2007]. Since IW molecules leave the layer after their confinement lifetimes of $\sim$ 100 ps, the maxima of their respective NGP are nearly at 100 ps (table 4.1). IW-Glyc being buried in the hydrophobic core of the lipid membrane (figure 2.1 a)) show the highest τ_{α_2} relaxation among IW molecules which are continuously residing for 100 ps. Interestingly, IW$_{\mathrm{CR400}}$ exhibits very strong non-Gaussian behavior for a longer period of time compared to other classes of IW molecules and decay after $\sim$ 340 ps which is again closer to their confinement lifetimes. The slow relaxations of all classes of IW molecules signify a strong structural arrest by their surrounding molecules similar to supercooled liquids exhibiting dynamical heterogeneity [Kob *et al.*, 1997; Vorselaars *et al.*, 2007; Youssef *et al.*, 2011]. The transition from the β to the α-relaxation occurs at a similar spatio-temporal scale where the respective MSD have transition from the sub-diffusive to the diffusive regime.

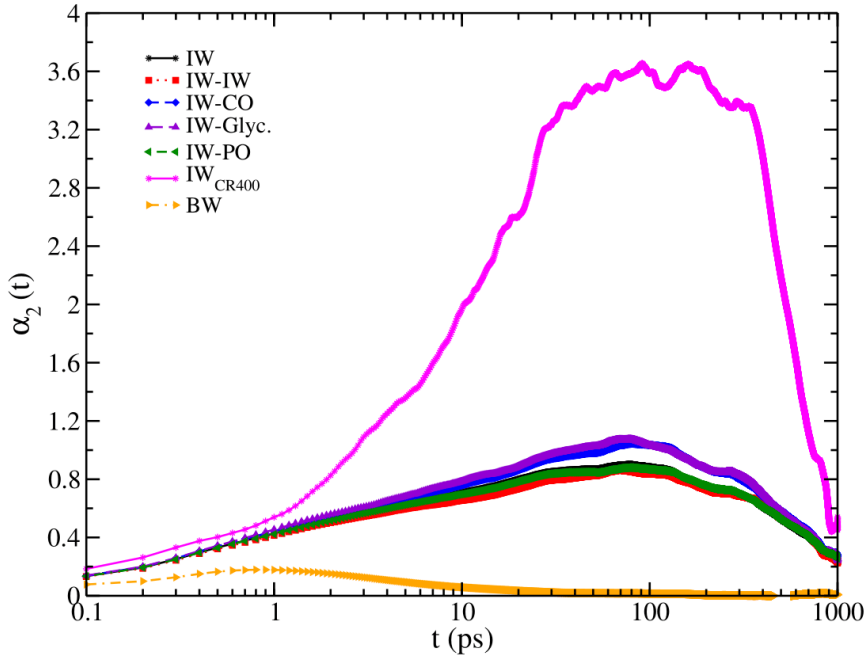

Figure 4.3: NGP (α_2(t)) for all classes of IW molecules and the BW molecules show a cross-over from β to α relaxation at the same time-scale when respective mean square displacements have transitions from sub-diffusive to diffusive region.

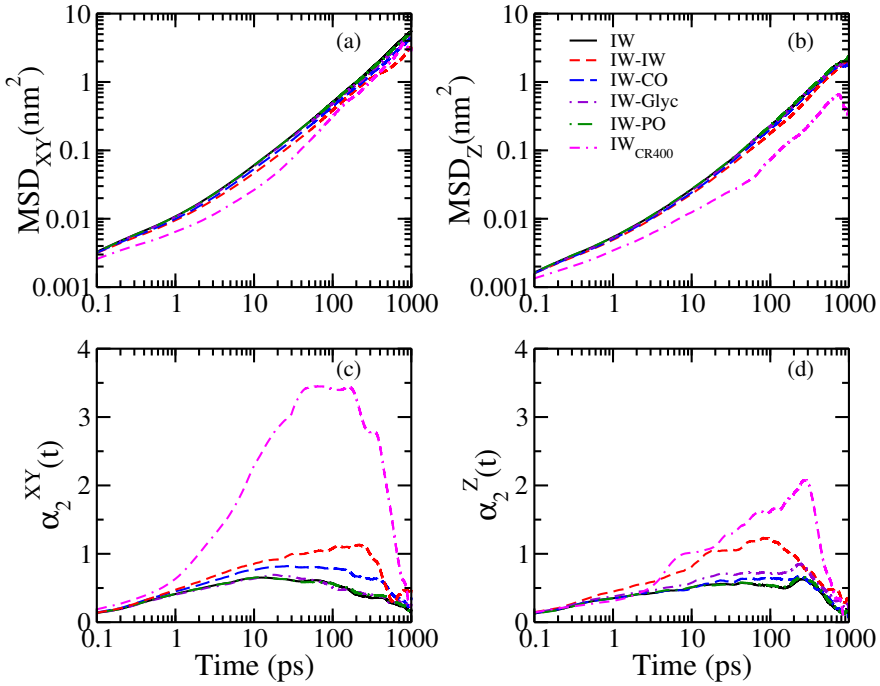

Figure 4.4: Translational mean square displacement for all classes of IW molecules along a) xy, b) z. NGP for all classes of IW molecules along c) xy and d) z.

Table 4.1: Relaxation time scales (τ_{α_2}) for all classes of IW and BW corresponding to peak of NGP.

Region	τ_{α_2} (ps)
IW	78.70
IW-IW	70.10
IW-CO	80.10
IW-Glyc.	82.80
IW-PO	78.40
IW_{CR400}	344.80
BW	0.90

4.6 VAN HOVE CORRELATION FUNCTION

For gaining deeper insights into the dynamical evolution of IW molecules associated with lipid moieties, the self part of the radial van Hove correlation function [Hopkins *et al.*, 2010] is calculated using the equation 1.1. Figure 4.5 shows the radial van Hove correlation function with a time interval (table 4.1) corresponding to the τ_{α_2}-relaxation of NGP where the dynamical heterogeneity is most significant for all classes of water. All classes of IW molecules show very strong deviations from Gaussianity where the BW follow Gaussian behavior. Due to the chemical confinement of different classes of IW in the vicinity of lipid heads, there is a strong correlation pertaining to longer length-scales which decays at a smaller length scale for the BW. Among different classes of IW, the van Hove correlation function of IW-Glyc which is buried towards the membrane core has the maximum amplitude depicting highest extent of correlation consistent with the highest correlation obtained from the respective NGP. Importantly, the van Hove correlation function of IW_{CR400} has two peaks and a shoulder unlike other classes of IW and their correlations decay at a smaller length scale than that for other classes of IW. Since IW_{CR400} has a larger time-window of 400 ps as the confinement lifetime, small numbers of IW_{CR400} are found on the bilayer surface which are inhomogeneously clustered on the bilayer surface. This might result in rattling or hopping of IW_{CR400} between cages which are not closely spaced on the bilayer surface unlike other classes of IW.

Since the bilayer is symmetric along the x and y directions where xy is the bilayer surface, one dimensional van Hove correlation function is calculated for all classes of water molecules along one of the directions to get a better description of deviations from Gaussianity. Figure 4.6 represents one dimensional van Hove correlation functions for time intervals corresponding to the same MSD_{xy} for all water molecules in the sub-diffusive regime. The time intervals used in the calculations are 5.12 ps, 5.2 ps, 6.74 ps, 5.51 ps, 5.01 ps, 5.12 ps and 0.9 ps for IW, IW-IW, IW-CO, IW-Glyc, IW-PO, IW_{CR400} and BW respectively. BW follow Gaussian dynamics and all classes of IW molecules show larger deviations from Gaussianity which have been manifested as an established behavior of dynamical heterogeneity in supercooled glass forming liquids [Chaudhuri *et al.*, 2007; Sengupta and Karmakar, 2014]. The origin of exponential tails for the IW molecules is the waiting time distributions for the subsequent jumps or hopping transitions between cages formed by the neighboring hydrogen bond networks.

4.7 SELF INTERMEDIATE SCATTERING FUNCTION

Since self intermediate scattering function (SISF, $F_s(q,t)$) is another universal feature of dynamical heterogeneity and the bilayer surface (xy plane) is symmetric along the x and y directions, two dimensional $F_s(q,t)$) is calculated using equation 1.2. Here $q = \frac{2\pi}{\lambda}$ where λ is the wavelength.

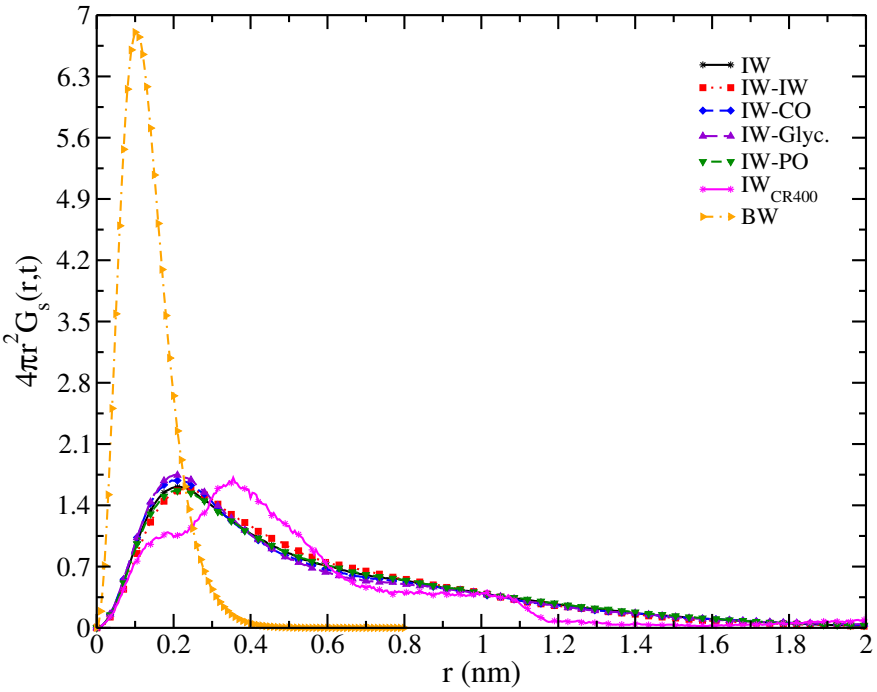

Figure 4.5: Self part of translational radial van Hove correlation function for all classes of IW and BW. The existence of larger correlation length indicates structured network of IW than BW.

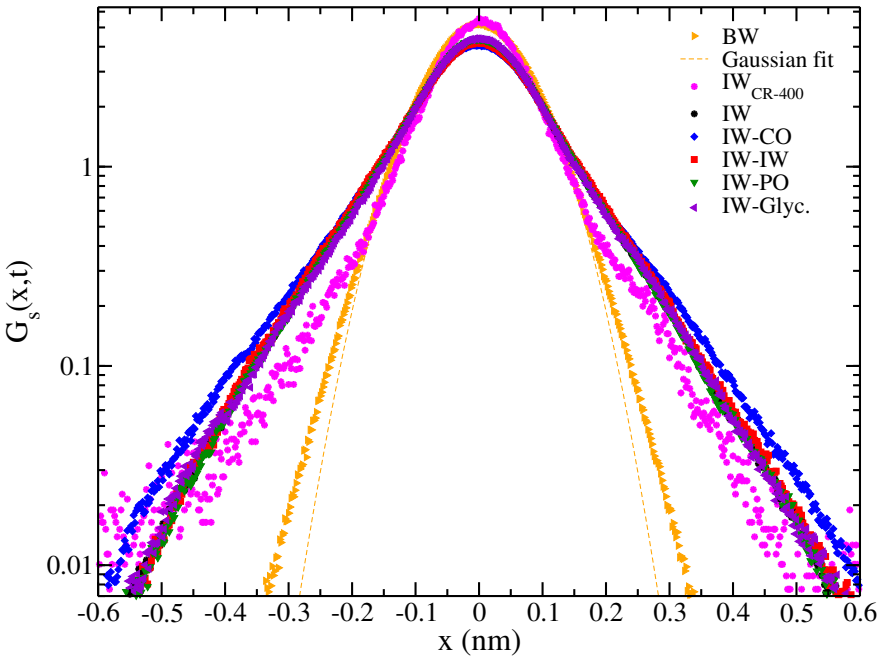

Figure 4.6: Self part of van Hove correlation function along x direction. Gaussian fitting for BW depicts Fickian dynamics while non-exponential tails for all classes of IW reveal deviations from Gaussian behavior.

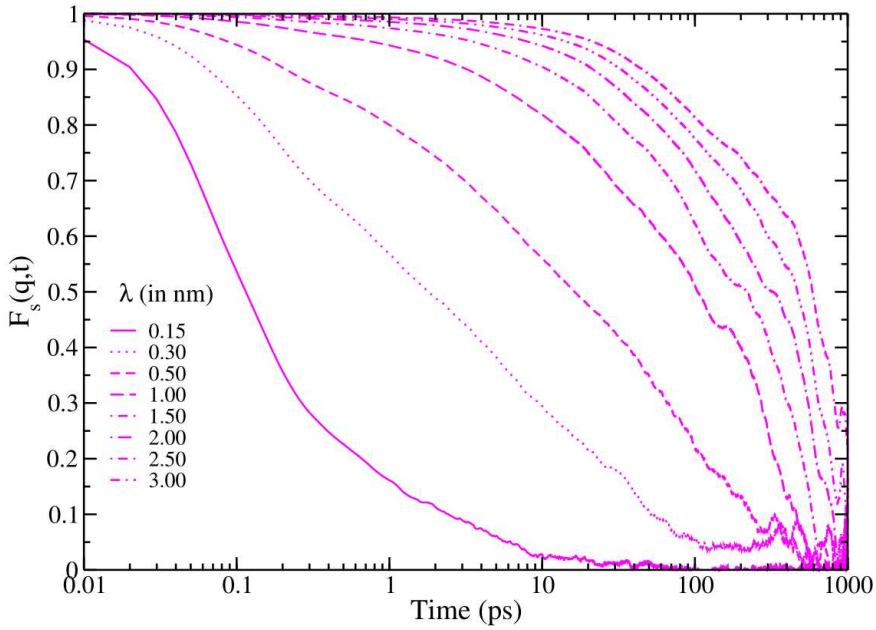

Figure 4.7: SISF of IW_{CR400} at λ values ranging from 0.50 nm to 3.00 nm.

To obtain the wave-vector dependence on the α-relaxation times, SISF are calculated at different values of λ. Figure 4.7 and 4.8 show the behavior of SISF at different λ for the IW_{CR400} and the BW.

Although the β and α-relaxation times of the IW molecules and the BW are not prominently disparate by characteristic Boson peaks as observed for the supercooled liquids [Hansen and McDonald, 2006], SISF very clearly scales up in different time regimes: very fast ballistic motion in a cage, cage relaxations and slow escape from the cage. Our BW data are fitted best to two relaxation time-scales using,

$$F_s(q,t) = (1 - f_Q)exp\Big(- \Big(\frac{t}{\tau_s}\Big)^2\Big) + f_Q exp\Big(- \Big(\frac{t}{\tau_\alpha}\Big)^{\beta_\alpha}\Big) \tag{4.1}$$

f_Q is known as the Debye-Waller factor, τ_s is the time-scale for ballistic motion and τ_α is the relaxation time-scale of the cage [Magno and Gallo, 2011]. The stretched exponential in the equation is known as the Kohlrausch-William-Watt (KWW) function [Camisasca *et al.*, 2016] where β_α can be correlated with the breakdown of the Stokes-Einstein relation for supercooled liquids [Bhowmik *et al.*, 2016]. Preservation or violation of the Stokes-Einstein equation has been calculated for the BW from its temperature dependence where the immobile component is characterized by slower τ_α and fast moving particles are characterized by τ_{α_2} [Kawasaki and Kim, 2017]. However, to establish such preservation or violation for the IW near the bilayer, one has to systematically analyze the breakdown temperature for the IW molecules. This investigation requires lipid bilayers at different phases at different temperatures which merits stand alone investigations in future. However, all classes of IW molecules are not fitted to the previous KWW function due to the appearance of a long time tail very similar to that for the IW molecules near proteins [Marzio *et al.*, 2016]. The SISF of IW molecules can be fitted for with three relaxation time-scales where one more stretched parameter is added to the KWW function as

$$F_s(q,t) = (1 - f_Q - f_Q^{'})exp\Big(- \Big(\frac{t}{\tau_s}\Big)^2\Big) + f_Q exp\Big(- \Big(\frac{t}{\tau_\alpha}\Big)^{\beta^\alpha}\Big) + f_Q^{'} exp\Big(- \Big(\frac{t}{\tau_l}\Big)^{\beta^l}\Big) \tag{4.2}$$

τ_l and β_l are longer relaxation time and stretching parameter respectively. Although such stretched long relaxation is not so common in glass-former liquids, similar τ_l for the IW molecules near

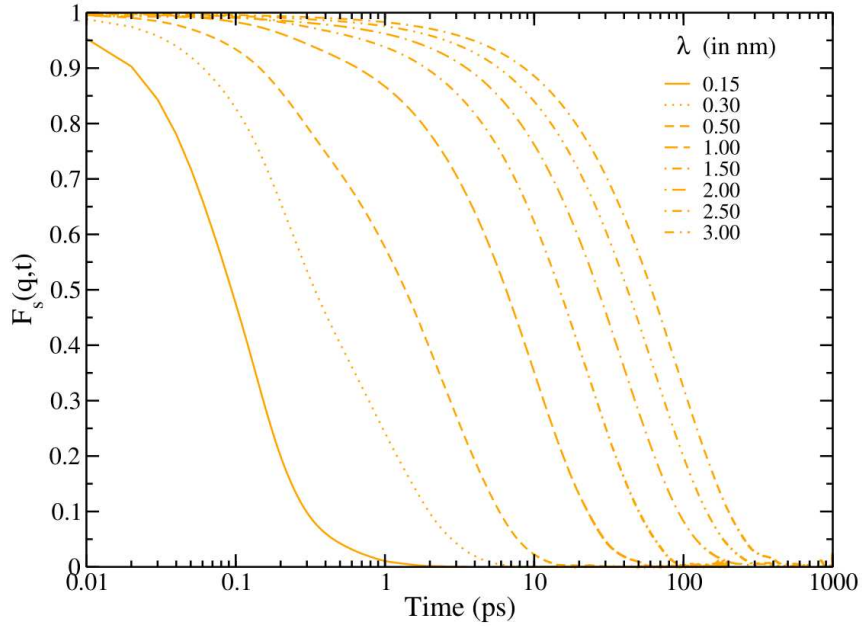

Figure 4.8: SISF of BW at λ values ranging from 0.50 nm to 3.00 nm.

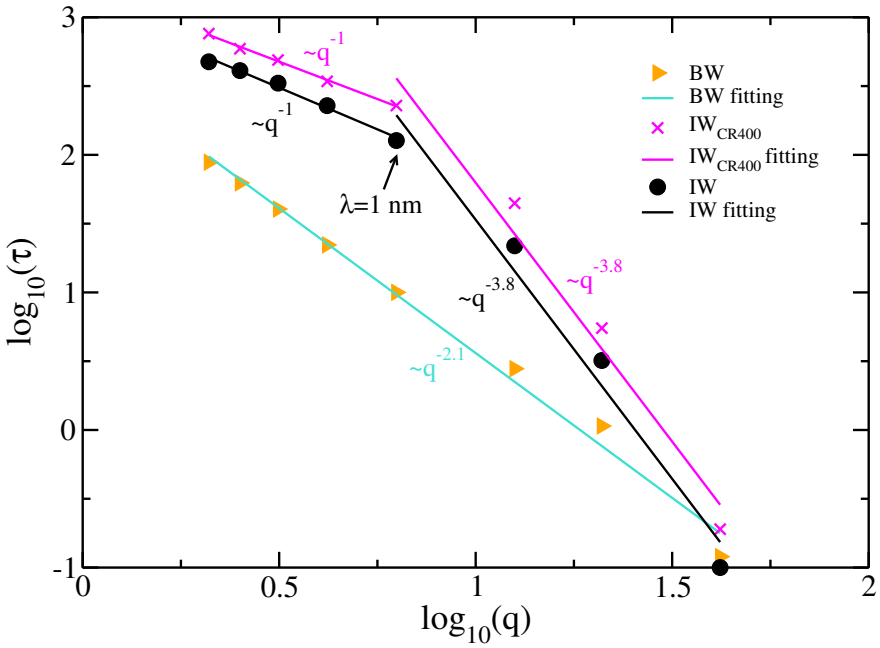

Figure 4.9: log(τ) vs log(q) plot for BW, $\mathrm{IW_{CR400}}$ and IW. Solid lines: fitting.

Table 4.2: Fitting parameters of SISFs for all classes of IW and BW. Correlation coefficients are >0.99. The relaxation times of IW (τ_l) and BW (τ_α) are compared with literature showing the suitability of Berger force fields in combination with TIP4P/2005 water model.

Region	τ_s (ps)	f_Q	τ_α (ps)	β_α	f'_Q	β_l	τ_l (ps)	τ_{HB} (ps)
IW	0.29	0.23	2.87	0.99	0.71	0.48	15.26	14.96
IW-IW	0.21	0.36	2.69	0.92	0.55	0.59	20.93	14.96
IW-CO	0.32	0.21	2.86	0.99	0.75	0.46	15.03	16.74
IW-Glyc	0.31	0.20	2.74	0.92	0.77	0.45	15.12	18.96
IW-PO	0.29	0.26	2.69	0.91	0.69	0.48	15.15	13.00
IW_{CR400}	0.17	0.22	2.72	0.82	0.70	0.68	85.31	122.85
BW	0.24	0.88	2.53	0.93				3.98
Reported literature (τ_l-IW and τ_α-BW)								
IW	Simulations	$\approx$ 10.00 ps [Magno and Gallo, 2011]						
BW	Simulations	$\approx$ 1.00 ps [Magno and Gallo, 2011]						

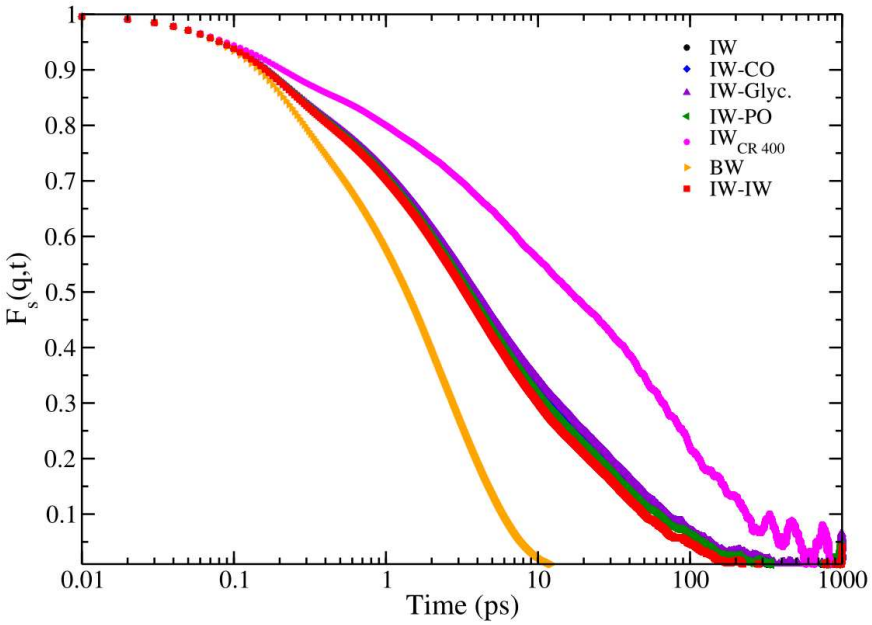

Figure 4.10: SISF for all classes of IW and BW at $\lambda = 0.50$ nm.

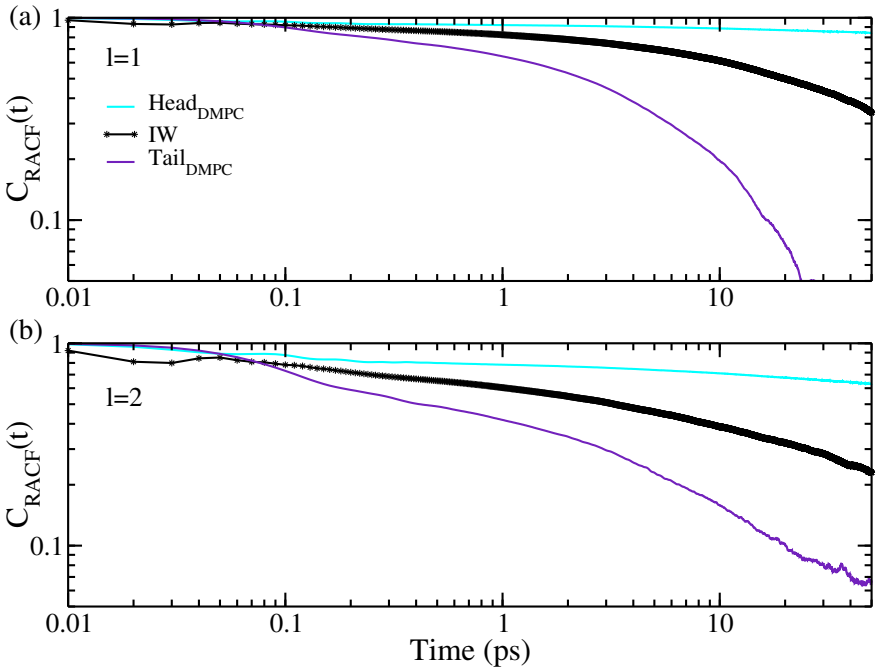

Figure 4.11: RACF for a) first and b) second order Legendre polynomial for lipid head, tail and IW.

Table 4.3: Reorientational correlation relaxation time scales for lipid head, tail and IW. All correlation coefficients were >0.99.

	Region	A_f	τ_f (ps)	A_s	τ_s (ps)
l=1	Head$_{DMPC}$	0.09	50	0.90	637.07
l=2		0.10	50	0.75	252.06
l=1	Tail$_{DMPC}$	0.48	2.75	0.36	14.32
l=2		0.25	1.01	0.40	11.94
l=1	IW	0.25	6.51	0.62	83.26
l=2		0.29	3.05	0.42	77.83

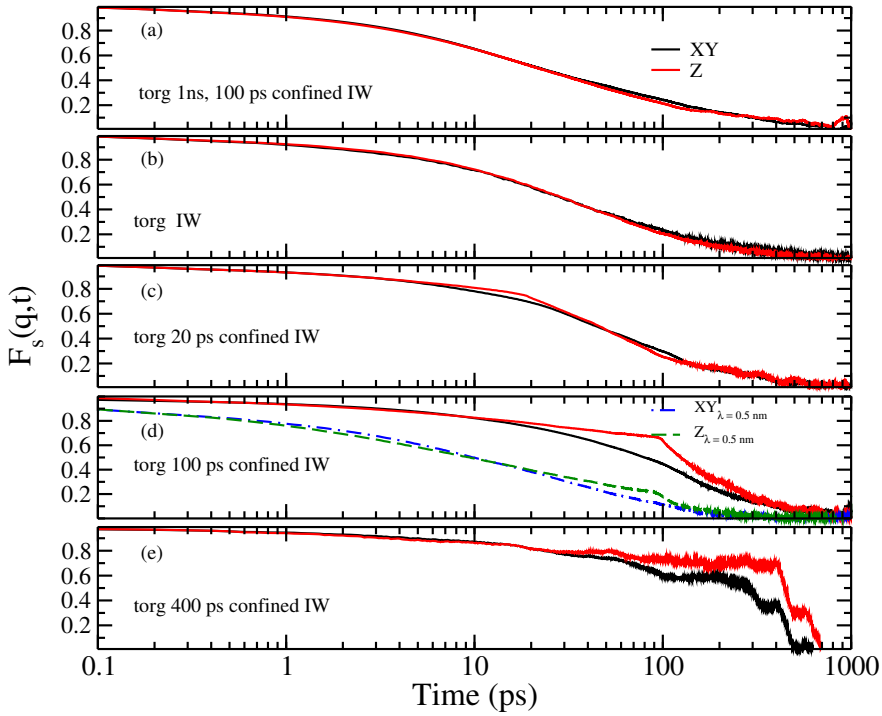

Figure 4.12: $F_s(q,t)$ of IW calculated along xy and z at $\lambda = 1$ nm. Time origins (torg) are averaged in two ways : a) torg over entire 1 ns run length for continuously residing IW for 100 ps, b)-e) torg over confinement time. b) IW for any frame, c) continuously residing IW for 20 ps, d) continuously residing IW for 100 ps at $\lambda = 1$ nm and $\lambda = 0.50$ nm and e) continuously residing IW for 400 ps.

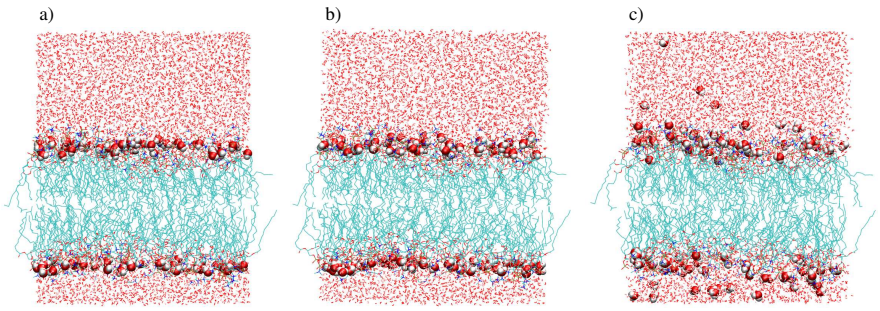

Figure 4.13: Snapshot of the DMPC bilayer at a) 50 ps, b) 100 ps and c) 150 ps. IW: CPK representation in red and white, DMPC lipids : line representations in cyan blue, remaining water : red dots.

proteins is known to follow Arrhenius dependence on temperatures with a cross-over due to the protein structure fluctuations [Marzio *et al.*, 2016]. τ_s and τ_α of all classes of IW show similar time-scales (table 4.2) as that of the BW and consistent with the time-scales obtained for hydration water near protein or sugar [Magno and Gallo, 2011; Marzio *et al.*, 2016].
To check the wavelength dependence of the slowest relaxations, log-log plot of the slowest relaxations and q are shown in figure 4.9. The slowest relaxation time (τ_α) follows a quadratic dependence on the q for the BW. The wavelength dependence of α-relaxation time-scales (τ_α) is generally characterized by the exponential decay of $F_s(q,t) = exp(-Dq^2t)$ at all wave lengths at room temperature. So the SISF of the BW have a q^{-2} dependence. In contrast, the slowest relaxation time of both IW and $\mathrm{IW_{CR400}}$ deviate from quadratic dependence indicating non-diffusive dynamics as seen earlier for liquids while supercooling [Bhattacharyya *et al.*, 2010]. However, the deviation from quadratic dependence on q for IW and $\mathrm{IW_{CR400}}$ is non-monotonic in nature. There are cross-overs from linear to quadratic behavior at $\lambda = 1$ nm for both IW and $\mathrm{IW_{CR400}}$. The non-diffusive dynamics of IW is influenced by confinement above a length-scale of 1 nm probably because the thickness of the interface layer is 0.6 nm along z, by definition.
SISF of the IW and the BW molecules are compared in figure 4.10 for $\lambda = 0.5$ nm which is slightly greater than the location of the first peak (0.3 nm) of the g(r) of water oxygens. This value of λ is chosen so that by this length scale all fast and slow relaxations of the IW molecules are over. Moreover, the differences in SISF between IW and BW are more prominent for $\lambda = 0.5$ nm than for $\lambda = 0.3$ nm. The IW-CO/IW-Glyc exhibit the slowest τ_s and τ_α since they are buried towards the hydrophobic region of the lipids. Interestingly, the τ_s and the τ_α for $\mathrm{IW_{CR400}}$ are 10 orders of magnitude slower than the remaining classes of water. However, all classes of water follow a long time stretched exponential tail (described by τ_l) which is clearly absent in the BW. Notably, the τ_l for $\mathrm{IW_{CR400}}$ is $4-6$ times larger than that for the remaining classes of IW molecules since they reside in the hydration layer for a longer time window. The emergence of τ_l is attributed to the very slow relaxation of the IW molecules arrested in a cage of hydrogen bond networks formed near the lipid head groups. To understand the physical origin of such stretched relaxation of IW molecules, intermittent hydrogen bond auto-correlation functions ($\mathrm{C}_{HB}(\mathrm{t})$) of IW molecules are calculated using

$$C_{HB}(t) = \frac{< h_{IW-HG}(0) h_{IW-HG}(t) >}{< h_{IW-HG} >} \tag{4.3}$$

where $\mathrm{h}_{IW-HG}(\mathrm{t})$ and $\mathrm{h}_{IW-HG}(0)$ represent hydrogen bonds between IW molecules and head-groups (HG) at time t and 0 respectively. h_{IW-HG} is 1 when a hydrogen bond is formed between the IW molecules and the HG and is 0 otherwise. Using reactive flux correlation analysis [Pasenkiewicz-Gierula *et al.*, 1999; Luzar, 2000], hydrogen bond relaxations (τ_{HB}) are calculated from the forward rate constants of hydrogen bond breaking reactions for all classes of IW discussed in the previous chapter. The hydrogen bond relaxations range from $13-19$ ps for IW-PO/IW/CO/Glyc [Srivastava and Debnath, 2018] and are very close to the values of τ_l mentioned in table 4.2. The hydrogen bond relaxation of $\mathrm{IW_{CR400}}$ is found to be ~ 100 ps which is again very close to the τ_l presented in table 4.2. Since the time-scales of τ_l for the IW molecules match well with their hydrogen bond relaxations (τ_{HB} in table 4.2), the hydrogen bond dynamics of the IW molecules can be the physical source of such long relaxations.
Earlier, bound water molecules are found to exhibit two time-scales, the fastest time-scale is connected to the BW dynamics and the slowest time-scale is found to be hydrogen bond relaxation time-scale [Nandi and Bagchi, 1997; Pal *et al.*, 2002]. However, translational MSD and rotational relaxations of lipid heads and tails are not straightforwardly connected to the MSD and rotational relaxations of the IW molecules (figure 4.11 and table 4.3). The rotational relaxation time-scales of lipid tails are closer to the relaxation time scale of IW molecules where the rotational time-scales of lipid heads are one order of magnitude slower than that of the IW molecules (table 4.3). This indicates that relaxations of the IW molecules are not governed by the relaxations of the lipid heads which are hydrogen bonded to the IW. The exact dependency between lipid and IW relaxations thus needs further intensive investigations.
Although, relaxations of $\mathrm{F}_s(\mathrm{q,t})$ shown in figure 4.10 capture the interlayer dynamics well through

hydrogen bond dynamics, the effect of confinement is not visible in the relaxations. This is because SISF in figure 4.10 is calculated at $\lambda = 0.5$ nm, a distance within the interface layer thickness (0.6 nm along the bilayer normal, z). F_s(q,t) at $\lambda = 1$ nm (a distance larger than the layer thickness) (figure 4.12) a)) has a τ_l value close to the confinement lifetime ($\sim$ 76 ps) and τ_α close to the hydrogen bond lifetime ($\sim$ 14 ps). However, the dynamics along xy and z are similar in nature. If IW molecules are probed at any time frame which may not reside in the layer for a finite time-span they too exhibit similar dynamics along xy and z (figure 4.12 b)) where the slowest relaxation time-scale is similar to their confinement lifetime ($\sim$ 82.25 ps). Survival probability of IW shows two time-scales (fast and slow, table 2.4) indicating distributions in lifetime for IW. If IW molecules which are continuously residing for $\sim$ 20 ps (close to its fastest survival time of $\sim$ 16.4 ps) are probed and averaged over time-origins (t_{org}) only over 20 ps, F_s(q,t) along z relaxes slower than F_s(q,t) along xy and the effect of confinement along z is clearly visible at $\sim$ 20 ps (figure 4.12 c)). The difference in xy and z is more prominent for IW continuously residing for 100 ps (figure 4.12 d)). Similar differences along xy and z are observed for SISF calculated at $\lambda = 0.50$ nm when averaged over torg only over 100 ps (figure 4.12 d)). The sudden drop of F_s(q,t) along z near 100 ps is because only those IW are probed which are confined in the interface layer along z continuously for 100 ps. These molecules relax very fast after the confinement lifetime. This is evident from the snapshots of the bilayers shown in figure 4.13. For the initial 50 ps, IW are residing at the layer, and at 100 ps the same molecules are still residing in the same layer, however at 150 ps, the same molecules are scattered to the bulk. So the movement of the IW for the initial 100 ps is more restricted than the next 50 ps along z when they no longer reside in the interface. Diffusion of the IW from interface to bulk just after the confinement lifetime is very fast with a high probability. This results in a sudden drop in F_s(q,t) along z. The effect of confinement on F_s(q,t) is examined for IW_{CR400} with a confinement lifetime of 400 ps. A similar drop in F_s(q,t) is found near their confinement lifetime of 400 ps (figure 4.12 e)).

4.8 VAN HOVE CORRELATION FUNCTIONS FROM BLOCK ANALYSIS

A block analysis approach is used to calculate the heterogeneity length scale present in the IW molecules at the membrane-water interface. The bilayer surface is divided into boxes of length L_B where $((L/L_B)^d)$ is the total number of boxes considered, L is the total boxlength and d is spatial dimension. To obtain sufficient statistics to evaluate the length scale associated with the dynamical heterogeneity [Karmakar *et al.*, 2009; Avila *et al.*, 2014; Chakrabarty *et al.*, 2017], one needs a large system size. Equilibration of such a large membrane using an all atom molecular dynamics simulation is expensive and thus we can reach a system size $\sim$ 4 times larger than our initial system size with a box-size of $12.6 \times 12.6 \times 7.7$ nm^3. The coarse grained displacement of one block is calculated by,

$$\Delta x_j^B(\tau) = \frac{1}{n_j} \sum_{i=1}^{n_j} [x_i(\tau) - x_i(0)] \tag{4.4}$$

where n_j is the number of IW molecules in the j^{th}th block. The blocked van Hove function is defined as,

$$G_s^B(x,\tau) = \left\langle \frac{1}{N_B} \sum_{j=1}^{N_B} \delta[x - \Delta x_j^B(\tau)] \right\rangle \tag{4.5}$$

$G_B^s(x,t)$ for each block is calculated with a time interval of 0.3 ps by which IW enter in the sub-diffusive regime. By considering different values of L_B , $G_B^s(x,t)$ of each block is calculated for 1 ns run-length averaging over 99970 time frames and shown in figure 4.14. With increase in L_B, the non-Gaussian distribution slowly becomes more and more Gaussian. A crossover from non-Gaussianity to Gaussianity is obtained at a coarse grained box length of 5.5 nm (figure 4.14)

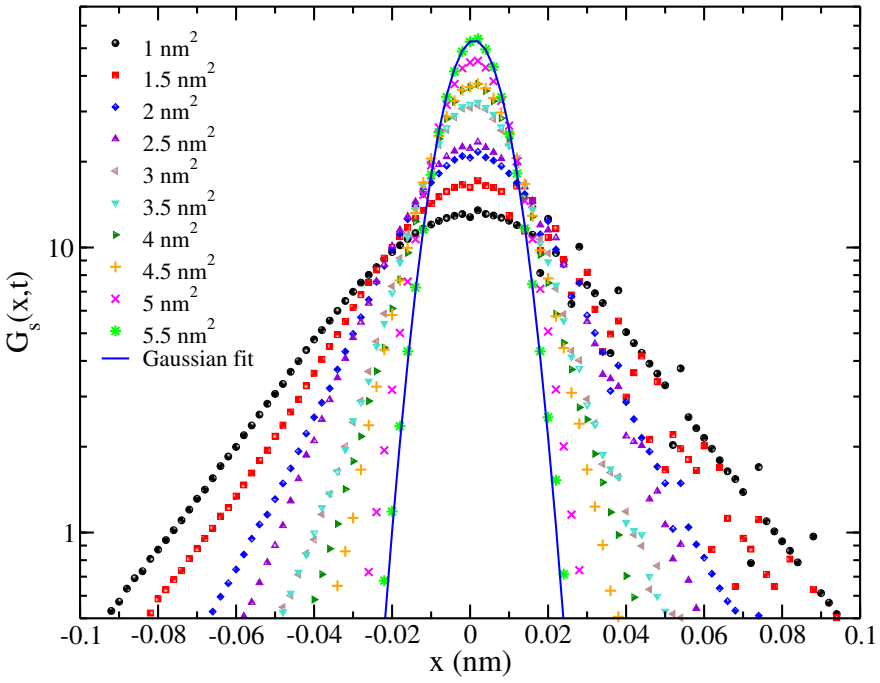

Figure 4.14: One dimensional van Hove correlation function for different coarse grained length scales. Solid blue line showed Gaussian fitting for coarse grained block area of 5.5×5.5 nm^2.

indicating the length-scale associated with the spatial heterogeneity in confined water. Although dynamics of water is expected to have a cross-over from non-Gaussian to Gaussian distribution once the numbers of particles increase to a large number with larger blocks according to the central limit theorem, block analysis enables one to predict the length-scale of the transition to Gaussianity which does not naturally come by central limit theorem. The length-scale of dynamical heterogeneity obtained from block analysis is examined earlier for different temperatures for glass-former liquids and compared with other independent methods [Bhowmik *et al.*, 2018].

To find the physical relevance of the heterogeneity length-scale of the confined water to the membrane structure, tilt of the tail to head vectors of the lipids [Schmid, 2013; Debnath *et al.*, 2014; Bradley and Radhakrishnan, 2016; Terzi and Deserno, 2017] are calculated as functions of lipid head group (x,y) coordinates on the bilayer surface using the following equation,

$$t(x,y) = cos^{-1}\frac{\vec{r}.\vec{n}}{\mid \vec{r} \mid} \tag{4.6}$$

where $\vec{r}$ is the tail to head vector of the lipid chain and $\hat{n}$ is the bilayer normal. A fast Fourier transform of t(x,y) provides the spectral intensity, and t(q) which is plotted on the xy plane of the membrane surface and shown in figure 4.15 a). The q value corresponding to the highest peak in figure 4.15 b) denotes the wave vector associated with the weak undulation of the membrane. Similar representative weak undulation is demonstrated in the side view of the bilayer snapshot in figure 4.15 c). The q vector of 1.14 nm^{-1} corresponding to the highest spectral intensity provides the wavelength ($\lambda = \frac{2\pi}{q} = 5.51$ nm) of the weak undulation.

The wave-length (5.51 nm) of the weak undulation of the bilayer obtained from intensity spectra of lipid tilts is similar to the dynamical heterogeneity length-scale (5.5 nm) of the IW molecules obtained by the block analysis approach. Although tilt is a small length-scale membrane undulation phenomenon unlike curvature, it has been recently shown that the bending and tilt modulus can be extracted from lipid longitudinal and transverse director fluctuations [Watson *et al.*, 2012; Terzi and Deserno, 2017; Chaurasia *et al.*, 2018]. Thus our finding suggests that the heterogeneity length-scale of interfacial water can be related to the small wavelength fluctuations of a fluid membrane. To

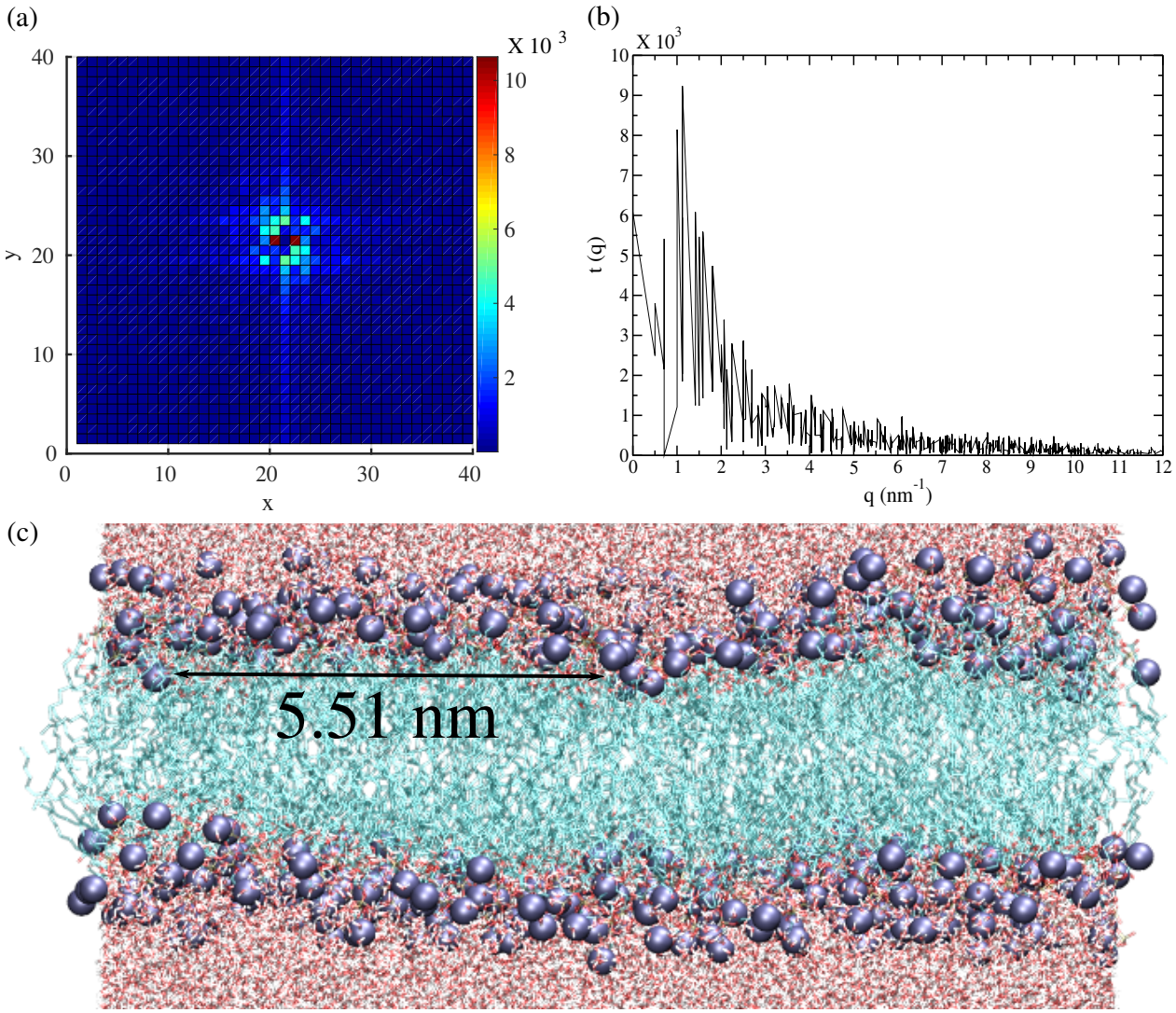

Figure 4.15: a) Top view of spectral intensity of DMPC tilt plotted on bilayer x-y plane showing emergence of peaks. x and y indicate the grids present on the surface and thus has no units. b) The spectral intensity t(q) vs q shows the q value with the highest intensity at 1.14 nm^{-1}. c) Side view of DMPC lipid bilayer showing the length scale of the local weak undulation of the lipid membrane.

put the observation on a strong ground, one has to extensively investigate the correlation between heterogeneity length scale and undulation wavelength of a rippled bilayer where the curvature is prominent. The correlation of dynamical heterogeneity length scale of the confined water with the wave-length of the weak undulation of the membranes indicates a tantalizing possibility of length-scale prediction from the phase of a membrane.

4.9 SUMMARY

In summary, this chapter provides evidence of spatio-temporal heterogeneities in interface water near lipid membranes at temperature well above room temperature using all-atom molecular dynamics simulations. Water molecules continuously residing in the interface layer for a time window of 100 ps are identified as IW. To investigate the influence of chemical confinement on their dynamics, the IW molecules which form hydrogen bonds to another IW molecule or to CO/PO/Glyc. lipid head groups for at least one time frame within their confinement time window are identified and referred to as IW-IW/CO/PO/Glyc. Dynamics of these different classes of water is relevant in understanding the structural or orientational heterogeneity of interface water near zwitterionic PC lipids or cationic or anionic lipid/surfactant interfaces previously reported using SFG spectroscopy and molecular dynamics simulations[Roy *et al.*, 2014; Inoue *et al.*, 2017; Cyran *et al.*, 2018]. The non-Gaussian parameters of all classes of IW molecules show β to α relaxations at similar spatio-temporal scale where their respective mean square displacements leave the sub-diffusive regions. IW-CO/Glyc. being buried deepest towards the hydrophobic core of the membrane have slowest β to α relaxations among all classes of IW. The slowest relaxation of IW-CO/Glyc. is attributed to the presence of a strong barrier of the membrane for water and ions at a location close to carbonyl head groups as seen in time-resolved fluorescence study [Koehorst *et al.*, 2010]. Such slow relaxations of IW are signatures of dynamical heterogeneities commonly found in glass former liquids [Kob *et al.*, 1997]. In contrast, the non-Gaussian parameter of bulk water molecules (BW) asymptotically decays to zero with a faster β to α relaxation exhibiting underlying Fickian dynamics. To understand the influence of confinement lifetime on the dynamics of IW, another class of IW molecules are identified which continuously reside in the interface layer for a longer time of 400 ps and are referred to as $\mathrm{IW_{CR400}}$. Since $\mathrm{IW_{CR400}}$ has the longest confinement lifetime, more profound dynamical heterogeneities are observed for these molecules. The β to α relaxation time scales of all classes of IW molecules are found to be closer to their confinement lifetimes.

The translational self part of the van Hove correlation function calculated at a time-interval of β to α relaxation time of NGP shows significant deviations from Gaussianity for all classes of IW. IW-Glyc. has the highest peak in the radial van Hove correlations among all classes of IW molecules very similar to their relaxations in NGP. $\mathrm{IW_{CR400}}$ with longest confinement lifetime has very few IW molecules inhomogeneously distributed over the bilayer surface. The inhomogeneous distribution can cause rattling or hopping of IW molecules between cages which are not spatially close leading to a peak and a shoulder in the radial van Hove correlation function. Since the bilayer is symmetric along the surface, one-dimensional van Hove correlation functions are calculated for all classes of water molecules at time-intervals having very similar values of MSD on the surface. BW follows a Gaussian fit in the one-dimensional van Hove correlation function where all classes of IW molecules show a significant amount of deviations. The exponential tails of the one dimensional van Hove correlation function are universal signatures of dynamical heterogeneity [Chaudhuri *et al.*, 2007; Sengupta and Karmakar, 2014] and are originated from the waiting time distributions for subsequent hopping transitions between cages formed by neighboring IW molecules hydrogen bonded to each other. Self intermediate scattering functions of all classes of IW molecules exhibit three well separated time scales unlike BW : fast ballistic motion in a cage, intermediate hopping transitions between neighboring cages and eventual relaxation of the cage. Although the long time cage relaxations are not so common in glass forming liquids, similar long relaxations are obtained for IW molecules near protein due to protein structure fluctuations [Camisasca *et al.*,

2016]. The long time relaxations of all classes of IW molecules are in excellent agreement with the respective hydrogen bond relaxations calculated from reactive flux correlation analysis [Srivastava and Debnath, 2018]. This confirms that the dynamical heterogeneity of IW molecules is originated from relaxation of hydrogen bonds due to hydrogen bond breaking irrespective of the confinement lifetime or the nature of the chemical confinement. To capture the confinement lifetime in the slowest relaxations, SISF should be calculated for a wavelength larger than the interface layer thickness. Importantly, the translational mean square displacement and rotational correlation functions of IW molecules are not straightforwardly coupled to that of the lipid heads or tails. However, this opens up a new direction to investigate the coupling between lipid and IW molecule dynamics in more detail.

The length scales of spatially heterogeneous dynamics are measured from van Hove correlation functions of IW molecules employing a block analysis approach. The IW molecules are coarse-grained over blocks of varying sizes on the membrane surface and one dimensional van Hove correlation functions are calculated for those blocks. A cross-over from non-Gaussianity to Gaussianity in van Hove correlation functions of IW molecules is found to occur at a specific length-scale which is identified as the dynamical heterogeneity length-scale of the IW. The spectral intensity calculated from the tilt of the lipids on the membrane surface estimates the wave-length of the weak undulations of the membrane in the fluid phase. The wave-length matches well with the dynamical heterogeneity length scale obtained from block analysis approach suggesting a correlation between the heterogeneity length scale and the membrane undulations. This correlation can be more profound for a membrane surface with a strong curvature which can be examined for a membrane in a rippled phase. Thus, we suggest an influence of the membrane phase on the length scale of dynamical heterogeneity of confined water, which merits further stand alone investigations.

Our calculations reveal that the slow relaxations of chemically confined water molecules near lipid membranes are governed by dynamical heterogeneities originated from hydrogen bonds rather than the dynamics of physically close lipid head groups. Moreover, the length-scale dependence of dynamical heterogeneity of confined water is predicted using the block analysis of the van Hove function. Importantly, the information of length-scale of dynamic heterogeneities is found to be possibly embedded in the length-scale of the lipid phase through its curvature. Thus the analyses can attempt to predict a length-scale for the membrane phase transition in future. Since confined biological water near membranes at room temperature exhibits similar dynamics to the super-cooled bulk water, the results can enhance our understanding of the mechanisms of bioprotection during freezing stresses and will be useful for mimicking cryo-preservation techniques at room temperature.

At the same time, our findings raise a few more questions : how strongly are the lipid dynamics coupled to the water dynamics? Is the coupling significant enough to influence the dynamics of lipids generating rafts, or skeleton fences? [Munro, 2003; Lingwood and Simons, 2010; He *et al.*, 2016] Is it relevant to the phase transitions of lipid bilayers?

5

Dynamic coupling of hydration water near a phospholipid membrane

5.1 INTRODUCTION

Biological water near lipid membranes has received a lot of attention since hydration sites of lipid membranes and hydrogen bonded network of hydration water are found to be crucial for understanding membrane-membrane interactions [Brzustowicz and Brunger, 2005; de Vries *et al.*, 2005; Polak *et al.*, 2014; Kučerka *et al.*, 2015; Fogarty *et al.*, 2015; Andoh *et al.*, 2016; Lin *et al.*, 2018]. To establish a relation between membrane and hydration layer dynamics and its connection to membrane functionalities, membrane associated protein-water dynamics have been analyzed where a correlation has been found to persist till 2.5 nm between two biosurfaces [Päslack *et al.*, 2019a]. 1H Overhauser dynamic nuclear polarization enhanced NMR relaxometry experiments show that dynamics of water near a membrane can be used as a predictor of membrane associated protein topology, structure, immersion depth [Cheng *et al.*, 2013]. Hydration water forms stronger hydrogen bonded networks with the phosphate group of lipid heads rather than other lipid head moieties [Re *et al.*, 2014]. All atom molecular dynamics simulations show that thermodynamical and dynamical properties of interface water near a bilayer follow a transition near the phase transition temperature of bilayers [Debnath *et al.*, 2013]. Molecular dynamics simulations and Overhauser DNP-enhanced NMR experiments show that water dynamics is strongly slowed down near the electrostatic interface of membrane-water and at larger distances away from the interface, it is dominated by the protein [Fisette *et al.*, 2016]. Distance dependency of hydration dynamics at the membrane interface has been investigated using molecular dynamics simulations revealing cooperative motion of water and lipid molecules [Das *et al.*, 2013]. Sum frequency generation spectroscopy and ab-initio molecular dynamics simulations show that continuous hydrogen bonded network can be formed from the bulk water to the carbonyl group of lipid molecules [Ohto *et al.*, 2015]. Correlated motions of water and protein and membrane have been identified in purple membranes [Tobias *et al.*, 2009]. Correlated motion of lipid molecules occurs over 3 nm which can consist of 4 lipid molecules with a time span from ps to close to ten ns [Rheinstädter *et al.*, 2008].

Similar to the hydration layers near membranes, coupled protein-water motions are observed over tens of ps for the slow relaxations [Li *et al.*, 2007]. Regional structure and dynamics of interface water near a protein are sensitive to the topological heterogeneity of the protein surface rather than to the chemical specificity of the protein structure [Dahanayake and Mitchell-Koch, 2018a]. Earlier experiments with limited energy resolutions of ~ 1 μev have prompted researchers to the idea of perfect coupling of protein dynamical transition (PDT) to the hydration water relaxation dynamics [Doster *et al.*, 1989; Chen *et al.*, 2006; Schiró *et al.*, 2015]. However, on the contrary, protein dynamical cross-overs have been reported at a temperature different from PDT or even at a dry state [Liu *et al.*, 2017]. Recent high resolution elastic neutron scattering experiment shows decoupling between protein and hydration water dynamics at low temperature [Benedetto, 2017]. This imposes serious questions on the well established thought of a perfect coupling between protein and hydration water.

At supercooled temperatures ranging from 100 K to 260 K, dynamic coupling between hydration water and membrane is no longer valid. For temperatures <260 K, membrane protein dynamics is not controlled by hydration water, rather, it is controlled by the dynamics of lipid [Wood *et al.*, 2007]. Similar to the protein-water coupling, it is not clear if the influence of water dynamics on membrane dynamics is significant enough to control the function of the membrane. If it is not significant,

what makes water dynamics a good predictor of membrane structure and topology is a topic of active research. The atomistic details of dynamic coupling between chemically confined hydration water and lipid interaction sites are still remain inconclusive. Controlling factors of heterogeneous distributions of hydration water near membrane surfaces leading to dynamical heterogeneities are not clearly understood.

Thus, in this chapter, we attempt to understand the coupling of hydration water and membrane dynamics by probing the membrane behavior from the hydrophobic core towards the hydrophilic region employing all atom molecular dynamics simulations. We calculate two dimensional mean square displacements, one dimensional van Hove Correlation functions of lipid components and interface water molecules on the membrane surface. van Hove correlation functions examine the presence of dynamical heterogeneity in both water molecules and the lipid bilayer at fluid phase. Earlier simulations have shown that lipid molecules exhibit dynamical heterogeneity in a membrane at L_β phase due to the presence of different mobility groups [Shafique *et al.*, 2016]. Dynamical heterogeneities have been observed in a binary lipid cholesterol membrane and even in a fluid membrane in absence of cholesterol on the scale of $80 - 150$ nm [Sarangi *et al.*, 2017; Roobala and K., 2017]. However, these results do not provide the correlations between local dynamics of membrane and the neighboring water dynamics contributing towards dynamical heterogeneity. To understand the origin of dynamical heterogeneity in the interface water under the influence of lipid molecules, we calculate probability distribution of logarithm of translational displacements. The probability distributions are calculated for different times for both lipids and water molecules to check the presence of a bimodal behavior. The bimodal behavior manifests intermittent dynamics in solute motion and can play a dominant role on Fickian and non-Gaussian behavior [Acharya *et al.*, 2017]. Colloidal systems are found to exhibit similar dynamics in crowded environments [Kwon *et al.*, 2014]. Representative trajectories of an interface water and a lipid molecule are plotted showing the presence of translational jump from one hydrogen bonded lipid partner to the other. Two dimensional self intermediate scattering functions are calculated for both lipid and interface water molecules on the bilayer surface. Multiple relaxation time scales present in the lipid molecules and the interface water are quantified. Correlations between relaxation times of lipid and interface water molecules are analyzed. These systematic analyses highlight the role of lipid moieties on the coupling or decoupling of interface water relaxations at multiple time-scales. Our results enhance the fundamental understanding on the influence of membrane dynamics on hydration layer dynamics which have future implications on sensing membrane functions due to external perturbations or chemical binding.

5.2 SIMULATION DETAILS

All atom molecular dynamics simulations are carried out for 128 DMPC lipid molecules fully hydrated with 5743 TIP4P/2005 [Abascal and Vega, 2005] water molecules. Thus ~ 45 water molecules per lipid are present which suffice the hydration number for DMPC as reported earlier in experiments [Lopez *et al.*, 2004; Zhao *et al.*, 2008; Trapp *et al.*, 2010]. DMPC force field parameters are obtained using Berger united atom force fields [Berger *et al.*, 1997; Cordomí *et al.*, 2012]. Berger force fields in combination with TIP4P/2005 water model is found to be suitable in calculating heterogeneity in the structure and dynamics of water near a membrane [Srivastava *et al.*, 2019b]. An NPT simulation is carried out for 100 ns with a 2 fs time step and 200 ps saving frequency. The bilayer is equilibrated at 308 K temperature using velocity rescaling method [Bussi *et al.*, 2007] with a 0.5 ps coupling constant. Pressure of 1 bar is maintained using Berendsen pressure coupling method [Berendsen *et al.*, 1984b] with a 0.1 ps coupling constant and compressibility of 4.5×10^{-5} bar^{-1}. van der Waals interactions are cutoff at 1 nm. Particle mesh Ewald method [Allen and Tildesley, 1987; Darden *et al.*, 1993; Essmann *et al.*, 1995b] is applied with a 0.12 nm grid size for corrections in long range interactions. Periodic boundary conditions are applied in all three directions. Bonds are kept constant using LINCS [Hess *et al.*, 1997] algorithm. Next, an NVT run

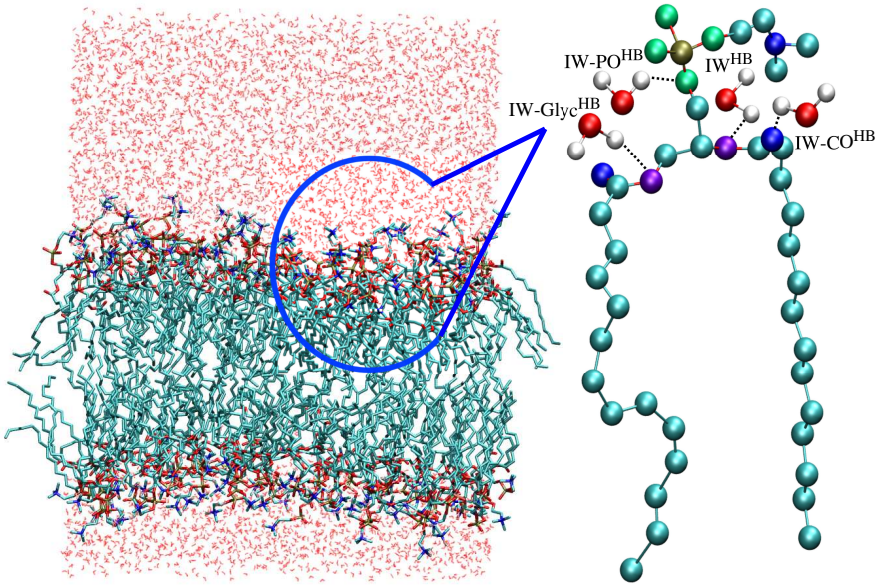

Figure 5.1: Snapshot of a hydrated DMPC bilayer and a DMPC molecule in presence of IW^{HB} molecules hydrogen bonded to lipid moieties residing near N head-groups.

is carried out for 20 ns with a 0.4 fs time step and a 10 fs saving frequency. Temperature and pressure coupling parameters, long and short range distance corrections are kept same for the NPT run. Box lengths of the bilayer are 6.24 nm in x and y and 7.95 nm in z direction. 10 sets of uncorrelated runs each with 1 ns run-length is used for the calculations of water dynamics. Each result is obtained by averaging over 10 uncorrelated blocks of data each with 10, 000 frames using in-house codes.
We also simulate bulk water (BW) using TIP4P/2005 water model consisting of 851 water molecules at 308 K temperature as discussed in the previous chapter. All simulations are performed with GROMACS-4.6.5 [Bekker *et al.*, 1993; Berendsen *et al.*, 1995; Lindahl *et al.*, 2001; Spoel *et al.*, 2005; Hess *et al.*, 2008] software package.

5.3 MEMBRANE DYNAMICS

For probing membrane dynamics, different lipid moieties are identified based on hydrophilic and hydrophobic characteristics exhibited by the lipids. The head-group hydrophilic moieties are N_{Head} (nitrogen), $Carb_{Head}$ (carbonyl carbons), $Glyc_{Head}$ (glycerol carbons) and P_{Head} (phosphorus). Hydrophobic alkyl chains are referred to as $B1_{Tail}$, $B2_{Tail}$ and $B3_{Tail}$. A snapshot of DMPC beads is shown in figure 5.2. For calculating dynamical properties, center of mass of same moiety from two hydrophobic alkyl chains of a DMPC molecule is considered. Interface water molecules are identified based on the geometric criteria of their proximity of ± 0.3 nm from the nitrogen head-group of DMPC and referred to as IW^{HB}. If a IW^{HB} is hydrogen bonded to phosphate or carbonyl or glycerol oxygens for even a single time frame during its confinement time, the molecule is referred to as IW-PO^{HB}, IW-CO^{HB} and IW-Glyc^{HB} respectively. these are identified in a similar way as mentioned in chapter 3, section 3.3. Density profiles for all classes of IW^{HB} exhibit restrained behavior near N head-group of DMPC for 100 ps confinement lifetime (figure 5.3 a)). The density profiles of IW^{HB} indicate that IW-PO^{HB}, IW-CO^{HB}, IW-Glyc^{HB} form hydrogen bonds to P, Carb and Glyc oxygens by residing close to the Nitrogen head-group density as they do not change their locations near the HB partners. Less associations of all classes of IW^{HB} near hydrophilic region are observed for 1 ns while more association of water near the head was found

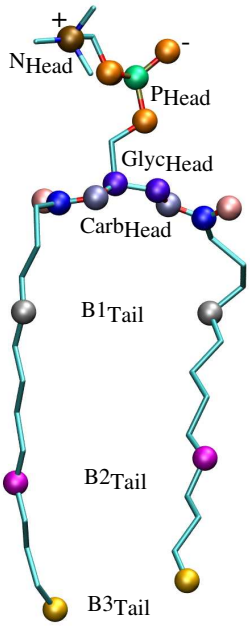

Figure 5.2: Hydrophilic and hydrophobic beads of a DMPC molecule for which dynamical calculations are performed. Color codes: VDW Ochre - Nitrogen (N_{Head}), Green - Phosphorus (P_{Head}), Orange - Oxygen atoms associated with phosphate group, Pink - Oxygen atoms of carbonyl moiety, Ice blue - Oxygen atoms of glycerol moiety, Violet - Carbon atoms of glycerol moiety ($Glyc_{Head}$), Blue - Carbon atoms of carbonyl moiety ($Carb_{Head}$), Silver - $B1_{Tail}$, Magenta - $B2_{tail}$ and Orange - $B3_{Tail}$.

for 100 ps. The molecules tend to diffuse into the bulk region from the hydrophilic head group regime when the density profiles are calculated for 1 ns (figure 5.3 b))

5.4 TRANSLATIONAL MEAN SQUARE DISPLACEMENT

For quantifying translational dynamics, we first calculate 2D translational mean square displacements (MSD_{XY}) of IW^{HB} and DMPC beads using equation 2.1. Figure 5.4 shows translational mean square displacement (MSD_{XY}) on the bilayer XY surface for DMPC beads and IW^{HB}. Bulk water molecules (BW) reach diffusive regime much faster ($\sim$ 10 ps) than that of IW^{HB}. IW^{HB} molecules enter into the diffusive regime with a diffusion exponent of $\sim$ 0.98 (figure 5.4) at $\sim$ 80 ps which is close to its confinement lifetime. They enter in the sub-diffusive regime within $\sim 5 - 10$ ps. (table 5.1). The lipid components reach similar values of MSD_{XY} at much later time $\sim 100 - 300$ ps (table 5.2). Interestingly, MSD_{XY} of lipid components increase from head-groups to tail (figure 5.4). $B3_{Tail}$ has the highest MSD_{XY} among all components of lipids although $B3_{Tail}$ situates at the midplane of the hydrophobic bilayer. This signifies that the translational motion of the end beads of the hydrophobic tails are faster than the heads since the alkyl tails are not hydrogen bonded. The behavior of MSD_{XY} of carbon and oxygens of Carb/Glyc and P and oxygens of PO show very similar sub-diffusive trends. MSD_{XY} of carbon and oxygen atoms of same moieties are calculated to check the effect of mass on MSD_{XY}. The MSD_{XY} of Glyc is slowest among all components of lipids. MSD_{XY} of IW^{HB} have been shown in figure 5.5. IW^{HB} do not show any significant difference in MSD_{XY} when identified based on their hydrogen bond partners such as IW-PO^{HB}, IW-CO^{HB} and IW-$Glyc^{HB}$ (inset in figure 5.5).
For gaining deeper insights on translational mobility of hydrogen bonded interfacial waters, retardation factor (RF) is calculated for all DMPC beads as well as for all classes of IW^{HB} which are

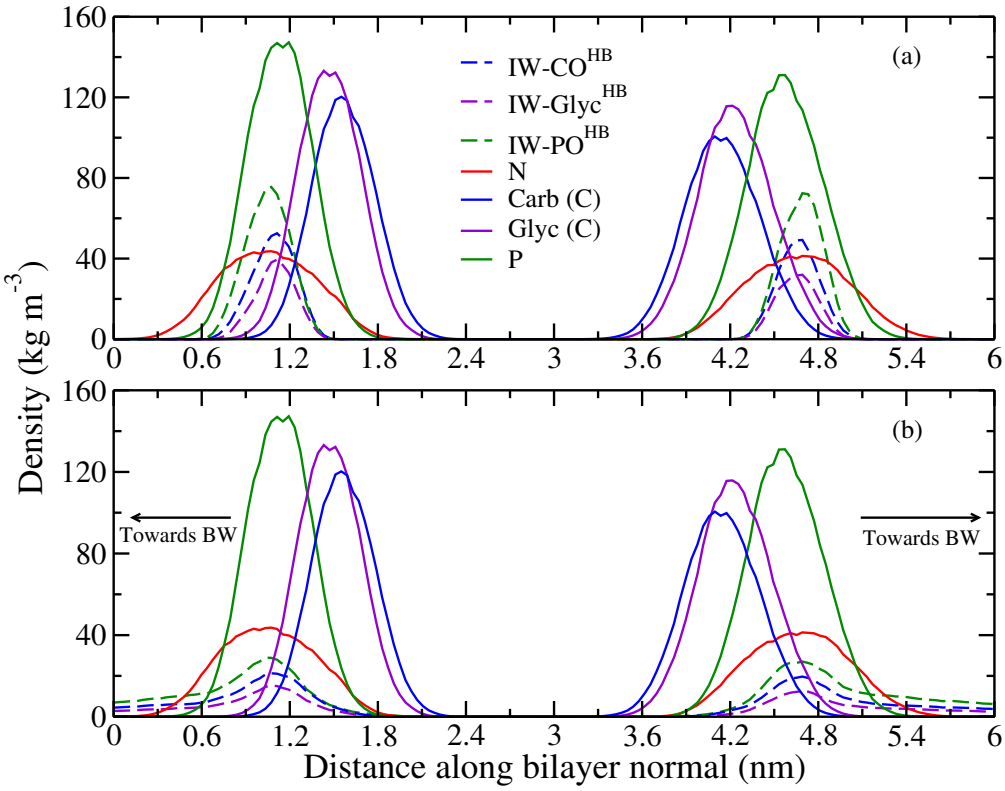

Figure 5.3: Density profiles of DMPC lipids and all classes of IW^{HB} along the bilayer normal. Density profiles of all classes of IW^{HB} are averaged over a) 100 ps and b) 1 ns.

averaged over 10 sets of uncorrelated data each of 1 ns run length. Retardation factor measures the slow down in mobility of solute with respect to the solvent [Abseher *et al.*, 1996; Franck *et al.*, 2015; Braun *et al.*, 2016; Barnes *et al.*, 2017; Dahanayake and Mitchell-Koch, 2018b]. RF is calculated as $\frac{MSD_{XY}(BW)}{MSD_{XY}(Lipid)}$ for DMPC and $\frac{MSD_{XY}(BW)}{MSD_{XY}(IW)}$ for IW^{HB}. For $MSD_{XY}(Lipid)$, COM of lipid is considered for MSD calculation. Figure 5.6 a) shows that Glyc. moiety of lipids have maximum RF followed by a decrease in RF as moving from P to N moieties of the lipid heads. This confirms a lowering in retardation of lipid moieties facing the outer most water regime. However, RF for all classes of IW^{HB} do not differ significantly as all of these IW^{HB} are confined near the N head-group and then form hydrogen bonds to the other lipid moieties. Ratio of retardation factors of lipids with respect to IW^{HB} are shown in figure 5.6 b). Glyc moiety buried deep in the hydrophobic core of the lipid show maximum retardation with respect to the IW-$Glyc^{HB}$ molecules. Since RF of different classes of IW^{HB} do not differ much, the ratio of RF of lipid to IW^{HB} follow similar trend as the RF of lipids.

5.5 TRANSLATIONAL VAN HOVE CORRELATION

For investigating heterogeneous dynamics on the bilayer surface, self part of one dimensional (1D) van Hove correlation function is calculated for all classes of IW^{HB} corresponding to time scales mentioned in table 5.1. Similarly, 1D van Hove correlation functions of DMPC are calculated for a time scale mentioned in table 5.2. It is to be noted that at these time scales, all classes of IW^{HB} and lipid moieties are still in sub-diffusive regime as mentioned in figure 5.5. Tails of lipids viz. $B1_{Tail}$, $B2_{Tail}$ and $B3_{Tail}$ deviate minimum from Gaussianity while maximum deviations from Gaussianity are observed for lipid heads (figure 5.7). On approaching the lipid-water from the hydrophobic core of lipids, deviations from Gaussianity are found to decrease (figure 5.8). Emergence of

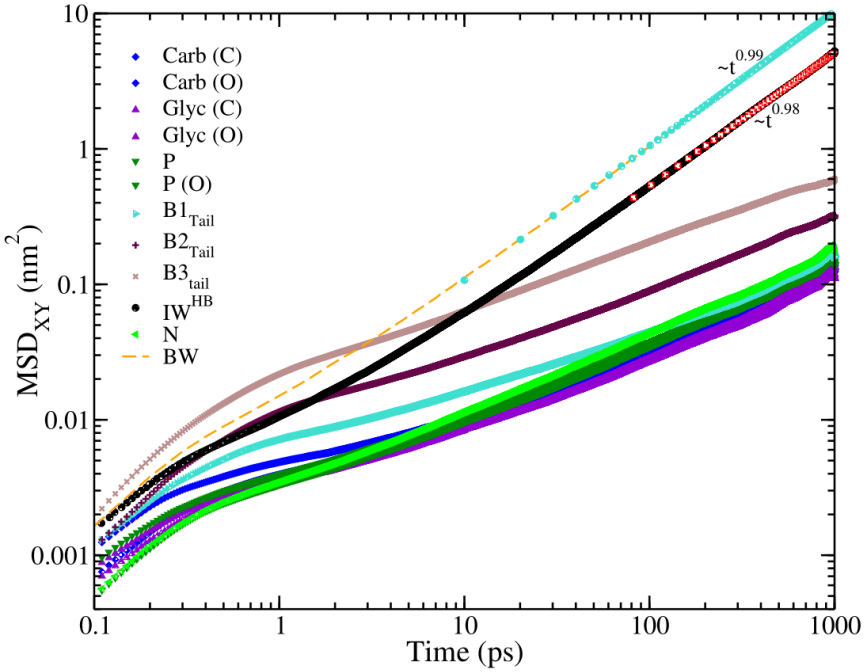

Figure 5.4: Two dimensional translational mean square displacement (MSD_{XY}) of all beads of DMPC, IW^{HB} and BW.

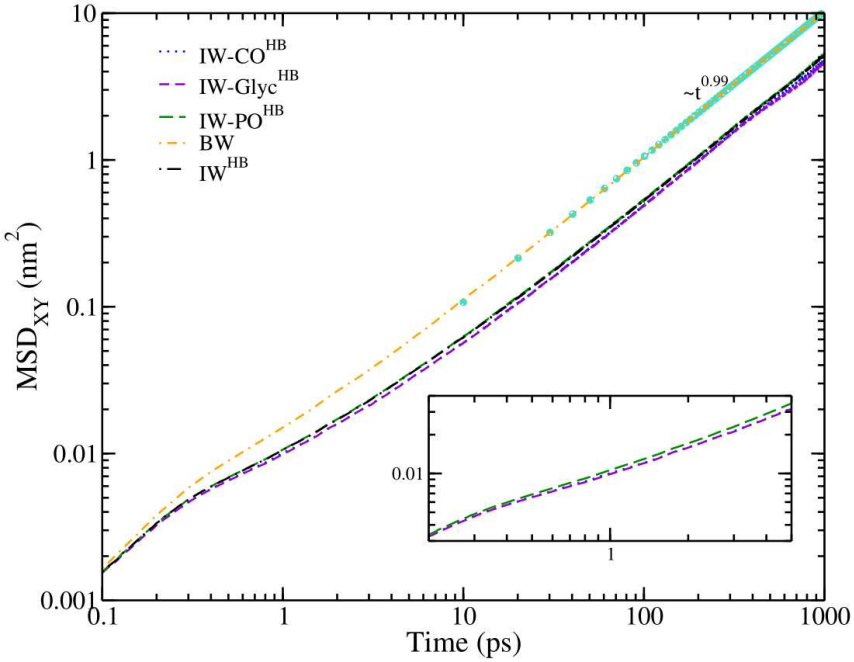

Figure 5.5: Two dimensional translational mean square displacement (MSD_{XY}) of all classes of IW^{HB} and BW. Inset: different classes of IW^{HB} show similar MSD_{XY}.

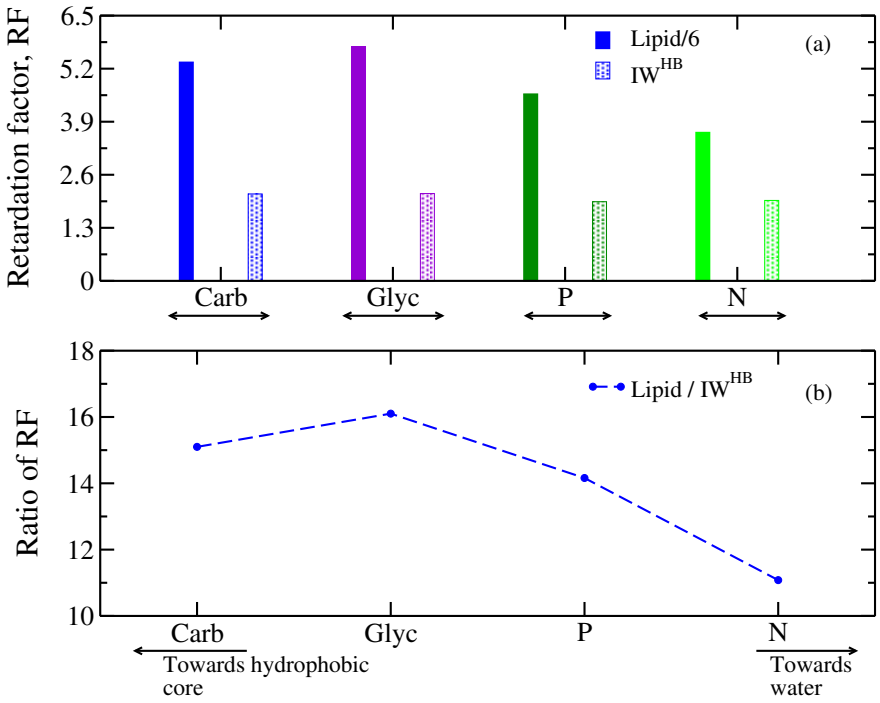

Figure 5.6: a) Retardation factor calculated for DMPC lipid moieties and IW^{HB} with respect to BW. Glyc beads show maximum retardation due to its buried nature in hydrophobic core. b) Ratio of RF showing retardation of lipids with respect to IW^{HB}. The ratio is maximum for Glyc moiety followed by a decrease from Carb to P to N.

non-Gaussianity in one dimensional van Hove correlation function is a universal feature of dynamical heterogeneity [Hove, 1954; Kegel and van Blaaderen, 2000; Puertas *et al.*, 2004; Chaudhuri *et al.*, 2007; Sengupta and Karmakar, 2014; Jaiswal *et al.*, 2015]. The heterogeneous behavior of IW^{HB} is due to their chemically confined nature. Non-Gaussianity in van Hove correlation function of lipid beads decreases as moving towards hydrophobic alkyl chains of the DMPC. $B3_{Tail}$ and N bead of the DMPC manifest least and strong deviations from Gaussianity respectively (figure 5.7). The maximum deviations of IW^{HB} hydrogen bonded to Glyc closer to the deep hydrophobic core and less deviations of lipid Glyc. components from Gaussianity with sub-diffusive dynamics are puzzling and contradictory at the first glance. According to the law of Brownian motion, a solute particle moving through a medium follows the theory of random walk. If the solute particle follows Fickian or diffusive behavior, the probability displacements of the particles should be Gaussian in nature [Einstein, 1906]. However recent report shows that particles with diffusing diffusivity in a crowded medium can have Fickian diffusion with non-Gaussian probability distributions in displacements [Jain and Sebastian, 2016]. So Fickian MSD_{XY} with prominent non-Gaussianity in G_s(x,t) of IW^{HB} and sub-linearity in MSD_{XY} with less non-Gaussian G_s(x,t) in lipid components need special attention and further analysis. These features confirm that MSD_{XY} is not a good measure to understand the laws of Brownian motion originally derived for motion of a solute through a medium. To understand the underlying phenomenon, $P(log_{10}(r(t))) = 4\pi r^3 ln(10) G_s(r,t)$ is calculated and shown in figure 5.9. For bulk water, the value of the most probable distribution of $P(\log_{10}r(t)) \approx 2.13$ at time 45 ps. This clearly indicates that the BW molecules follow Gaussian distributions with Fickian dynamics. A departure from the value 2.13 indicates deviations from Gaussianity [Acharya *et al.*, 2017]. The value of the distribution for the IW^{HB} is much lower than 2.13 with highly non-Gaussian probability distribution at 5.12 ps because the IW^{HB} molecules are at sub-diffusive regime at that time. At a later time of 78.7 ps, IW^{HB} molecules reach the linear behavior in MSD_{XY}, but have a very distinct bi-modal nature characterizing intermittency in dynamics of IW^{HB}. Similar intermittent dynamics is common in supercooled liquids due to

domain formation. In the case of IW^{HB}, there is no domain formation, but IW^{HB} molecules are still stuck at a transient cage formed by the lipid head-groups for some time and then hop or jump from there to another transient cage leading to intermittency in dynamics. At a much longer time (at 154) ps which is ~ 4 times the value of diffusive time, the bi-modal nature still persists. At 610 ps, the peak of $P(\log_{10}r(t))$ of IW^{HB} shifts to the right hand side in figure 5.9. Although the bimodal nature is not retained, the peak value is much lower than 2.13. The time evolution of $P(\log_{10}r(t))$ of IW^{HB} does not lead to Gaussian behavior even at ~ 7.7 times of diffusive limiting time. The probability distribution is calculated for a lipid head (P) to check the correlation between membrane and IW^{HB} dynamics. Time evolution of $P(\log_{10}r(t))$ of P lipid head does not show much changes in their behavior within 200 ps indicating very slow dynamics of P lipid heads compared to the IW^{HB}. The peak value of $P(\log_{10}r(t))$ of the lipid is close to 2.13 and consistent with less deviations from Gaussianity in their $G_s(x,t)$. The less deviations from Gaussianity probably originate from their vibrations in the cage formed by the neighboring lipid heads. The time evolution of $P(\log_{10}r(t))$ for both IW^{HB} and lipid head P, clearly demonstrate the presence of intermittency in IW^{HB} dynamics and the absence of perfect coupling in lipid and IW^{HB} dynamics via same relaxation time scales throughout the entire observation time period.

The intermittency in dynamics of IW^{HB} and the imperfect coupling of lipids and IW^{HB} are clearly observed when a trajectory of a single IW^{HB} molecule is plotted and shown in figure 5.10. The trajectories of single IW^{HB} molecule and two lipid head-groups, viz. Carb and P are shown. The trajectories of the IW^{HB}, Carb, and P of lipids are shown in black, blue and green respectively. The trajectory of the IW^{HB} molecule shows the presence of three sticky segments S1, S2 and S3. The IW^{HB} molecule transiently spends some time in each sticky segment followed by a translational jump from one segment to another. This is a clear manifestation of intermittency in dynamics of IW^{HB}. The IW^{HB} molecule is hydrogen bonded to the carbonyl (Carb) oxygen of a lipid molecule while residing in the segment S1 as shown in figure 5.10. After it resides in the transient cage of S1, it jumps from S1 to S2 and form a hydrogen bond to the P oxygen of another lipid molecule and reside in that transient cage S2. After some time, the IW^{HB} molecule again jumps from segment S2 to S3. Similar translational jump has been found to be the origin of decoupling between translational diffusion and viscosity in supercooled bulk water molecules [Dueby *et al.*, 2019]. While the IW^{HB} molecule jumps from S1 to S2 to S3 after residing at each segment or cage for a small duration, the hydrogen bonded lipid partners do not move or jump coherently with the IW^{HB} molecule. Instead they remain stationary near the respective segments for more time and then move after a time lag. This clearly shows that the IW^{HB} and the lipid molecules in the membrane do not obey the concept of perfect coupling. Perfect coupling exists if the relaxation dynamics of two or more processes are occurring on the same time scale. For instance, in proteins, fluctuations in the bulk water are coupled with large scale motion of proteins. The internal motion of proteins are coupled with β-relaxations of the hydration water [Frauenfelder *et al.*, 2009]. Similarly, for membranes, hydration water dynamics and membrane dynamics should be of the same order. However, it is reported that lower temperatures, the concept of perfect coupling no longer holds valid and hydration water dynamics and membrane/protein dynamics are decoupled [Wood *et al.*, 2007; Benedetto, 2017]. The coupling between IW^{HB} and lipids occur with some scaling factor which is discussed later.

Table 5.1: Time of entrance to the sub-diffusive regime for different classes of IW^{HB} as obtained from 10 sets of MSD_{XY}.

Beads	Δt_1 (ps)	Δt_2 (ps)	Δt_3 (ps)	Δt_4 (ps)	Δt_5 (ps)	Δt_6 (ps)	Δt_7 (ps)	Δt_8 (ps)	Δt_9 (ps)	Δt_{10} (ps)
IW^{HB}	6.07	5.11	5.75	6.51	5.02	5.08	7.86	5.51	6.58	5.37
IW-CO^{HB}	6.94	5.93	6.22	7.06	5.71	5.56	8.56	5.68	6.70	6.03
IW-$Glyc^{HB}$	6.26	5.22	6.05	8.11	5.60	5.89	10.70	5.87	6.74	6.11
IW-PO^{HB}	6.14	5.06	5.74	6.46	3.73	5.10	7.44	5.45	6.34	5.31

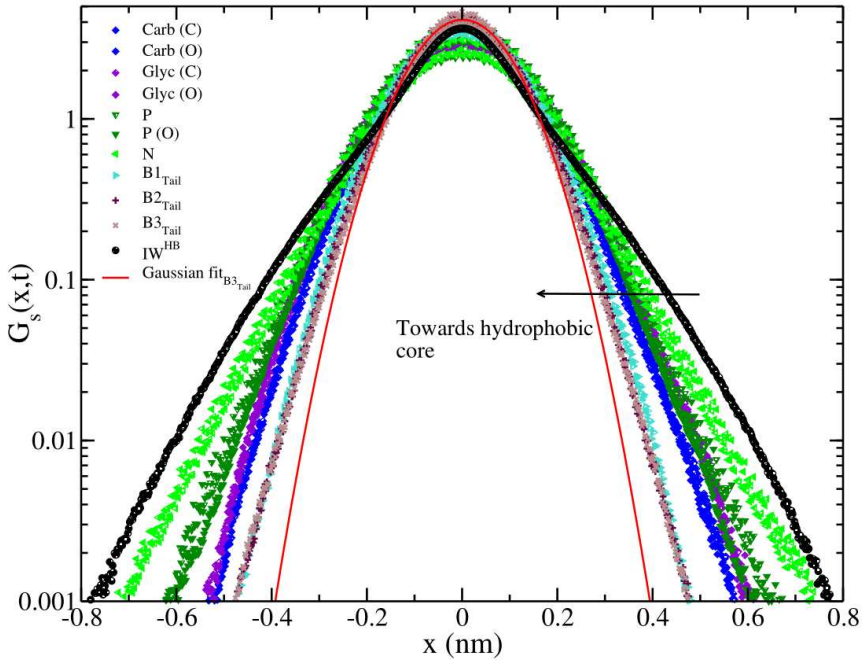

Figure 5.7: One dimensional van Hove correlation function of DMPC beads and IW^{HB}. End beads of lipid tails have minimum deviations from Gaussianity.

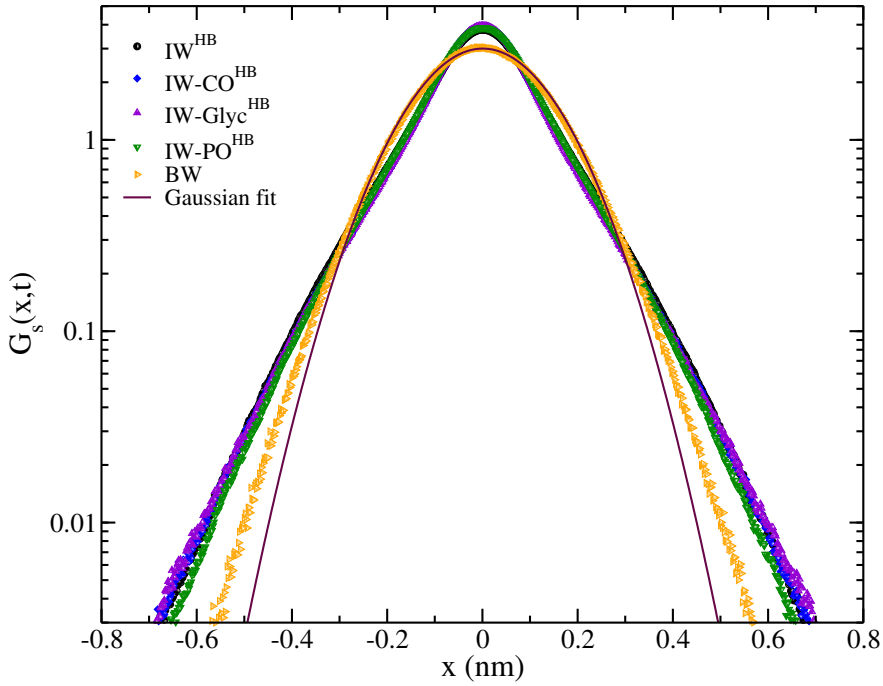

Figure 5.8: One dimensional van Hove correlation function of all classes of IW^{HB}. IW-PO^{HB} close to the lipid-water interface have minimum deviations from Gaussianity.

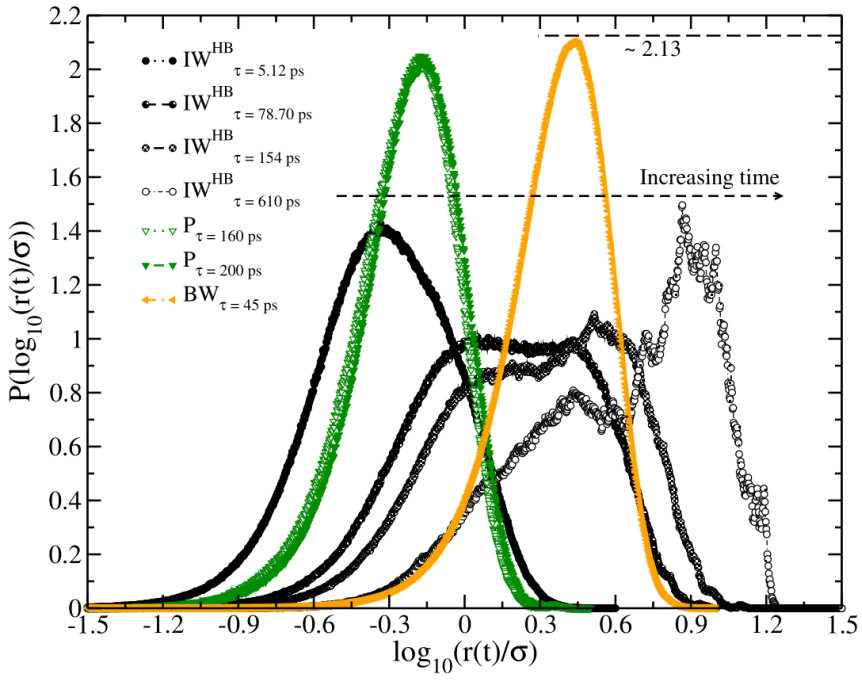

Figure 5.9: Time evolution of P ($\log_{10}(r(t)/\sigma)$) of IW^{HB}, P (phosphate) and BW. The peak of BW at $\sim$ 2.13 corresponds to Gaussianity. IW^{HB} molecules reveal a bimodal nature characterizing presence of intermittency at a time scale when Fickian dynamics is followed.

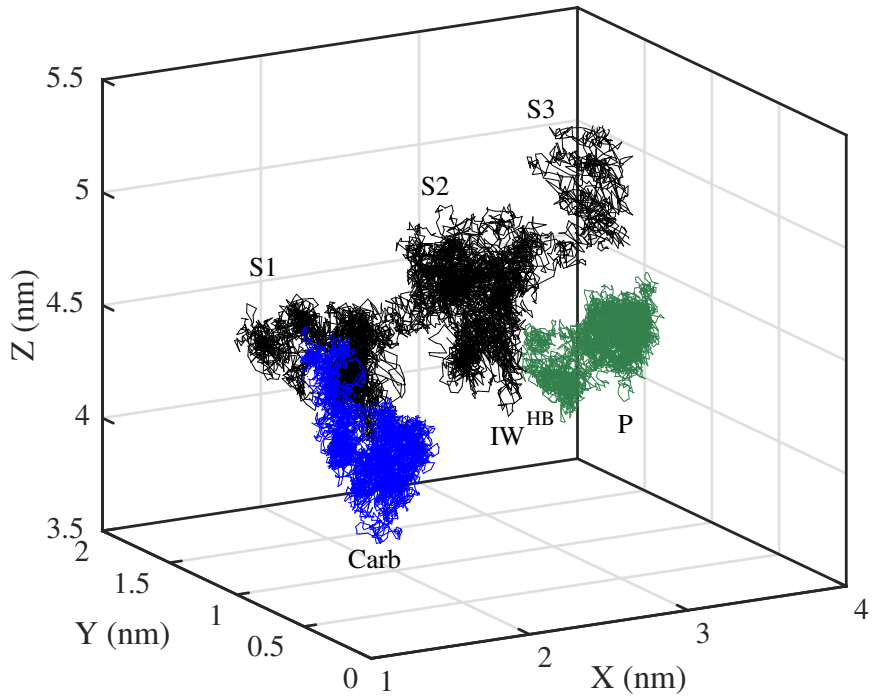

Figure 5.10: Trajectory of an atom of IW^{HB}, carbonyl carbon (Carb) and phosphorus (P) for 1 ns run length. S1, S2 and S3 represent three segments of the IW^{HB} trajectory showing three regions with consequent hopping from one region to the other. IW^{HB} remains hydrogen bonded to oxygens of Carb and P in these regions.

Table 5.2: Time of entrance to the sub-diffusive regime of DMPC beads as obtained from average of 10 sets of MSD_{XY}.

Beads	Δ t (ps)
Carb $(C)_{Head}$	156.32 ± 37.64
Carb $(O)_{Head}$	160.56 ± 27.58
Glyc $(C)_{Head}$	201.40 ± 57.56
Glyc $(O)_{Head}$	201.50 ± 40.76
P_{Head}	131.90 ± 29.47
P $(O)_{Head}$	119.67 ± 15.35
N_{Head}	81.34 ± 6.19
$B1_{Tail}$	79.33 ± 7.07
$B2_{Tail}$	18.99 ± 0.47
$B3_{Tail}$	2.93 ± 0.09

5.6 SELF INTERMEDIATE SCATTERING FUNCTION

Self intermediate scattering function (SISF) is another universal feature characterizing dynamical heterogeneities. Two dimensional SISF on the bilayer surface is calculated by equation 1.2. For quantifying membrane and IW heterogeneity, SISF are calculated for all moieties of DMPC lipids and IW^{HB} at $\lambda = 0.60$ nm for a run-length of 10 ns (figure 5.11). As the first peaks of g(r) are at ~ 0.3 nm and 0.9 nm for $IW^{HB}$and N head of DMPC respectively, an intermediate wavelength, $\lambda = 0.60$ nm, is chosen to calculate SISF. Tails (B1, B2, B3) of the lipids relax faster than the head-groups (Carb, Glyc, P) of the lipids. Since there are no IW^{HB} in the midplane of the bilayer, tails of the lipids get free space for flexible motion and at the same time no hydrogen bonds can restrict their motion. SISF of carbon oxygen and phosphorus oxygen of the same moiety show similar behavior. SISF of lipid moieties are fitted with Kohlrausch-William-Watt (KWW) function (4.1). The fitted parameters, f_Q, τ_s, τ_α, β_α are listed in table 5.3. SISF of IW-CO/PO/Glyc hydrogen bonded to different moieties of lipid head groups are shown in figure 5.12 after averaging over 10 blocks of data sets each with a run-length of 1 ns. In compared with the BW, all IW^{HB} relax much slower where IW-CO^{HB}/$Glyc^{HB}$ buried most in the hydrophobic core relax slowest. F_s(q,t) of IW-PO^{HB} and IW-CO^{HB}/$Glyc^{HB}$ show small differences in relaxations. However, SISF of IW^{HB} are not fit to the KWW function due to the appearance of long time tails τ_l. Similar long time tail has been identified earlier for interface water molecules near proteins and lipids [Marzio *et al.*, 2016; Srivastava *et al.*, 2019a]. F_s(q,t) of IW^{HB} are fitted with equation 4.2. The fitted parameters are mentioned in Table 5.4.

5.7 CORRELATIONS IN LIPID AND IW DYNAMICS

In order to understand the coupling between IW^{HB} and lipid relaxations, τ_s of both lipids and IW^{HB} are plotted in figure 5.13 a). τ_s of lipids decrease from Carb to Glyc to P to N as N is the outermost head group facing bulk water and thus is most mobile. However, τ_s of IW^{HB} does not follow similar trend as moving from inner core towards the outer surface. Note, that the values of τ_s are in the sub-ps range and therefore the differences in τ_s between various classes of IW^{HB} are also very small. To measure the extent of coupling between the fast relaxations of lipids and IW^{HB}, $\frac{\tau_s(lipid)}{\tau_s(IW)}$ is plotted in figure 5.13 b). For all classes of IW^{HB}, the ratios decrease from Carb to Glyc to P to N and the ratio is ~ 1.1 for N. This suggests that the fast relaxations of all classes of IW^{HB} and respective lipid moieties occur at very similar time scale. The fastest relaxations are strongly coupled because both IW^{HB} and respective lipid moieties vibrate in the local cage formed by the nearest neighbors and regionally relax together.

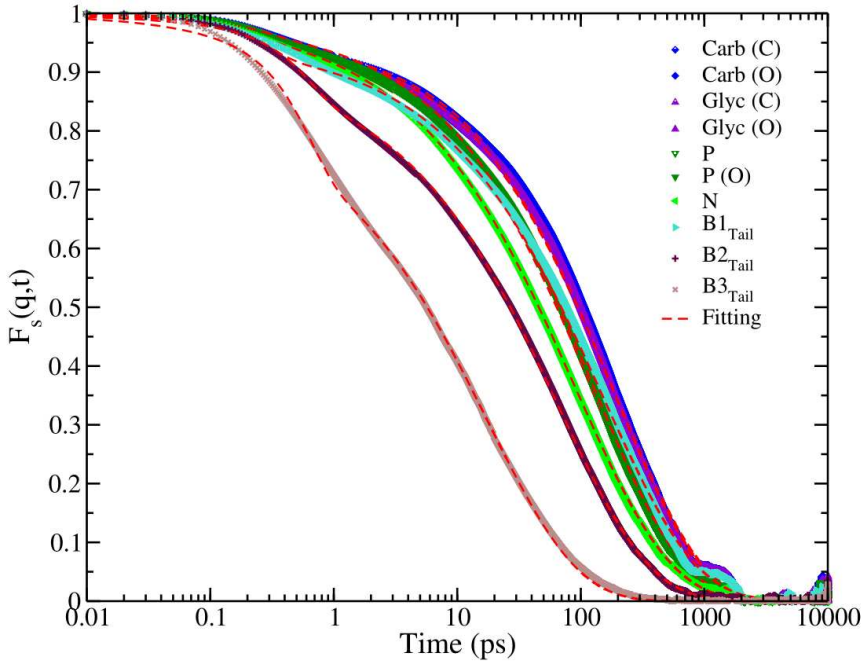

Figure 5.11: SISF of different beads of DMPC lipids for $\lambda = 0.60$ nm. Two ends of a lipid chain relax faster compared to the moieties situated in the middle.

Table 5.3: Fitted parameters of SISF of different moieties of DMPC molecule for $\lambda = 0.60$ nm along the chain. All correlation coefficients are >0.99.

Region	τ_s (ps)	f_Q	τ_α (ps)	β_α
N $_{\text{Head}}$	0.29	0.97	91.65	0.57
P $_{\text{Head}}$	0.31	0.98	124.75	0.60
P (O)$_{\text{Head}}$	0.31	0.98	129.35	0.60
Carb (C)$_{\text{Head}}$	0.40	0.96	197.32	0.63
Carb (O)$_{\text{Head}}$	0.40	0.95	189.06	0.63
Glyc (C)$_{\text{Head}}$	0.33	0.97	179.91	0.62
Glyc (O)$_{\text{Head}}$	0.33	0.96	186.33	0.62
B1$_{\text{Tail}}$	0.37	0.95	150.94	0.58
B2$_{\text{Tail}}$	0.71	0.90	66.89	0.59
B3$_{\text{Tail}}$	0.69	0.82	18.32	0.58

Table 5.4: Fitted parameters of SISF of all classes of IW^{HB} for $\lambda = 0.60$ nm. Correlation coefficients are >0.99.

Region	τ_s (ps)	f_Q	τ_α (ps)	β_α	$f_{Q'}$	τ_l (ps)	β_l
IW^{HB}	0.24	0.50	3.49	0.91	0.45	43.00	0.62
IW-CO^{HB}	0.25	0.36	4.03	0.94	0.59	31.54	0.53
IW-Glyc^{HB}	0.22	0.33	3.90	0.99	0.64	30.64	0.54
IW-PO^{HB}	0.21	0.41	3.40	0.93	0.58	24.42	0.51
BW	0.10	0.90	3.54	0.94			

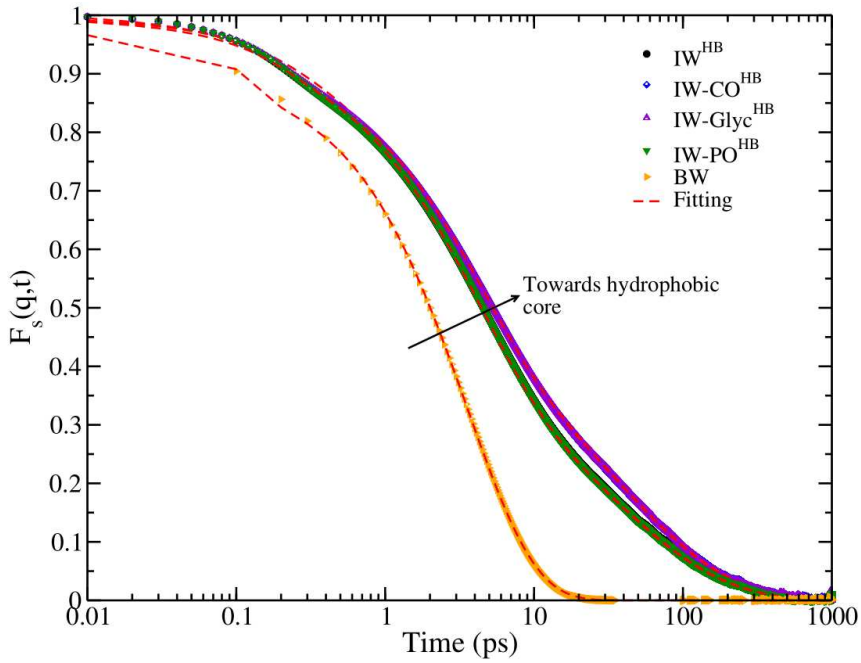

Figure 5.12: SISF for all classes of IW^{HB} at $\lambda = 0.60$ nm. IW-$Glyc^{HB}$ molecules buried deep in the hydrophobic core relax slowest.

A comparison of τ_α of lipids and IW^{HB} is shown in figure 5.14 a). τ_α of all classes of IW^{HB} and the respective lipid moieties decrease coherently from Carb to Glyc to P to N as reaching the outermost water like the BW. The ratio of the respective τ_α of lipid and IW^{HB} (figure 5.14 b) decreases following similar trend. Since the ratio ranges between $20 - 50$, τ_α of the lipid moieties and the respective IW^{HB} do not relax at the same time and not follow perfect coupling, but correlated by a scaling factor. To understand if the slowest dynamics of lipid and IW^{HB} are coupled or not, the slowest relaxation times of both lipids and IW^{HB} are plotted in figure 5.15 a). Since lipids do not have additional τ_l as the IW^{HB}, τ_α of lipids are compared with τ_l of IW^{HB}. τ_α of lipids become faster from Carb to Glyc to P to N as lipid moieties become more mobile towards lipid-water interface facing outermost water molecules. To understand the extent of correlations between the slowest dynamics of lipids and IW^{HB}, ratios of τ_l to τ_α are plotted in figure 5.15 b). Since the relaxations of different classes of IW^{HB} do not differ much, the ratios follow similar trend as the lipid head-groups. The ratio is closest to 1 for N facing outermost water molecules. More imperfect is the coupling, the ratio deviates more from 1. Since the lipid moieties are geometrically more constraint compared to the IW^{HB}, they move much slower compared to the IW^{HB} molecules and can not have perfectly coupled relaxations occurring at the same timescale as the confined IW^{HB} molecules. The long time relaxation obtained from SISF can also be characterized by the time SISF reaches value of $\frac{1}{e}$ [Michele *et al.*, 2011; Flenner and Szamel, 2013; Kim and Saito, 2013; Kuon *et al.*, 2017] which is associated with the escape of the molecules from their respective cages. Ratio for $\frac{1}{e}$ relaxation of lipids and IW^{HB} follow the same trend as obtained from the fitting of the SISF (figure 5.15 b)). Although the slowest relaxations between IW^{HB} and lipids are not perfectly coupled (the ratio is not equal to 1), they are closest to 1 for the outermost N among different head moieties. Similar trend is followed for the ratios from τ_s, τ_α and τ_l.

To understand the regional dynamics of a lipid membrane and its coupling with the IW^{HB}, both lipid components and IW^{HB} molecules are colormapped in terms of the fastest and slowest relaxation times and shown in figure 5.16. The fastest relaxation times, τ_s, decrease from the tail to the head groups of the lipids. τ_s of the lipid heads are strongly coupled with the nearest interface water as evident from the similar color maps (figure 5.16 a)). However, the slowest relaxation times, τ_α, of

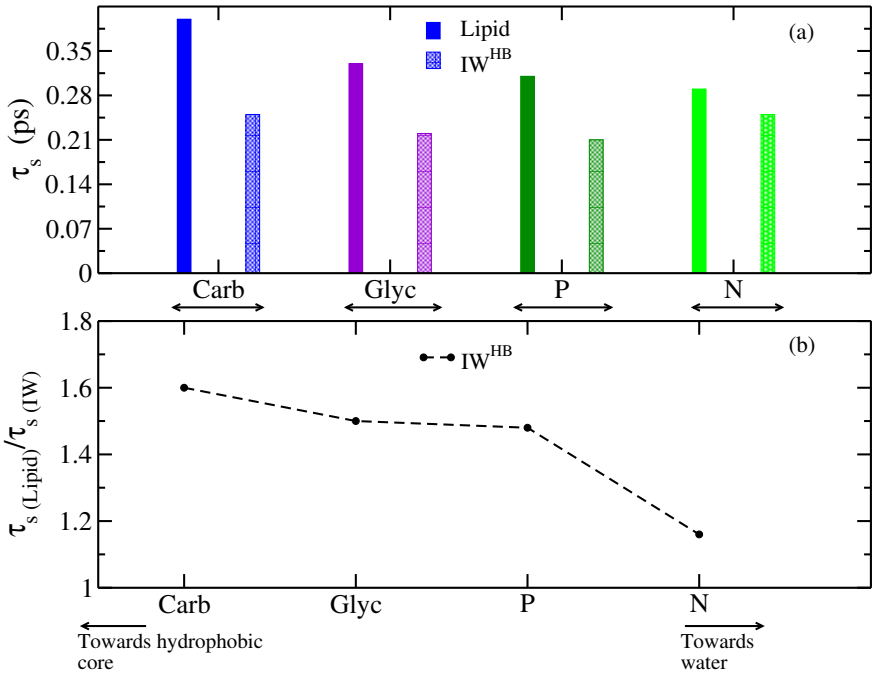

Figure 5.13: a) Shortest relaxation time scales, τ_s, are compared for the lipid head moieties and the IW^{HB} hydrogen bonded to the respective lipid heads. The values of τ_s are obtained in table 5.3 and 5.4. b) Ratio of τ_s of the lipid moieties and the IW^{HB}.

the lipids do not follow monotonic behavior from the tail to the head groups like their τ_s values. Instead the dynamics is fastest at both ends (head and tail) of the lipids and slowest in the middle (figure 5.16 b). The relaxation times of the lipid heads and the IW^{HB} confined close the head are correlated and therefore have close colormaps. The strong coupling in the fast relaxations as well as the correlations in the slow relaxations of the lipids and the confined IW^{HB} imply that the regional dynamics of different lipid head group moieties can be sensed by the respective IW^{HB} molecules. Therefore, any perturbation near lipid heads occurred by binding of a guest molecule should be monitored by the closest spatially resolved IW^{HB} dynamics. However the extents of correlations depend on the value of λ for which SISF is calculated. It has been observed that although the numerical values of the ratio of relaxation change with λ, the trend of coherent lipid and physically close IW^{HB} dynamics remains unaltered.

5.8 SUMMARY

In summary, the chapter investigates the complex multiple time-scale coupling between interface water and a lipid bilayer using all-atom molecular dynamics simulations at 308 K. Water molecules which reside in the interface layer located within ±3 Å away from the density of N head groups of the bilayer for a continuous time window of 100 ps are identified as IW^{HB}. The 100 ps time window is chosen for the confinement lifetime since the residence time of the IW^{HB} is $\sim$ 100 ps [Debnath *et al.*, 2010; Srivastava *et al.*, 2019a]. To understand the influence of the hydrogen bond on the coupling of the hydration layer and the bilayer these IW^{HB} are further classified based on their hydrogen bond partners, viz., P, Glyc, Carb and referred to as IW-PO^{HB}/$Glyc^{HB}$/CO^{HB} respectively. Previous experiments using SFG spectroscopy and molecular dynamics simulations reveal significance of similar chemically confined water molecules on the orientational or structural heterogeneity of interface water near cationic or anionic surfactant/lipid interfaces or zwitterionic phospholipids [Re *et al.*, 2014; Roy *et al.*, 2014; Ohto *et al.*, 2015; Inoue *et al.*, 2017; Cyran *et al.*,

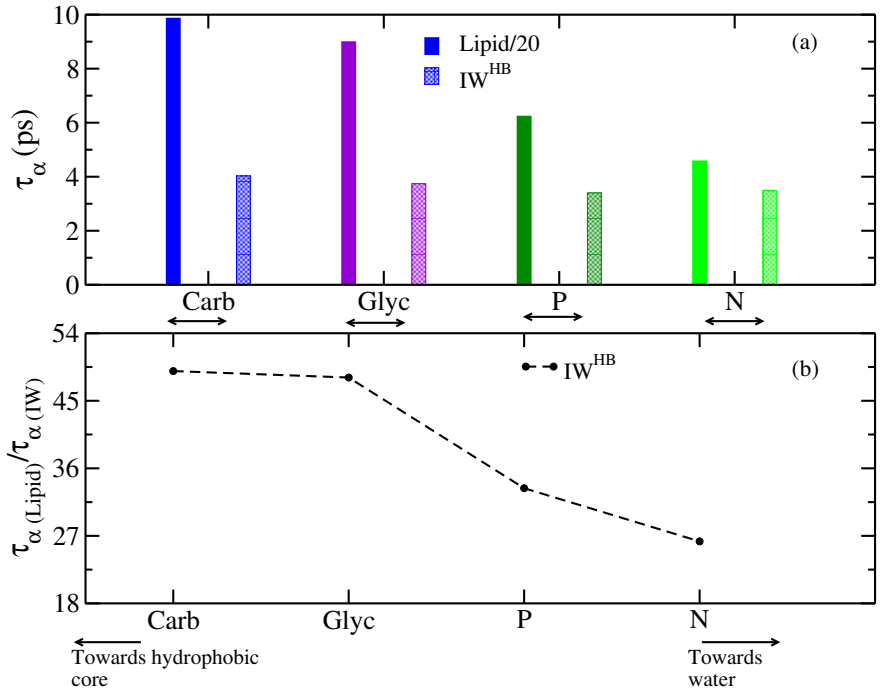

Figure 5.14: a) τ_α are compared for the lipid moieties and the IW. The values of τ_α are obtained from table 5.3 and 5.4. τ_α of lipids is divided by 20 for the clarity. b) Ratio of τ_α of the lipid moieties and the respective IW decreases as moving towards outer water.

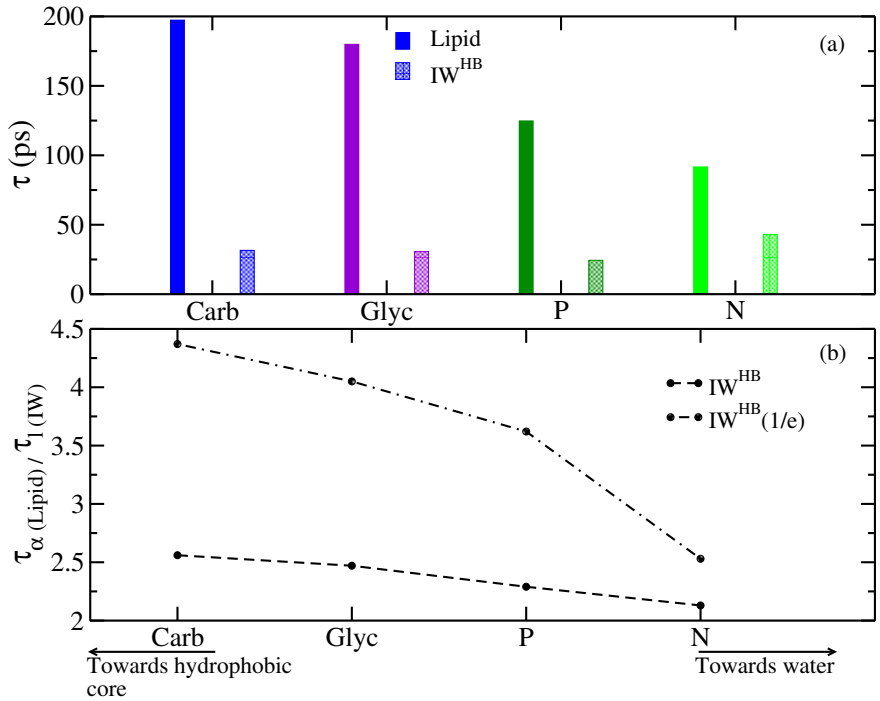

Figure 5.15: a) Slowest relaxation time scales are compared for lipid moieties (τ_α) and the IW^{HB} molecules (τ_l) hydrogen bonded to those lipid moieties. The time scales are obtained in table 5.3 and 5.4. b) Ratio of the slowest time-scales of the lipids and the IW obtained from SISF fitting and $\frac{1}{e}$ cut-off. τ_l of IW^{HB} obtained from $\frac{1}{e}$ is divided by 4.

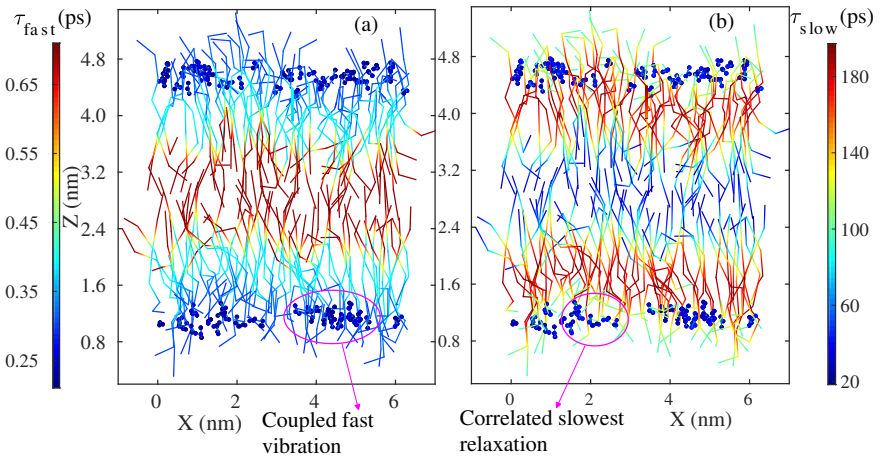

Figure 5.16: Colormap of a snapshot of a lipid bilayer and the IW^{HB} in terms of a) fast and b) relaxations for SISF calculated at $\lambda = 0.6$ nm for both DMPC and IW^{HB}. The fast relaxations are obtained from τ_s values in table 5.3 and 5.4. The slow relaxations for lipids and IW^{HB} are obtained from their τ_α (table 5.3) and τ_l (table 5.4) values respectively.

2018]. The retardation factors of the lipid head moieties decrease from the deeper hydrophobic side to the outermost water side.

The previous chapter discusses that the slow relaxations of IW^{HB} is originated from dynamical heterogeneity even at room temperature [Srivastava *et al.*, 2019a]. As the lipid components approach from the head to the tail lying on the midplane of the hydrophobic core, the van Hove correlation functions approach Gaussianity. The Gaussian distribution of the end tail beads are attributed to their flexible and less constraint mobility in the absence of IW^{HB}. On the other side, the distribution is non-Gaussian at the end head beads of lipids to which IW^{HB} molecules reside closest. Since the lipid components move much slower compared to the IW^{HB} molecules as evident from their MSD, the underlying distribution of lipids should be more non-Gaussian compared to the IW^{HB}. To understand the opposite trend of IW^{HB} and lipids in van Hove correlation functions, distribution of logarithm of displacements of the IW^{HB} and the P lipid heads are calculated. With time, the IW^{HB} molecules develop a bimodal nature which is a characteristic of intermittent behavior leading to dynamical heterogeneity. The time by which the IW^{HB} follow Fickian behavior are still intermittent and non-Gaussian in nature. This clearly confirms that MSD_{XY} is not an appropriate measure for deciphering underlying dynamics. The IW^{HB} molecules do not reach Gaussianity even at a time-scale 7 times slower than the time of linear behavior in MSD. The IW^{HB} molecule vibrates for sometime in a cage or segment formed by the hydrogen bonds to a lipid head followed by a translational jump to another segment where it is hydrogen bonded to another lipid head. Although the IW^{HB} molecule jumps from one segment to the other segment, the hydrogen bonded lipid molecule does not jump coherently with the IW^{HB} not resulting in a perfect coupling between them. The decoupling in individual lipid-IW^{HB} dynamics and the intermittency in the IW^{HB} result in dynamical heterogeneity in the IW^{HB}. Intermittency is known to be present in supercooled bulk water due to fluctuations in high density 5 coordinated and low density 4 coordinated water molecules [Jana and Bagchi, 2009]. Although lipid and IW^{HB} molecules do not relax at the same time scale, dynamics of IW^{HB} molecules are significantly influenced by the regional dynamics of lipids.

Self intermediate scattering functions of the lipid moieties exhibit two time-scales: fast ballistic motion in a cage and long relaxations of the cage. Interestingly, IW^{HB} molecules show an additional long time scale with an intermediate hopping time scale. Such three well separated time-scales are found earlier for water in the vicinity of protein due to the fluctuations in protein structure [Marzio *et al.*, 2016]. On comparing both fast and slow relaxations of IW^{HB} with that of the lipid moieties,

fast relaxations of both IW^{HB} and respective lipids are found to be coupled as they vibrate together in the local cage formed either by physically close neighboring molecules or connected by hydrogen bonds. The fast relaxations of lipid moieties in the respective cages are slower from the head to the tail beads approaching the bilayer midplane. However, the slow relaxations of the lipid components are more complex in nature and do not follow any monotonic change from the head to the tail. Instead, the slow relaxations are faster at the two ends of a chain compared to the relaxations of beads at the middle. Ratio of slow relaxations of the lipids and the IW^{HB} is closest to 1 near the outermost N head-group among the remaining moieties. This is because N heads are most mobile at the lipid head-water interface with faster relaxation time scales and different classes of IW^{HB} have similar relaxation time scales since all of them reside closest to N head-groups. Thus our analysis sheds light on quantification of coupling between lipid and IW^{HB} multiple time-scale relaxations at a fluid phase. Very similar coupling has been found for protein-water interface using component wise molecular dynamics study [Wohlfromm and Vogel, 2019]. Our results explain the origin of dynamical heterogeneity in IW^{HB} through intermittency due to the hydrogen bond breaking and formation with different lipid moieties in the interface. Our calculations show that the IW^{HB} relaxations can not influence the dynamics of lipids occurring on different time-scales, but regional dynamics of lipids can be reflected in the regional dynamics of IW^{HB}. This strongly supports the idea that IW^{HB} can act as a sensor for capturing the regional complex dynamics of lipids which is not easy to access through experiments. At the same time, our findings pave the way to a better understanding on membrane-protein or membrane-drug interactions through water dynamics in future. The analysis will have implications towards IW^{HB} dynamics used as a finer tool to monitor the dynamics of lipids generating skeleton fences, molecular recognition, rafts and so on [Munro, 2003; Lingwood and Simons, 2010; He *et al.*, 2016].

References

Abascal, J. L. F. and Vega, C. (2005), "A general purpose model for the condensed phases of water: TIP4P/2005", *The Journal of Chemical Physics*, Vol. 123, pp. 234505–1–12

Abseher, R., Schreiber, H., and Steinhauser, O. (1996), "The influence of a protein on water dynamics in its vicinity investigated by molecular dynamics simulation", *Proteins: Structure, Function, and Bioinformatics*, Vol. 25, pp. 366–378

Acharya, S., Nandi, U. K., and Bhattacharyya, S. M. (2017), "Fickian yet non-Gaussian behaviour: A dominant role of the intermittent dynamics", *The Journal of Chemical Physics*, Vol. 146, p. 134504

A.Einstein (1905), "Zur Elektrodynamik bewegter Körper", *Annalen der Physik*, Vol. 322, pp. 891–921

Allen, M. P. and Tildesley, D. J., *Computer Simulation of Liquids*, Clarendon Press, New York, NY, USA 1987

Almeida, P. F. and Vaz, W. L. (1995), "Lateral diffusion in membranes", *Handbook of biological physics*, Vol. 1, pp. 305–357

Alsop, R. J., Dhaliwal, A., and Rheinstädter, M. C. (2017), "Curcumin Protects Membranes through a Carpet or Insertion Model Depending on Hydration", *Langmuir*, Vol. 33, pp. 8516–8524

A.Luzar and Chandler, D. (1996), "Hydrogen-Bond Kinetics in Liquid Water", *Nature*, Vol. 379, pp. 55–57

Andoh, Y., Aoki, N., and Okazaki, S. (2016), "Molecular dynamics study of lipid bilayers modeling the plasma membranes of mouse hepatocytes and hepatomas", *The Journal of Chemical Physics*, Vol. 144, p. 085104

Angell, C. (1985), "Spectroscopy simulation and scattering, and the medium range order problem in glass", *Journal of Non-Crystalline Solids*, Vol. 73, pp. 1–17

Angell, C. A. and Rodgers, V. (1984), "Near infrared spectra and the disrupted network model of normal and supercooled water", *The Journal of Chemical Physics*, Vol. 80, pp. 6245–6252

Arbe, A., de Molina, P. M., Alvarez, F., Frick, B., and Colmenero, J. (2016), "Dielectric Susceptibility of Liquid Water: Microscopic Insights from Coherent and Incoherent Neutron Scattering", *Physical Review Letters*, Vol. 117, p. 185501

Aussenac, F., Laguerre, M., Schmitter, J.-M., and Dufourc, E. J. (2003), "Detailed Structure and Dynamics of Bicelle Phospholipids Using Selectively Deuterated and Perdeuterated Labels. 2H NMR and Molecular Mechanics Study", *Langmuir*, Vol. 19, pp. 10468–10479

Avila, K. E., Castillo, H. E., Fiege, A., Vollmayr-Lee, K., and Zippelius, A. (2014), "Strong Dynamical Heterogeneity and Universal Scaling in Driven Granular Fluids", *Physical Review Letters*, Vol. 113, p. 025701

Bagchi, B., *Water in Biological and Chemical Processes*, Cambridge University Press 2013

Balasubramanian, S., Pal, S., and Bagchi, B. (2002), "Hydrogen Bond Dynamics Near A Micellar Surface: Origin of the Universal Slow Relaxation at Complex Aqueous Interfaces", *Physical Review Letters*, Vol. 89, p. 115505

Ball, P. (2008), "Water- an enduring mystery", *Nature*, Vol. 452, pp. 291–292

Barnes, R., Sun, S., Fichou, Y., Dahlquist, F. W., Heyden, M., and Han, S. (2017), "Spatially Heterogeneous Surface Water Diffusivity around Structured Protein Surfaces at Equilibrium", *Journal of the American Chemical Society*, Vol. 139, pp. 17890–17901

Bechinger, B. and Seelig, J. (1991), "Conformational changes of the phosphatidylcholine headgroup due to membrane dehydration. A 2H-NMR study", *Chemistry and Physics of Lipids*, Vol. 58, pp. 1–5

Bekker, H., Berendsen, H., Dijkstra, E., Achterop, S., Vondrumen, R., van der Spoel, D., Sijbers, A., Keegstra, H., and Renardus, M. (1993), "GROMACS - A Parallel Computer For Molecular-Dynamics Simulations", pp. 252–256

Bellissent-Funel, M. (2001), "Structure of confined water", *Journal of Physics: Condensed Matter*, Vol. 13, pp. 9165–9177

Bellissent-Funel, M.-C. (1998), "Structure and dynamics of water near hydrophilic surfaces", *Journal of Molecular Liquids*, Vol. 78, pp. 19–28

BellissentFunel, M. and Bosio, L. (1995), "A neutron scattering study of liquid D2O under pressure and at various temperatures", *The Journal of Chemical Physics*, Vol. 102, pp. 3727–3735

BellissentFunel, M. C., Bosio, L., Hallbrucker, A., Mayer, E., and SridiDorbez, R. (1992), "Xray and neutron scattering studies of the structure of hyperquenched glassy water", *The Journal of Chemical Physics*, Vol. 97, pp. 1282–1286

Benavides, A. L., Portillo, M. A., Chamorro, V. C., Espinosa, J. R., Abascal, J. L. F., and Vega, C. (2017), "A potential model for sodium chloride solutions based on the TIP4P/2005 water model", *The Journal of Chemical Physics*, Vol. 147, p. 104501

Benedetto, A. (2017), "Low-Temperature Decoupling of Water and Protein Dynamics Measured by Neutron Scattering", *The Journal of Physical Chemistry Letters*, Vol. 8, pp. 4883–4886

Berendsen, H., Vangunsteren, W., Postma, J., and Hermans, J. (1984a), "A Consistent Emperical Potential for Water-Protein Interactions", *Biopolymers*, Vol. 23, pp. 1513–1518

Berendsen, H., van der Spoel, D., and van Drunen, R. (1995), "GROMACS - A Message-Passing Parallel Molecular-Dynamics Implementation", *Computer Physics Communications*, Vol. 91, pp. 43–56

Berendsen, H. J. C., Postma, J. P. M., van Gunsteren, W. F., and Hermans, J., *Interaction Models for Water in Relation to Protein Hydration*, pp. 331–342 1981

Berendsen, H. J. C., Postma, J. P. M., van Gunsteren, W. F., DiNola, A., and Haak, J. R. (1984b), "Molecular dynamics with coupling to an external bath", *The Journal of Chemical Physics*, Vol. 81, pp. 3684–3690

Berger, O., Edholm, O., and Jähnig, F. (1997), "Molecular dynamics simulations of a fluid bilayer of dipalmitoylphosphatidylcholine at full hydration, constant pressure, and constant temperature", *Biophysical Journal*, Vol. 72, pp. 2002–2013

Bhattacharyya, S. M., Bagchi, B., and Wolynes, P. G. (2010), "Subquadratic wavenumber

dependence of the structural relaxation of supercooled liquid in the crossover regime", *The Journal of Chemical Physics*, Vol. 132, p. 104503

Bhide, S. Y. and Berkowitz, M. L. (2005), "Structure and dynamics of water at the interface with phospholipid bilayers", *The Journal of Chemical Physics*, Vol. 123, p. 224702

Bhide, S. Y. and Berkowitz, M. L. (2006), "The behavior of reorientational correlation functions of water at the water-lipid bilayer interface", *The Journal of Chemical Physics*, Vol. 125, p. 094713

Bhowmik, B. P., Das, R., and Karmakar, S. (2016), "Understanding the Stokes–Einstein relation in supercooled liquids using random pinning", *Journal of Statistical Mechanics: Theory and Experiment*, Vol. 2016, p. 074003

Bhowmik, B. P., Tah, I., and Karmakar, S. (2018), "Non-Gaussianity of the van Hove function and dynamic-heterogeneity length scale", *Physical Review E*, Vol. 98, p. 022122

Biswas, R., Furtado, J., and Bagchi, B. (2013), "Layerwise decomposition of water dynamics in reverse micelles: A simulation study of two-dimensional infrared spectrum", *The Journal of Chemical Physics*, Vol. 139, p. 144906

Blicher, A., Wodzinska, K., Fidorra, M., Winterhalter, M., and Heimburg, T. (2009), "The Temperature Dependence of Lipid Membrane Permeability, its Quantized Nature, and the Influence of Anesthetics", *Biophysical Journal*, Vol. 96, pp. 4581–4591

Borgnia, M., Nielsen, S., Engel, A., and Agre, P. (1999), "Cellular and Molecular Biology of the Aquaporin Water Channels", *Annual Review of Biochemistry*, Vol. 68, pp. 425–458

Borle, F. and Seelig, J. (1983), "Hydration of Escherichia coli lipids: Deuterium T1 relaxation time studies of phosphatidylglycerol, phosphatidylethanolamine and phosphatidylcholine", *Biochimica et Biophysica Acta (BBA) - Biomembranes*, Vol. 735, pp. 131–136

Bosio, L., Chen, S. H., and Teixeira, J. (1983), "Isochoric temperature differential of the x-ray structure factor and structural rearrangements in low-temperature heavy water", *Physical Review A*, Vol. 27, pp. 1468–1475

Bradley, R. P. and Radhakrishnan, R. (2016), "Curvature–undulation coupling as a basis for curvature sensing and generation in bilayer membranes", *Proceedings of the National Academy of Sciences*, Vol. 113, pp. E5117–E5124

Braun, D., Schmollngruber, M., and Steinhauser, O. (2016), "Rotational dynamics of water molecules near biological surfaces with implications for nuclear quadrupole relaxation", *Physical Chemistry Chemical Physics*, Vol. 18, pp. 24620–24630

Brochard-Wyart, F., Gennes, P., and Pfeuty, P. (1976), "Surface tension and deformations of membrane structures: relation to two-dimensional phase transitions", *Journal de Physique*, Vol. 37, pp. 1099–1104

Brzustowicz, M. R. and Brunger, A. T. (2005), "X-ray scattering from unilamellar lipid vesicles", *Journal of Applied Crystallography*, Vol. 38, pp. 126–131

Burton, E. F. and Oliver, W. F. (1935), "The crystal structure of ice at low temperatures", *Proceeding of the Royal Society A*, Vol. 153, pp. 166–172

Bussi, G., Donadio, D., and Parrinello, M. (2007), "Canonical sampling through velocity rescaling", *The Journal of Chemical Physics*, Vol. 126, p. 014101

Camisasca, G., Marzio, M. D., Corradini, D., and Gallo, P. (2016), "Two structural relaxations in

protein hydration water and their dynamic crossovers", *The Journal of Chemical Physics*, Vol. 145, p. 044503

Capponi, S., Arbe, A., Cerveny, S., Busselez, R., Frick, B., Embs, J. P., and Colmenero, J. (2011), "Quasielastic neutron scattering study of hydrogen motions in an aqueous poly(vinyl methyl ether) solution", *The Journal of Chemical Physics*, Vol. 134, p. 204906

Capponi, S., White, S. H., Tobias, D. J., and Heyden, M. (2019), "Structural Relaxation Processes and Collective Dynamics of Water in Biomolecular Environments", *The Journal of Physical Chemistry B*, Vol. 123, pp. 480–486

Cavagna, A. (2009), "Supercooled liquids for pedestrians", *Physics Reports*, Vol. 476, pp. 51–124

Cerveny, S., Colmenero, J., and A.Alegría (2005), "Dielectric Investigation of the Low-Temperature Water Dynamics in the Poly(vinyl methyl ether)/H2O System", *Macromolecules*, Vol. 38, pp. 7056–7063

Cerveny, S., Mallamace, F., Swenson, J., Vogel, M., and Xu, L. (2016), "Confined Water as Model of Supercooled Water", *Chemical Reviews*, Vol. 116, pp. 7608–7625

Chakrabarty, S., Tah, I., Karmakar, S., and Dasgupta, C. (2017), "Block Analysis for the Calculation of Dynamic and Static Length Scales in Glass-Forming Liquids", *Physical Review Letters*, Vol. 119, p. 205502

Chakraborty, D. and Chandra, A. (2011), "Hydrogen bonded structure and dynamics of liquid-vapor interface of water-ammonia mixture: An ab initio molecular dynamics study", *The Journal of Chemical Physics*, Vol. 135, p. 114510

Chanda, J., Chakraborty, S., and Bandyopadhyay, S. (2006), "Sensitivity of Hydrogen Bond Lifetime Dynamics to the Presence of Ethanol at the Interface of a Phospholipid Bilayer", *The Journal of Physical Chemistry B*, Vol. 110, pp. 3791–3797

Chandra, A. (2000), "Effects of Ion Atmosphere on Hydrogen-Bond Dynamics in Aqueous Electrolyte Solutions", *Physical Review Letters*, Vol. 85, pp. 768–771

Chandrasekhar, I., Kastenholz, M., Lins, R. D., Oostenbrink, C., Schuler, L. D., Tieleman, D. P., and van Gunsteren, W. F. (2003), "A consistent potential energy parameter set for lipids: dipalmitoylphosphatidylcholine as a benchmark of the GROMOS96 45A3 force field", *European Biophysics Journal*, Vol. 32, pp. 67–77

Chatham, J. C. and Blackband, S. J. (2001), "Nuclear Magnetic Resonance Spectroscopy and Imaging in Animal Research", *ILAR Journal*, Vol. 42, pp. 189–208

Chaudhuri, P., Berthier, L., and Kob, W. (2007), "Universal Nature of Particle Displacements close to Glass and Jamming Transitions", *Physical Review Letters*, Vol. 99, p. 060604

Chaurasia, A. K., Rukangu, A. M., Philen, M. K., Seidel, G. D., and Freeman, E. C. (2018), "Evaluation of bending modulus of lipid bilayers using undulation and orientation analysis", *Physical Review E*, Vol. 97, p. 032421

Chen, R., Poger, D., and Mark, A. E. (2011), "Effect of High Pressure on Fully Hydrated DPPC and POPC Bilayers", *The Journal of Physical Chemistry B*, Vol. 115, pp. 1038–1044

Chen, S.-H., Liu, L., Fratini, E., Baglioni, P., Faraone, A., and Mamontov, E. (2006), "Observation of fragile-to-strong dynamic crossover in protein hydration water", *Proceedings of the National Academy of Sciences*, Vol. 103, pp. 9012–9016

Chen, X., Weber, I., and Harrison, R. W. (2008), "Hydration Water and Bulk Water in Proteins Have Distinct Properties in Radial Distributions Calculated from 105 Atomic Resolution Crystal Structures", *The Journal of Physical Chemistry B*, Vol. 112, pp. 12073–12080

Chen, X., Hua, W., Huang, Z., and Allen, H. C. (2010), "Interfacial Water Structure Associated with Phospholipid Membranes Studied by Phase-Sensitive Vibrational Sum Frequency Generation Spectroscopy", *Journal of the American Chemical Society*, Vol. 132, pp. 11336–11342

Cheng, C.-Y., Varkey, J., Ambroso, M. R., Langen, R., and Han, S. (2013), "Hydration dynamics as an intrinsic ruler for refining protein structure at lipid membrane interfaces", *Proceedings of the National Academy of Sciences*, Vol. 110, pp. 16838–16843

Cheng, Y.-K. and Rossky, P. J. (1998), "Surface topography dependence of biomolecular hydrophobic hydration", *Nature*, Vol. 392, pp. 696–699

Chiu, S. W., Clark, M., Balaji, V., Subramaniam, S., Scott, H. L., and Jakobsson, E. (1995), "Incorporation of surface tension into molecular dynamics simulation of an interface: a fluid phase lipid bilayer membrane", *Biophysical Journal*, Vol. 69, pp. 1230–1245

Cicerone, M. T., Blackburn, F. R., and Ediger, M. D. (1995), "How do molecules move near Tg? Molecular rotation of six probes in oterphenyl across 14 decades in time", *The Journal of Chemical Physics*, Vol. 102, pp. 471–479

Cipcigan, F., Sokhan, V., Martyna, G., and Crain, J. (2018), "Structure and hydrogen bonding at the limits of liquid water stability", *Scientific Reports*, Vol. 8, p. 1718

Cola, D. D., Deriu, A., Sampoli, M., and Torcini, A. (1996), "Proton dynamics in supercooled water by molecular dynamics simulations and quasielastic neutron scattering", *The Journal of Chemical Physics*, Vol. 104, pp. 4223–4232

Cordomí, A., Caltabiano, G., and Pardo, L. (2012), "Membrane Protein Simulations Using AMBER Force Field and Berger Lipid Parameters", *Journal of Chemical Theory and Computation*, Vol. 8, pp. 948–958

Costard, R., Heisler, I. A., and Elsaesser, T. (2014), "Structural Dynamics of Hydrated Phospholipid Surfaces Probed by Ultrafast 2D Spectroscopy of Phosphate Vibrations", *The Journal of Physical Chemistry Letters*, Vol. 5, pp. 506–511

Cowan, M. L., Bruner, B., Huse, N., Dwyer, J., Chugh, B., Nibbering, E., Elasaesser, T., and Miller, R. (2005), "Ultrafast memory loss and energy redistribution in the hydrogen bond network of liquid H2O", Vol. 434, pp. 199–202

Cyran, J. D., Backus, E. H. G., Nagata, Y., and Bonn, M. (2018), "Structure from Dynamics: Vibrational Dynamics of Interfacial Water as a Probe of Aqueous Heterogeneity", *The Journal of Physical Chemistry B*, Vol. 122, pp. 3667–3679

D. van der Spoel, B. H., E. Lindahl and the GROMACS development team. (2013), "GROMACS User Manual version 4.6.5", URL `http://www.gromacs.org`

Dahanayake, J. and Mitchell-Koch, K. (2018a), "Entropy connects water structure and dynamics in protein hydration layer", *Physical Chemistry Chemical Physics*, Vol. 20, pp. 14765–14777

Dahanayake, J. N. and Mitchell-Koch, K. R. (2018b), "How Does Solvation Layer Mobility Affect Protein Structural Dynamics ?", *Frontiers in Molecular Biosciences*, Vol. 5, p. 65

Damodaran, K. V., Merz, K. M., and Gaber, B. P. (1992), "Structure and dynamics of the

dilauroylphosphatidylethanolamine lipid bilayer", *Biochemistry*, Vol. 31, pp. 7656–7664

Darden, T., York, D., and Pedersen, L. (1993), "Particle mesh Ewald: An Nlog(N) method for Ewald sums in large systems", *The Journal of Chemical Physics*, Vol. 98, pp. 10089–10092

D'Arrigo, G., Maisano, G., Mallamace, F., Migliardo, P., and Wanderlingh, F. (1981), "Raman scattering and structure of normal and supercooled water", *The Journal of Chemical Physics*, Vol. 75, pp. 4264–4270

Das, J., Flenner, E., and Kosztin, I. (2013), "Anomalous diffusion of water molecules in hydrated lipid bilayers", *The Journal of Chemical Physics*, Vol. 139, p. 065102

Das, S., Biswas, R., and Mukherjee, B. (2015), "Reorientational Jump Dynamics and Its Connections to Hydrogen Bond Relaxation in Molten Acetamide: An All-Atom Molecular Dynamics Simulation Study", *The Journal of Physical Chemistry B*, Vol. 119, pp. 274–283

de Vries, A. H., Chandrasekhar, I., van Gunsteren, W. F., and Hünenberger, P. H. (2005), "Molecular Dynamics Simulations of Phospholipid Bilayers: Influence of Artificial Periodicity, System Size, and Simulation Time", *The Journal of Physical Chemistry B*, Vol. 109, pp. 11643–11652

Debnath, A. and Schäfer, L. V. (2015), "Structure and Dynamics of Phospholipid Nanodiscs from All-Atom and Coarse-Grained Simulations", *The Journal of Physical Chemistry B*, Vol. 119, No. 23, pp. 6991–7002

Debnath, A., Mukherjee, B., Ayappa, K. G., Maiti, P. K., and Lin, S.-T. (2010), "Entropy and dynamics of water in hydration layers of a bilayer", *The Journal of Chemical Physics*, Vol. 133, pp. 174704–1–14

Debnath, A., Ayappa, K. G., and Maiti, P. K. (2013), "Simulation of Influence of Bilayer Melting on Dynamics and Thermodynamics of Interfacial Water", *Physical Review Letters*, Vol. 110, pp. 018303–1–5

Debnath, A., Thakkar, F. M., Maiti, P. K., Kumaran, V., and Ayappa, K. G. (2014), "Laterally structured ripple and square phases with one and two dimensional thickness modulations in a model bilayer system", *Soft Matter*, Vol. 10, pp. 7630–7637

DelloStritto, M., Piontek, S. M., Klein, M. L., and Borguet, E. (2018), "Relating Interfacial Order to Sum Frequency Generation with Ab Initio Simulations of the Aqueous Al2O3(0001) and (1120) Interfaces", *The Journal of Physical Chemistry C*, Vol. 122, pp. 21284–21294

Dill, K. A. (1990), "Dominant forces in protein folding", *Biochemistry*, Vol. 29, pp. 7133–7155

Dingley, A. J. and Grzesiek, S. (1998), "Direct Observation of Hydrogen Bonds in Nucleic Acid Base Pairs by Internucleotide 2JNN Couplings", *Journal of the American Chemical Society*, Vol. 120, pp. 8293–8297

Donati, C., Douglas, J. F., Kob, W., Plimpton, S. J., Poole, P. H., and Glotzer, S. C. (1998), "Stringlike Cooperative Motion in a Supercooled Liquid", *Physical Review Letters*, Vol. 80, pp. 2338–2341

Doster, W., Cusack, S., and Petry, W. (1989), "Dynamical transition of myoglobin revealed by inelastic neutron scattering", *Nature*, Vol. 337, pp. 754–756

Dueby, S., Dubey, V., and Daschakraborty, S. (2019), "Decoupling of Translational Diffusion from the Viscosity of Supercooled Water: Role of Translational Jump Diffusion", *The Journal of*

Physical Chemistry B, Vol. 123, pp. 7178–7189

Eaves, J. D., Loparo, J. J., Fecko, C. J., Roberts, S. T., Tokmakoff, A., and Geissler, P. L. (2005), "Hydrogen bonds in liquid water are broken only fleetingly", *Proceedings of the National Academy of Sciences*, Vol. 102, pp. 13019–13022

Ediger, M. D. (2000), "Spatially Heterogeneous Dynamics in Supercooled Liquids", *Annual Review of Physical Chemistry*, Vol. 51, pp. 99–128

Efimov, A. V. and Brazhnikov, E. V. (2003), "Relationship between intramolecular hydrogen bonding and solvent accessibility of side-chain donors and acceptors in proteins", *FEBS Letters*, Vol. 554, pp. 389–393

Einstein, A. (1906), "Zur Theorie der Brownschen Bewegung", *Annals of Physics*, Vol. 19, p. 371

Emwas, A.-H. M., *The Strengths and Weaknesses of NMR Spectroscopy and Mass Spectrometry with Particular Focus on Metabolomics Research*, pp. 161–193, Springer New York 2015

Essmann, U., Perera, L., and Berkowitz, M. L. (1995a), "The Origin of the Hydration Interaction of Lipid Bilayers from MD Simulation of Dipalmitoylphosphatidylcholine Membranes in Gel and Liquid Crystalline Phases", *Langmuir*, Vol. 11, pp. 4519–4531

Essmann, U., Perera, L., Berkowitz, M. L., Darden, T., Lee, H., and Pedersen, L. G. (1995b), "A smooth particle mesh Ewald method", *The Journal of Chemical Physics*, Vol. 103, pp. 8577–8593

Faraone, A., Liu, L., and Chen, S.-H. (2003), "Model for the translation-rotation coupling of molecular motion in water", *The Journal of Chemical Physics*, Vol. 119, pp. 6302–6313

Fecko, C. J., Eaves, J. D., Loparo, J. J., Tokmakoff, A., and Geissler, P. L. (2003), "Ultrafast Hydrogen-Bond Dynamics in the Infrared Spectroscopy of Water", *Science*, Vol. 301, pp. 1698–1702

Fenn, E. E., Wong, D. B., and Fayer, M. D. (2009), "Water dynamics at neutral and ionic interfaces", *Proceedings of the National Academy of Sciences*, Vol. 106, pp. 15243–15248

Ferrario, V. and Pleiss, J. (2019), "Simulation of protein diffusion: a sensitive probe of proteinsolvent interactions", *Journal of Biomolecular Structure and Dynamics*, Vol. 37, pp. 1534–1544

Fisette, O., Päslack, C., Barnes, R., Isas, J. M., Langen, R., Heyden, M., Han, S., and Schäfer, L. V. (2016), "Hydration Dynamics of a Peripheral Membrane Protein", *Journal of the American Chemical Society*, Vol. 138, pp. 11526–11535

Flenner, E. and Szamel, G. (2013), "Dynamic heterogeneities above and below the mode-coupling temperature: Evidence of a dynamic crossover", *The Journal of Chemical Physics*, Vol. 138, p. 12A523

Flenner, E., Das, J., Rheinstädter, M. C., and Kosztin, I. (2009), "Subdiffusion and lateral diffusion coefficient of lipid atoms and molecules in phospholipid bilayers", *Physical Review E*, Vol. 79, p. 011907

Fogarty, A. C. and Laage, D. (2014), "Water Dynamics in Protein Hydration Shells: The Molecular Origins of the Dynamical Perturbation", *The Journal of Physical Chemistry B*, Vol. 118, pp. 7715–7729

Fogarty, J. C., Arjunwadkar, M., Pandit, S. A., and Pan, J. (2015), "Atomically detailed lipid bilayer models for the interpretation of small angle neutron and X-ray scattering data", *Biochimica et*

Biophysica Acta (BBA) - Biomembranes, Vol. 1848, pp. 662–672

Franck, J. M., Ding, Y., Stone, K., Qin, P. Z., and Han, S. (2015), "Anomalously Rapid Hydration Water Diffusion Dynamics Near DNA Surfaces", *Journal of the American Chemical Society*, Vol. 137, pp. 12013–12023

Frauenfelder, H., Chen, G., Berendzen, J., Fenimore, P. W., Jansson, H., McMahon, B. H., Stroe, I. R., Swenson, J., and Young, R. D. (2009), "A unified model of protein dynamics", *Proceedings of the National Academy of Sciences*, Vol. 106, pp. 5129–5134

Fröchtenicht, R., Kaloudis, M., Koch, M., and Huisken, F. (1996), "Vibrational spectroscopy of small water complexes embedded in large liquid helium clusters", *The Journal of Chemical Physics*, Vol. 105, pp. 6128–6140

Furse, K. E. and Corcelli, S. A. (2008), "The Dynamics of Water at DNA Interfaces: Computational Studies of Hoechst 33258 Bound to DNA", *Journal of the American Chemical Society*, Vol. 130, pp. 13103–13109

Gabriel, B. and Teissié, J. (1996), "Proton long-range migration along protein monolayers and its consequences on membrane coupling", *Proceedings of the National Academy of Sciences*, Vol. 93, pp. 14521–14525

Gallo, P., Sciortino, F., Tartaglia, P., and Chen, S.-H. (1996), "Slow Dynamics of Water Molecules in Supercooled States", *Physical Review Letters*, Vol. 76, pp. 2730–2733

Gallo, P., Rovere, M., and Spohr, E. (2000a), "Glass transition and layering effects in confined water: A computer simulation study", *The Journal of Chemical Physics*, Vol. 113, pp. 11324–11335

Gallo, P., Rovere, M., and Spohr, E. (2000b), "Supercooled Confined Water and the Mode Coupling Crossover Temperature", *Physical Review Letters*, Vol. 85, pp. 4317–4320

Gallot, G., Bratos, S., Pommeret, S., Lascoux, N., Leicknam, J.-C., Koziński, M., Amir, W., and Gale, G. M. (2002), "Coupling between molecular rotations and OH-O motions in liquid water: Theory and experiment", *The Journal of Chemical Physics*, Vol. 117, pp. 11301–11309

Gennis, R. B., *Biomembranes : molecular structure and function*, Springer-Verlag 1989

Golosov, A. A. and Karplus, M. (2007), "Probing Polar Solvation Dynamics in Proteins: A Molecular Dynamics Simulation Analysis", *The Journal of Physical Chemistry B*, Vol. 111, pp. 1482–1490

González, M. A. and Abascal, J. L. F. (2010), "The shear viscosity of rigid water models", *The Journal of Chemical Physics*, Vol. 132, p. 096101

Gorter, E. and Grendel, F. (2004), "On Bimolecular Layers of Lipoids on the Chromocytes of the Blood", *The Journal of Experimental Medicine*, Vol. 41, pp. 439–443

Götze, W. (2008), "Complex Dynamics of Glass-Forming Liquids: A Mode-Coupling Theory", 2008

Gotze, W. and Sjogren, L. (1992), "Relaxation processes in supercooled liquids", *Reports on Progress in Physics*, Vol. 55, pp. 241–376

Gowrishankar, K., Ghosh, S., Saha, S., Rumamol, C., Mayor, S., and Rao, M. (2012), "Active Remodeling of Cortical Actin Regulates Spatiotemporal Organization of Cell Surface Molecules", *Cell*, Vol. 149, pp. 1353–1367

Gruenbaum, S. M. and Skinner, J. L. (2013), "Vibrational spectroscopy of water in hydrated lipid multi-bilayers. III. Water clustering and vibrational energy transfer", *The Journal of Chemical*

Physics, Vol. 139, p. 175103

Guevara-Carrion, G., Vrabec, J., and Hasse, H. (2011), "Prediction of self-diffusion coefficient and shear viscosity of water and its binary mixtures with methanol and ethanol by molecular simulation", *The Journal of Chemical Physics*, Vol. 134, p. 074508

Gurtovenko, A. A. and Vattulainen, I. (2005), "Pore Formation Coupled to Ion Transport through Lipid Membranes as Induced by Transmembrane Ionic Charge Imbalance: Atomistic Molecular Dynamics Study", *Journal of the American Chemical Society*, Vol. 127, pp. 17570–17571

Gurtovenko, A. A., Patra, M., Karttunen, M., and Vattulainen, I. (2004), "Cationic DMPC/DMTAP lipid bilayers: molecular dynamics study.", *Biophysical journal*, Vol. 86, pp. 3461–72

Hagamanasa, K. H., Gokhale, S., Sood, A. K., , and Ganapathy, R. (2015), "Direct measurements of growing amorphous order and non-monotonic dynamic correlations ina colloidal glass-former", *Nature Physics*, Vol. 11, pp. 403–408

Handle, P. H., Loerting, T., and Sciortino, F. (2017), "Supercooled and glassy water: Metastable liquid(s), amorphous solid(s), and a no-man's land", *Proceedings of the National Academy of Sciences*, Vol. 114, pp. 13336–13344

Hansen, J.-P. and McDonald, I. R., *Theory of Simple Liquids (Third Edition)*, Academic Press 2006

Hartkamp, R., Moore, T. C., Iacovella, C. R., Thompson, M. A., Bulsara, P. A., Moore, D. J., and McCabe, C. (2018), "Composition Dependence of Water Permeation Across Multicomponent Gel-Phase Bilayers", *The Journal of Physical Chemistry B*, Vol. 122, pp. 3113–3123

He, S. and Maibaum, L. (2017), "Lipid Phase Heterogeneity and Size Dependence in Quarternary Lipid Bilayer System: A Coarse-Grained Molecular Dynamics Study", *Biophysical Journal*, Vol. 112, p. 224a

He, W., Song, H., Su, Y., Geng, Ackerson, B. J., Peng, H. B., and Tong, P. (2016), "Dynamic heterogeneity and non-Gaussian statistics for acetylcholine receptors on live cell membrane", *Nature Communications*, Vol. 7, p. 11701

Heid, E. and Braun, D. (2019), "Fundamental limitations of the time-dependent Stokes shift for investigating protein hydration dynamics", *Physical Chemistry Chemical Physics*, Vol. 21, pp. 4435–4443

Heide, H.-G. (1984), "Observations on ice layers", *Ultramicroscopy*, Vol. 14, pp. 271–278

Hemley, R. J., Chen, L. C., , and Mao, H. K. (1989), "New transformations between crystalline and amorphous ice", *Nature*, Vol. 338, pp. 638–640

Hess, B., Bekker, H., Berendsen, H. J. C., and Fraaije, J. G. E. M. (1997), "LINCS : A linear constraint solver for molecular simulations", *Journal of Computational Chemistry*, Vol. 18, pp. 1463–1472

Hess, B., Kutzner, C., van der Spoel, D., and Lindahl, E. (2008), "GROMACS 4: Algorithms for Highly Efficient, Load-Balanced, and Scalable Molecular Simulation", *Journal of Chemical Theory and Computation*, Vol. 4, pp. 435–447

Högberg, C.-J. and Lyubartsev, A. P. (2006), "A Molecular Dynamics Investigation of the Influence of Hydration and Temperature on Structural and Dynamical Properties of a Dimyristoylphosphatidylcholine Bilayer", *The Journal of Physical Chemistry B*, Vol. 110, pp.

14326–14336

Holz, M., Heil, S. R., and Sacco, A. (2000), "Temperature-dependent self-diffusion coefficients of water and six selected molecular liquids for calibration in accurate 1H NMR PFG measurements", *Physical Chemistry Chemical Physics*, Vol. 2, pp. 4740–4742

Hopkins, P., Fortini, A., Archer, A. J., and Schmidt, M. (2010), "The van Hove distribution function for Brownian hard spheres: Dynamical test particle theory and computer simulations for bulk dynamics", *The Journal of Chemical Physics*, Vol. 133, p. 224505

Hosseinpour, S., Tang, F., Wang, F., Livingstone, R. A., Schlegel, S. J., Ohto, T., Bonn, M., Nagata, Y., and Backus, E. H. G. (2017), "Chemisorbed and Physisorbed Water at the TiO2/Water Interface", *The Journal of Physical Chemistry Letters*, Vol. 8, pp. 2195–2199

Hove, L. V. (1954), "Correlations in Space and Time and Born Approximation Scattering in Systems of Interacting Particles", *Physical Review*, Vol. 95, pp. 249–262

Hsieh, C. H. and Wu, W. G. (1997), "Structure and dynamics of primary hydration shell of phosphatidylcholine bilayers at subzero temperatures", *Biophysical journal*, Vol. 71, pp. 3278–87

Hu, Z. and Jiang, J. (2010), "Assessment of biomolecular force fields for molecular dynamics simulations in a protein crystal", *Journal of Computational Chemistry*, Vol. 31, pp. 371–380

Huang, Z. S. and Miller, R. E. (1988), "SubDoppler resolution infrared spectroscopy of water dimer", *The Journal of Chemical Physics*, Vol. 88, pp. 8008–8009

Huang, Z. S. and Miller, R. E. (1989), "Highresolution nearinfrared spectroscopy of water dimer", *The Journal of Chemical Physics*, Vol. 91, pp. 6613–6631

Huggins, C. M. and Pimentel, G. C. (1956), "Systematics of the Infrared Spectral Properties of Hydrogen Bonding Systems: Frequency Shift, Half Width and Intensity", *The Journal of Physical Chemistry*, Vol. 60, pp. 1615–1619

Hummer, G. and Tokmakoff, A. (2014), "Preface: Special Topic on Biological Water", *The Journal of Chemical Physics*, Vol. 141, pp. 22D101–2

Humphrey, W., Dalke, A., and Schulten, K. (1996), "VMD – Visual Molecular Dynamics", *Journal of Molecular Graphics*, Vol. 14, pp. 33–38

Hung, W.-C., Chen, F.-Y., Lee, C.-C., Sun, Y., Lee, M.-T., and Huang, H. W. (2008), "Membrane-Thinning Effect of Curcumin", *Biophysical Journal*, Vol. 94, pp. 4331–4338

Ingolfsson, H. I., Koeppe, R. E., and Andersen, O. S. (2007), "Curcumin is a Modulator of Bilayer Material Properties", *Biochemistry*, Vol. 46, pp. 10384–10391

Inoue, K., Singh, P. C., Nihonyanagi, S., Yamaguchi, S., and Tahara, T. (2017), "Cooperative Hydrogen-Bond Dynamics at a Zwitterionic Lipid/Water Interface Revealed by 2D HD-VSFG Spectroscopy", *The Journal of Physical Chemistry Letters*, Vol. 8, pp. 5160–5165

Isaacs, E. D., Shukla, A., Platzman, P. M., Hamann, D. R., Barbiellini, B., and Tulk, C. A. (1999), "Covalency of the Hydrogen Bond in Ice: A Direct X-Ray Measurement", *Physical Review Letters*, Vol. 82, pp. 600–603

Izadi, S. and Onufriev, A. V. (2016), "Accuracy limit of rigid 3-point water models", *The Journal of Chemical Physics*, Vol. 145, p. 074501

Jahn, R., Lang, T., and Südhof, T. C. (2003), "Membrane Fusion", *Cell*, Vol. 112, pp. 519–533

Jähnig, F. (1996), "What is the Surface Tension of a Lipid Bilayer Membrane ?", *Biophysical Journal*, Vol. 71, pp. 1348–1349

Jain, R. and Sebastian, K. L. (2016), "Diffusion in a Crowded, Rearranging Environment", *The Journal of Physical Chemistry B*, Vol. 120, pp. 3988–3992

Jaiswal, A., Egami, T., and Zhang, Y. (2015), "Atomic-scale dynamics of a model glass-forming metallic liquid: Dynamical crossover, dynamical decoupling, and dynamical clustering", *Physical Review B*, Vol. 91, p. 134204

Jämbeck, J. P. M. and Lyubartsev, A. P. (2012a), "Derivation and Systematic Validation of a Refined All-Atom Force Field for Phosphatidylcholine Lipids", *The Journal of Physical Chemistry B*, Vol. 116, pp. 3164–3179

Jämbeck, J. P. M. and Lyubartsev, A. P. (2012b), "An Extension and Further Validation of an All-Atomistic Force Field for Biological Membranes", *Journal of Chemical Theory and Computation*, Vol. 8, pp. 2938–2948

Jana, B. and Bagchi, B. (2009), "Intermittent Dynamics, Stochastic Resonance and Dynamical Heterogeneity in Supercooled Liquid Water", *The Journal of Physical Chemistry B*, Vol. 113, pp. 2221–2224

Jana, B., Pal, S., and Bagchi, B. (2008), "Hydrogen Bond Breaking Mechanism and Water Reorientational Dynamics in the Hydration Layer of Lysozyme", *The Journal of Physical Chemistry B*, Vol. 112, pp. 9112–9117

Janssen, L. M. C. (2018), "Mode-Coupling Theory of the Glass Transition: A Primer", *Frontiers in Physics*, Vol. 6, p. 97

Javanainen, M., Lamberg, A., Cwiklik, L., Vattulainen, I., and Ollila, O. H. S. (2018), "Atomistic Model for Nearly Quantitative Simulations of Langmuir Monolayers", *Langmuir*, Vol. 34, pp. 2565–2572

Ji, M., Odelius, M., and Gaffney, K. J. (2010), "Large Angular Jump Mechanism Observed for Hydrogen Bond Exchange in Aqueous Perchlorate Solution", *Science*, Vol. 328, pp. 1003–1005

Jiang, F. Y., Bouret, Y., and Kindt, J. T. (2004), "Molecular dynamics simulations of the lipid bilayer edge.", *Biophysical journal*, Vol. 87, pp. 182–92

Johari, G., Hallbrucker, A., and Mayer, E. (1987), "The glass-liquid transition of hyperquenched water", *Nature*, Vol. 330, pp. 552–553

Jójárt, B. and Martinek, T. A. (2007), "Performance of the general amber force field in modeling aqueous POPC membrane bilayers", *Journal of Computational Chemistry*, Vol. 28, pp. 2051–2058

Jonas, J., DeFries, T., and Wilbur, D. J. (1976), "Molecular motions in compressed liquid water", *The Journal of Chemical Physics*, Vol. 65, pp. 582–588

Jorgensen, W. L. (1979), "Quantum and statistical mechanical studies of liquids. 3. Deriving intermolecular potential functions for the water dimer from ab initio calculations", *Journal of the American Chemical Society*, Vol. 101, pp. 2011–2016

Jorgensen, W. L. (1981), "Transferable intermolecular potential functions for water, alcohols, and ethers. Application to liquid water", *Journal of the American Chemical Society*, Vol. 103, pp. 335–340

Jorgensen, W. L., Chandrasekhar, J., Madura, J. D., Impey, R. W., and Klein, M. L. (1983),

"Comparison of simple potential functions for simulating liquid water", *The Journal of Chemical Physics*, Vol. 79, pp. 926–935

Jung, J., Kobayashi, C., and Sugita, Y. (2019), "Optimal Temperature Evaluation in Molecular Dynamics Simulations with a Large Time Step", *Journal of Chemical Theory and Computation*, Vol. 15, pp. 84–94

Jungwirth, P. (2015), "Biological Water or Rather Water in Biology?", *The Journal of Physical Chemistry Letters*, Vol. 6, pp. 2449–2451

Karmakar, S., Dasgupta, C., and Sastry, S. (2009), "Growing length and time scales in glass-forming liquids", *Proceedings of the National Academy of Sciences*, Vol. 106, pp. 3675–3679

Kasson, P. M. and Pande, V. S. (2004), "Molecular Dynamics Simulation of Lipid Reorientation at Bilayer Edges", *Biophysical Journal*, Vol. 86, pp. 3744–3749

Kasson, P. M., Lindahl, E., and Pande, V. S. (2011), "Water Ordering at Membrane Interfaces Controls Fusion Dynamics", *Journal of the American Chemical Society*, Vol. 133, pp. 3812–3815

Kawasaki, T. and Kim, K. (2017), "Identifying time scales for violation/preservation of Stokes-Einstein relation in supercooled water", *Science Advances*, Vol. 3

Kegel, W. K. and van Blaaderen, A. (2000), "Direct Observation of Dynamical Heterogeneities in Colloidal Hard-Sphere Suspensions", *Science*, Vol. 287, No. 5451, pp. 290–293

Keutsch, F. N. and Saykally, R. J. (2001), "Water clusters: Untangling the mysteries of the liquid, one molecule at a time", *Proceedings of the National Academy of Sciences*, Vol. 98, pp. 10533–10540

Khakbaz, P. and Klauda, J. B. (2018), "Investigation of phase transitions of saturated phosphocholine lipid bilayers via molecular dynamics simulations", *Biochimica et Biophysica Acta (BBA) - Biomembranes*, Vol. 1860, pp. 1489–1501

Khatib, R., Backus, E. H. G., Bonn, M., Perez-Haro, M.-J., Gaigeot, M.-P., and Sulpizi, M. (2016), "Water orientation and hydrogen-bond structure at the fluorite/water interface", *Scientific Reports*, Vol. 6, p. 24287

Khondker, A., Dhaliwal, A., Alsop, R. J., Tang, J., Backholm, M., Shi, A.-C., and Rheinstädter, M. C. (2017), "Partitioning of caffeine in lipid bilayers reduces membrane fluidity and increases membrane thickness", *Physical Chemistry Chemical Physics*, Vol. 19, pp. 7101–7111

Killian, J. (1998), "Hydrophobic mismatch between proteins and lipids in membranes", *Biochimica et Biophysica Acta (BBA) - Reviews on Biomembranes*, Vol. 1376, pp. 401–416

Kim, K. and Saito, S. (2013), "Multiple length and time scales of dynamic heterogeneities in model glass-forming liquids: A systematic analysis of multi-point and multi-time correlations", *The Journal of Chemical Physics*, Vol. 138, p. 12A506

Klauda, J. B., Venable, R. M., Freites, J. A., OConnor, J. W., Tobias, D. J., Mondragon-Ramirez, C., Vorobyov, I., MacKerell, A. D., and Pastor, R. W. (2010), "Update of the CHARMM All-Atom Additive Force Field for Lipids: Validation on Six Lipid Types", *The Journal of Physical Chemistry B*, Vol. 114, pp. 7830–7843

Kob, W., Donati, C., Plimpton, S. J., Poole, P. H., and Glotzer, S. C. (1997), "Dynamical Heterogeneities in a Supercooled Lennard-Jones Liquid", *Physical Review Letters*, Vol. 79, pp. 2827–2830

Koehorst, R. B. M., Laptenok, S., van Oort, B., van Hoek, A., Spruijt, R. B., van Stokkum, I. H. M., van Amerongen, H., and Hemminga, M. A. (2010), "Profiling of dynamics in protein-lipid-water systems: a time-resolved fluorescence study of a model membrane protein with the label BADAN at specific membrane depths", *European Biophysics Journal*, Vol. 39, pp. 647–656

Korolev, N., Lyubartsev, A. P., Laaksonen, A., and Nordenskiöld, L. (2002), "On the Competition between Water, Sodium Ions, and Spermine in Binding to DNA: A Molecular Dynamics Computer Simulation Study", *Biophysical Journal*, Vol. 82, pp. 2860–2875

Krynicki, K., Green, C. D., and Sawyer, D. W. (1978a), "Pressure and temperature dependence of self-diffusion in water", *Faraday Discussions of the Chemical Society*, Vol. 66, pp. 199–208

Krynicki, K., Green, C. D., and Sawyer, D. W. (1978b), "Pressure and temperature dependence of self-diffusion in water", *Faraday Discussions Chemical Society*, Vol. 66, pp. 199–208

Kumar, P. (2008), "Temperature dependence of isothermal compressibility of water and other liquids.", `http://polymer.bu.edu/~hes/water/thesis-kumar.pdf` 2008

Kumar, P., Franzese, G., and Stanley, H. E. (2008), "Predictions of Dynamic Behavior under Pressure for Two Scenarios to Explain Water Anomalies", *Physical Review Letters*, Vol. 100, p. 105701

Kumar, P., Buldyrev, S. V., and Stanley, H. E. (2009), "A tetrahedral entropy for water", *Proceedings of the National Academy of Sciences*, Vol. 106, pp. 22130–22134

Kundu, A., asiak, B. B., Lim, J.-H., Kwak, K., and Cho, M. (2016a), "Water Hydrogen-Bonding Network Structure and Dynamics at Phospholipid Multibilayer Surface: Femtosecond Mid-IR PumpProbe Spectroscopy", *The Journal of Physical Chemistry Letters*, Vol. 7, pp. 741–745

Kundu, A., Kwak, K., and Cho, M. (2016b), "Water Structure at the Lipid Multibilayer Surface: Anionic Versus Cationic Head Group Effects", *The Journal of Physical Chemistry B*, Vol. 120, pp. 5002–5007

Kundu, A., Kumar, P., Ha, J.-H., and Cho, M. (2017), "Studying Water Hydrogen-Bonding Network near the Lipid Multibilayer with Multiple IR Probes", *The Journal of Physical Chemistry A*, Vol. 121, pp. 1435–1441

Kuon, N., Milischuk, A. A., Ladanyi, B. M., and Flenner, E. (2017), "Self-intermediate scattering function analysis of supercooled water confined in hydrophilic silica nanopores", *The Journal of Chemical Physics*, Vol. 146, p. 214501

Kučerka, N., Nieh, M.-P., and Katsaras, J. (2011), "Fluid phase lipid areas and bilayer thicknesses of commonly used phosphatidylcholines as a function of temperature", *Biochimica et Biophysica Acta (BBA) - Biomembranes*, Vol. 1808, pp. 2761–2771

Kučerka, N., Heberle, F. A., Pan, J., and Katsaras, J. (2015), "Structural Significance of Lipid Diversity as Studied by Small Angle Neutron and X-ray Scattering", *Membranes*, Vol. 5, pp. 454–472

Kwon, G., Sung, B. J., and Yethiraj, A. (2014), "Dynamics in Crowded Environments: Is Non-Gaussian Brownian Diffusion Normal?", *The Journal of Physical Chemistry B*, Vol. 118, pp. 8128–8134

Laage, D., Stirnemann, G., Sterpone, F., Rey, R., and Hynes, J. T. (2011), "Reorientation and Allied Dynamics in Water and Aqueous Solutions", *Annual Review of Physical Chemistry*, Vol. 62, pp. 395–416

Lawrence, C. P. and Skinner, J. L. (2003), "Vibrational spectroscopy of HOD in liquid D2O. VII. Temperature and frequency dependence of the OH stretch lifetime", *The Journal of Chemical Physics*, Vol. 119, pp. 3840–3848

Li, C. and Liu, M. (2013), "Protein dynamics in living cells studied by in-cell NMR spectroscopy", *FEBS Letters*, Vol. 587, pp. 1008–1011

Li, J., Shaikh, S. A., Enkavi, G., Wen, P.-C., Huang, Z., and Tajkhorshid, E. (2013), "Transient formation of water-conducting states in membrane transporters", *Proceedings of the National Academy of Sciences*, Vol. 110, pp. 7696–7701

Li, T., Hassanali, A. A., Kao, Y.-T., Zhong, D., and Singer, S. J. (2007), "Hydration Dynamics and Time Scales of Coupled WaterProtein Fluctuations", *Journal of the American Chemical Society*, Vol. 129, pp. 3376–3382

Liang, C., Jeon, J., and Cho, M. (2019), "Ab initio Modeling of the Vibrational Sum-Frequency Generation Spectrum of Interfacial Water", *The Journal of Physical Chemistry Letters*, Vol. 10, pp. 1153–1158

Lin, X., Nair, V., Zhou, Y., and Gorfe, A. A. (2018), "Membrane potential and dynamics in a ternary lipid mixture: insights from molecular dynamics simulations", *Physical Chemistry Chemical Physics*, Vol. 20, pp. 15841–15851

Lindahl, E., Hess, B., and van der Spoel, D. (2001), "GROMACS 3.0: a package for molecular simulation and trajectory analysis", *Molecular modeling annual*, Vol. 7, pp. 306–317

Lingwood, D. and Simons, K. (2010), "Lipid Rafts As a Membrane-Organizing Principle", *Science*, Vol. 327, pp. 46–50

Lipscomb, L. A., Peek, M. E., Zhou, F. X., Bertrand, J. A., VanDerveer, D., and Williams, L. D. (1994), "Water Ring Structure at DNA Interfaces: Hydration and Dynamics of DNA-Anthracycline Complexes", *Biochemistry*, Vol. 33, pp. 3649–3659

Liu, J., He, X., Zhang, J. Z. H., and Qi, L.-W. (2018), "Hydrogen-bond structure dynamics in bulk water: insights from ab initio simulations with coupled cluster theory", *Chemical Science*, Vol. 9, pp. 2065–2073

Liu, Z., Huang, J., Tyagi, M., ONeill, H., Zhang, Q., Mamontov, E., Jain, N., Wang, Y., Zhang, J., Smith, J. C., and Hong, L. (2017), "Dynamical Transition of Collective Motions in Dry Proteins", *Physical Review Letters*, Vol. 119, p. 048101

Lopez, C. F., Nielsen, S. O., Klein, M. L., and Moore, P. B. (2004), "Hydrogen Bonding Structure and Dynamics of Water at the Dimyristoylphosphatidylcholine Lipid Bilayer Surface from a Molecular Dynamics Simulation", *The Journal of Physical Chemistry B*, Vol. 108, pp. 6603–6610

Luzar, A. (2000), "Resolving the hydrogen bond dynamics conundrum", *The Journal of Chemical Physics*, Vol. 113, pp. 10663–10675

Luzar, A. and Chandler, D. (1996), "Effect of Environment on Hydrogen Bond Dynamics in Liquid Water", *Physical Review Letters*, Vol. 76, pp. 928–931

Lyubartsev, A. P. and Rabinovich, A. L. (2016), "Force Field Development for Lipid Membrane Simulations", *Biochimica et Biophysica Acta (BBA) - Biomembranes*, Vol. 1858, pp. 2483–2497

MacDowell, L. G. and Vega, C. (2010), "Dielectric Constant of Ice Ih and Ice V: A Computer Simulation Study", *The Journal of Physical Chemistry B*, Vol. 114, pp. 6089–6098

MacKerell, A. D., Wiorkiewicz-Kuczera, J., and Karplus, M. (1995), "An all-atom empirical energy function for the simulation of nucleic acids", *Journal of the American Chemical Society*, Vol. 117, pp. 11946–11975

MacKerell, A. D., Bashford, D., Bellott, M., Dunbrack, R. L., Evanseck, J. D., Field, M. J., Fischer, S., Gao, J., Guo, H., Ha, S., Joseph-McCarthy, D., Kuchnir, L., Kuczera, K., Lau, F. T. K., Mattos, C., Michnick, S., Ngo, T., Nguyen, D. T., Prodhom, B., Reiher, W. E., Roux, B., Schlenkrich, M., Smith, J. C., Stote, R., Straub, J., Watanabe, M., Wiórkiewicz-Kuczera, J., Yin, D., and Karplus, M. (1998), "All-Atom Empirical Potential for Molecular Modeling and Dynamics Studies of Proteins", *The Journal of Physical Chemistry B*, Vol. 102, pp. 3586–3616

Magno, A. and Gallo, P. (2011), "Understanding the Mechanisms of Bioprotection: A Comparative Study of Aqueous Solutions of Trehalose and Maltose upon Supercooling", *The Journal of Physical Chemistry Letters*, Vol. 2, pp. 977–982

Maiti, P. K. and Bagchi, B. (2006), "Structure and Dynamics of DNA-Dendrimer Complexation: Role of Counterions, Water, and Base Pair Sequence", *Nano Letters*, Vol. 6, pp. 2478–2485

Majumdar, S., Duvvuri, S., and Mitra, A. K. (2004), "Membrane transporter/receptor-targeted prodrug design: strategies for human and veterinary drug development", *Advanced Drug Delivery Reviews*, Vol. 56, pp. 1437–1452

Mallamace, F., Corsaro, C., and Stanley, H. E. (2013), "Possible relation of water structural relaxation to water anomalies", *Proceedings of the National Academy of Sciences*, Vol. 110, pp. 4899–4904

Mandal, A. and van der Wel, P. C. (2016), "MAS 1H NMR Probes Freezing Point Depression of Water and Liquid-Gel Phase Transitions in Liposomes", *Biophysical Journal*, Vol. 111, pp. 1965–1973

Marchi, M., Sterpone, F., and Ceccarelli, M. (2002), "Water Rotational Relaxation and Diffusion in Hydrated Lysozyme", *Journal of the American Chemical Society*, Vol. 124, pp. 6787–6791

Mark, P. and Nilsson, L. (2001), "Structure and Dynamics of the TIP3P, SPC, and SPC/E Water Models at 298 K", *The Journal of Physical Chemistry A*, Vol. 105, pp. 9954–9960

Markiewicz, M., Baczyński, K., and Pasenkiewicz-Gierula, M. (2015), "Properties of water hydrating the galactolipid and phospholipid bilayers: a molecular dynamics simulation study", *Acta Biochimica Polonica*, Vol. 62, pp. 475–481

Markovitch, O. and Agmon, N. (2008), "Reversible geminate recombination of hydrogen-bonded water molecule pair", *The Journal of Chemical Physics*, Vol. 129, p. 084505

Marrink, S.-J. and Berendsen, H. J. C. (1994), "Simulation of water transport through a lipid membrane", *The Journal of Physical Chemistry*, Vol. 98, pp. 4155–4168

Marrink, S. J. and Berendsen, H. J. C. (1996), "Permeation Process of Small Molecules across Lipid Membranes Studied by Molecular Dynamics Simulations", *The Journal of Physical Chemistry*, Vol. 100, pp. 16729–16738

Marzio, M. D., Camisasca, G., Rovere, M., and Gallo, P. (2016), "Mode coupling theory and fragile to strong transition in supercooled TIP4P/2005 water", *The Journal of Chemical Physics*, Vol. 144, p. 074503

Marzio, M. D., Camisasca, G., Rovere, M., and Gallo, P. (2017), "Microscopic origin of the fragile to strong crossover in supercooled water: The role of activated processes", *The Journal of Chemical*

Physics, Vol. 146, p. 084502

Masayasu, S., Hiroshi, S., and Syûzô, S. (1968), "Calorimetric Study of the Glassy State. IV. Heat Capacities of Glassy Water and Cubic Ice", *Bulletin of the Chemical Society of Japan*, Vol. 41, pp. 2591–2599

Mazza, M. G., Giovambattista, N., Starr, F. W., and Stanley, H. E. (2006), "Relation between Rotational and Translational Dynamic Heterogeneities in Water", *Physical Review Letters*, Vol. 96, p. 057803

McDaniel, J. G. and Yethiraj, A. (2017), "Coupling between the Dynamics of Water and Surfactants in Lyotropic Liquid Crystals", *The Journal of Physical Chemistry B*, Vol. 121, pp. 5048–5057

McMillan, J. A. and Los, S. C. (1965), "Vitreous Ice : Irreversible Transformation During Warm-Up", *Nature*, Vol. 206, pp. 806–807

Mezei, P. J. M. (2001), "Orientational Order of the Water Molecules Across a Fully Hydrated DMPC Bilayer : A Monte Carlo Simulation Study", *The Journal of Physical Chemistry B*, Vol. 105, pp. 3614–3623

Michele, C. D., Gado, E. D., and Leporini, D. (2011), "Scaling between structural relaxation and particle caging in a model colloidal gel", *Soft Matter*, Vol. 7, pp. 4025–4031

Mills, R. (1973), "Self-diffusion in normal and heavy water in the range 1-45.deg.", *The Journal of Physical Chemistry*, Vol. 77, pp. 685–688

Mishima, O. and Stanley, H. E. (1998), "The relationship between liquid, supercooled and glassy water", *Nature*, Vol. 396, pp. 329–335

Moilanen, D. E., Wong, D., Rosenfeld, D. E., Fenn, E. E., and Fayer, M. D. (2009), "Ion-water hydrogen-bond switching observed with 2D IR vibrational echo chemical exchange spectroscopy", *Proceedings of the National Academy of Sciences*, Vol. 106, pp. 375–380

Molugu, T. R., Xu, X., Lee, S., Mallikarjunaiah, K. J., and Brown, M. F., *Solid-State 2H NMR Studies of Water-Mediated Lipid Membrane Deformation* 2018

Mondal, J. A., Nihonyanagi, S., Yamaguchi, S., and Tahara, T. (2012), "Three Distinct Water Structures at a Zwitterionic Lipid/Water Interface Revealed by Heterodyne-Detected Vibrational Sum Frequency Generation", *Journal of the American Chemical Society*, Vol. 134, pp. 7842–7850

Moore, P. B., Lopez, C. F., and Klein, M. L. (2001), "Dynamical Properties of a Hydrated Lipid Bilayer from a Multinanosecond Molecular Dynamics Simulation", *Biophysical Journal*, Vol. 81, pp. 2484–2494

Mouritsen, O. G. and Jørgensen, K. (1992), "Problems and paradigms: Dynamic lipidbilayer heterogeneity: A mesoscopic vehicle for membrane function?", *BioEssays*, Vol. 14, pp. 129–136

Munro, S. (2003), "Lipid Rafts: Elusive or Illusive?", *Cell*, Vol. 115, pp. 377–388

Nagata, Y. and Mukamel, S. (2010), "Vibrational Sum-Frequency Generation Spectroscopy at the Water/Lipid Interface: Molecular Dynamics Simulation Study", *Journal of the American Chemical Society*, Vol. 132, pp. 6434–6442

Nagle, J. F. and Tristram-Nagle, S. (2000), "Structure of lipid bilayers", *Biochimica et Biophysica Acta (BBA) - Reviews on Biomembranes*, Vol. 1469, pp. 159–195

Nandi, N. and Bagchi, B. (1997), "Dielectric Relaxation of Biological Water", *The Journal of*

Physical Chemistry B, Vol. 101, pp. 10954–10961

Nandi, P. K., English, N. J., Futera, Z., and Benedetto, A. (2017), "Hydrogen-bond dynamics at the biowater interface in hydrated proteins : a molecular-dynamics study", *Physical Chemistry Chemical Physics*, Vol. 19, pp. 318–329

Narten, A. H. and Levy, H. A. (1971), "Liquid Water: Molecular Correlation Functions from XRay Diffraction", *The Journal of Chemical Physics*, Vol. 55, pp. 2263–2269

Nathanson, J. (1984), "Caffeine and related methylxanthines: possible naturally occurring pesticides", *Science*, Vol. 226, pp. 184–187

Nehlig, A., Daval, J.-L., and Debry, G. (1992), "Caffeine and the central nervous system: mechanisms of action, biochemical, metabolic and psychostimulant effects", *Brain Research Reviews*, Vol. 17, pp. 139–170

Nienhuys, H.-K., Woutersen, S., van Santen, R. A., and Bakker, H. J. (1999), "Mechanism for vibrational relaxation in water investigated by femtosecond infrared spectroscopy", *The Journal of Chemical Physics*, Vol. 111, pp. 1494–1500

Nienhuys, H.-K., van Santen, R. A., and Bakker, H. J. (2000), "Orientational relaxation of liquid water molecules as an activated process", *The Journal of Chemical Physics*, Vol. 112, pp. 8487–8494

Nojima, Y., Suzuki, Y., and Yamaguchi, S. (2017), "Weakly Hydrogen-Bonded Water Inside Charged Lipid Monolayer Observed with Heterodyne-Detected Vibrational Sum Frequency Generation Spectroscopy", *The Journal of Physical Chemistry C*, Vol. 121, pp. 2173–2180

Ohto, T., Backus, E. H. G., Hsieh, C.-S., Sulpizi, M., Bonn, M., and Nagata, Y. (2015), "Lipid Carbonyl Groups Terminate the Hydrogen Bond Network of Membrane-Bound Water", *The Journal of Physical Chemistry Letters*, Vol. 6, pp. 4499–4503

Ollila, O. H. S., Heikkinen, H. A., and Iwaï, H. (2018), "Rotational Dynamics of Proteins from Spin Relaxation Times and Molecular Dynamics Simulations", *The Journal of Physical Chemistry B*, Vol. 122, pp. 6559–6569

O.Mishima, Calvert, L., and Whalley, E. (1984), "'Melting ice' I at 77 K and 10 kbar : a new method of making amorphous solids", *Nature*, Vol. 310, pp. 393–395

O.Mishima, Calvert, L., and Whalley, E. (1985), "An apparently first-order transition between two amorphous phases of ice induced by pressure", *Nature*, Vol. 314, pp. 76–78

Onufriev, A. V. and Izadi, S. (2018), "Water models for biomolecular simulations", *Wiley Interdisciplinary Reviews: Computational Molecular Science*, Vol. 8, p. e1347

Orbach, E. and Finkelstein, A. (1980), "The nonelectrolyte permeability of planar lipid bilayer membranes.", *The Journal of General Physiology*, Vol. 75, No. 4, pp. 427–436

Pal, S., Maiti, P. K., and Bagchi, B. (2006), "Exploring DNA groove water dynamics through hydrogen bond lifetime and orientational relaxation", *The Journal of Chemical Physics*, Vol. 125, p. 234903

Pal, S. K., Peon, J., Bagchi, B., and Zewail, A. H. (2002), "Biological Water: Femtosecond Dynamics of Macromolecular Hydration", *The Journal of Physical Chemistry B*, Vol. 106, pp. 12376–12395

Pal, S. K., Zhao, L., and Zewail, A. H. (2003), "Water at DNA surfaces: Ultrafast dynamics in minor groove recognition", *Proceedings of the National Academy of Sciences*, Vol. 100, pp. 8113–8118

Paolantoni, M., Sassi, P., Morresi, A., and Santini, S. (2007), "Hydrogen bond dynamics and water structure in glucose-water solutions by depolarized Rayleigh scattering and low-frequency Raman spectroscopy", *The Journal of Chemical Physics*, Vol. 127, p. 024504

Papahadjopoulos, D., Nir, S., and Ohki, S. (1972), "Permeability properties of phospholipid membranes: Effect of cholesterol and temperature", *Biochimica et Biophysica Acta (BBA) - Biomembranes*, Vol. 266, pp. 561–583

Pasenkiewicz-Gierula, M., Takaoka, Y., Miyagawa, H., Kitamura, K., and Kusumi, A. (1997), "Hydrogen Bonding of Water to Phosphatidylcholine in the Membrane As Studied by a Molecular Dynamics Simulation: Location, Geometry, and LipidLipid Bridging via Hydrogen-Bonded Water", *The Journal of Physical Chemistry A*, Vol. 101, pp. 3677–3691

Pasenkiewicz-Gierula, M., Takaoka, Y., Miyagawa, H., Kitamura, K., and Kusumi, A. (1999), "Charge Pairing of Headgroups in Phosphatidylcholine Membranes: A Molecular Dynamics Simulation Study", *Biophysical Journal*, Vol. 76, pp. 1228–1240

Päslack, C., Schäfer, L. V., and Heyden, M. (2019a), "Atomistic characterization of collective protein-water-membrane dynamics", *Physical Chemistry Chemical Physics*, Vol. 21, pp. 15958–15965

Päslack, C., Smith, J. C., Heyden, M., and Schäfer, L. V. (2019b), "Hydration-mediated stiffening of collective membrane dynamics by cholesterol", *Physical Chemistry Chemical Physics*, Vol. 21, pp. 10370–10376

Patra, M., Karttunen, M., Hyvnen, M., Falck, E., Lindqvist, P., and Vattulainen, I. (2003), "Molecular Dynamics Simulations of Lipid Bilayers: Major Artifacts Due to Truncating Electrostatic Interactions", *Biophysical Journal*, Vol. 84, pp. 3636–3645

Pauling, L. (1941), "The nature of the chemical bond and the structure of molecules and crystals", *Journal of the American Pharmaceutical Association (Scientific ed.)*, Vol. 30, p. 30

Persson, E. and Halle, B. (2008), "Cell water dynamics on multiple time scales", *Proceedings of the National Academy of Sciences*, Vol. 105, pp. 6266–6271

Pestana, L. R., Marsalek, O., Markland, T. E., and Head-Gordon, T. (2018), "The Quest for Accurate Liquid Water Properties from First Principles", *The Journal of Physical Chemistry Letters*, Vol. 9, pp. 5009–5016

Petrache, H. I., Dodd, S. W., and Brown, M. F. (2000), "Area per Lipid and Acyl Length Distributions in Fluid Phosphatidylcholines Determined by 2H NMR Spectroscopy", *Biophysical Journal*, Vol. 79, pp. 3172–3192

Pezzotti, S., Galimberti, D. R., Shen, Y. R., and Gaigeot, M.-P. (2018), "Structural definition of the BIL and DL: a new universal methodology to rationalize non-linear $\chi^{(2)}(\omega)$ SFG signals at charged interfaces, including $\chi^{(3)}(\omega)$ contributions", *Physical Chemistry Chemical Physics*, Vol. 20, pp. 5190–5199

Piggot, T. J., Allison, J. R., Sessions, R. B., and Essex, J. W. (2017), "On the Calculation of Acyl Chain Order Parameters from Lipid Simulations", *Journal of Chemical Theory and Computation*, Vol. 13, pp. 5683–5696

Poger, D. and Mark, A. E. (2010), "On the Validation of Molecular Dynamics Simulations of Saturated and cis-Monounsaturated Phosphatidylcholine Lipid Bilayers: A Comparison with Experiment", *Journal of Chemical Theory and Computation*, Vol. 6, pp. 325–336

Poger, D., Gunsteren, W. F. V., and Mark, A. E. (2010), "A new force field for simulating phosphatidylcholine bilayers", *Journal of Computational Chemistry*, Vol. 31, pp. 1117–1125

Polak, A., Tarek, M., Tomšič, M., Valant, J., Ulrih, N. P., Jamnik, A., Kramar, P., and Miklavčič, D. (2014), "Structural Properties of Archaeal Lipid Bilayers: Small-Angle X-ray Scattering and Molecular Dynamics Simulation Study", *Langmuir*, Vol. 30, pp. 8308–8315

Pronk, S., Lindahl, E., and Kasson, P. M. (2014), "Dynamic heterogeneity controls diffusion and viscosity near biological interfaces", *Nature Communications*, Vol. 5, p. 3034

Pronk, S., Lindahl, E., and Kasson, P. M. (2015), "Coupled Diffusion in Lipid Bilayers upon Close Approach", *Journal of the American Chemical Society*, Vol. 137, pp. 708–714

Puertas, A. M., Fuchs, M., and Cates, M. E. (2004), "Dynamical heterogeneities close to a colloidal gel", *The Journal of Chemical Physics*, Vol. 121, pp. 2813–2822

Pugliano, N. and Saykally, R. (1992), "Measurement of quantum tunneling between chiral isomers of the cyclic water trimer", *Science*, Vol. 257, No. 5078, pp. 1937–1940

Pugliano, N., Cruzan, J. D., Loeser, J. G., and Saykally, R. J. (1993), "Vibrational and K!'a dependencies of the multidimensional tunneling dynamics in the 82.6 cm-1 intermolecular vibration of the water dimer-d4", *The Journal of Chemical Physics*, Vol. 98, pp. 6600–6617

Purusottam, R. N., Sénicourt, L., Lacapére, J.-J., and Tekely, P. (2015), "Probing the gel to liquid-crystalline phase transition and relevant conformation changes in liposomes by 13C magic-angle spinning NMR spectroscopy", *Biochimica et Biophysica Acta (BBA) - Biomembranes*, Vol. 1848, pp. 3134–3139

Qiao, B., Jiménez-Ángeles, F., Nguyen, T. D., and de la Cruz, M. O. (2019), "Water follows polar and nonpolar protein surface domains", *Proceedings of the National Academy of Sciences*, Vol. 116, pp. 19274–19281

Qvist, J. and Halle, B. (2008), "Thermal Signature of Hydrophobic Hydration Dynamics", *Journal of the American Chemical Society*, Vol. 130, pp. 10345–10353

Rahman, A. (1964), "Correlations in the Motion of Atoms in Liquid Argon", *Physical Review*, Vol. 136, pp. A405–A411

Rasaiah, J. C., Garde, S., and Hummer, G. (2008), "Water in Nonpolar Confinement: From Nanotubes to Proteins and Beyond", *Annual Review of Physical Chemistry*, Vol. 59, pp. 713–740

Raschke, T. M. (2006), "Water structure and interactions with protein surfaces", *Current Opinion in Structural Biology*, Vol. 16, pp. 152–159

Rayleigh (1891), "Surface Tension", *Nature*, Vol. 43, pp. 437–439

Re, S., Nishima, W., Tahara, T., and Sugita, Y. (2014), "Mosaic of Water Orientation Structures at a Neutral Zwitterionic Lipid/Water Interface Revealed by Molecular Dynamics Simulations", *The Journal of Physical Chemistry Letters*, Vol. 5, pp. 4343–4348

Reinsberg, S. A., Qiu, X. H., Wilhelm, M., Spiess, H. W., and Ediger, M. D. (2001), "Length scale of dynamic heterogeneity in supercooled glycerol near Tg", *The Journal of Chemical Physics*, Vol. 114, pp. 7299–7302

Rey, R., Mller, K. B., and Hynes, J. T. (2002), "Hydrogen Bond Dynamics in Water and Ultrafast Infrared Spectroscopy", *The Journal of Physical Chemistry A*, Vol. 106, pp. 11993–11996

Rezai, T., Bock, J. E., Zhou, M. V., Kalyanaraman, C., Lokey, R. S., and Jacobson, M. P. (2006), "Conformational Flexibility, Internal Hydrogen Bonding, and Passive Membrane Permeability: Successful in Silico Prediction of the Relative Permeabilities of Cyclic Peptides", *Journal of the American Chemical Society*, Vol. 128, pp. 14073–14080

Rezus, Y. L. A. and Bakker, H. J. (2006), "Orientational dynamics of isotopically diluted H2O and D2O", *The Journal of Chemical Physics*, Vol. 125, p. 144512

Rheinstädter, M. C., Das, J., Flenner, E. J., Brüning, B., Seydel, T., and Kosztin, I. (2008), "Motional Coherence in Fluid Phospholipid Membranes", *Physical Review Letter*, Vol. 101, p. 248106

Ricci, M. A., Bruni, F., and Giuliani, A. (2009), "Similarities between confined and supercooled water", *Faraday Discussions*, Vol. 141, pp. 347–358

Richert, R. (2002), "Heterogeneous dynamics in liquids: fluctuations in space and time", *Journal of Physics: Condensed Matter*, Vol. 14, pp. R703–R738

Roobala, C. and K., J. B. (2017), "Emergence of compositionally tunable nanoscale dynamical heterogeneity in model binary lipid biomembranes", *Soft Matter*, Vol. 13, pp. 4598–4606

Ropp, J., Lawrence, C., Farrar, T. C., and Skinner, J. L. (2001), "Rotational Motion in Liquid Water Is Anisotropic: A Nuclear Magnetic Resonance and Molecular Dynamics Simulation Study", *Journal of the American Chemical Society*, Vol. 123, pp. 8047–8052

Rose, D., Rendell, J., Lee, D., Nag, K., and Booth, V. (2008), "Molecular dynamics simulations of lung surfactant lipid monolayers", *Biophysical Chemistry*, Vol. 138, pp. 67–77

Rosso, L. and Gould, I. R. (2008), "Structure and dynamics of phospholipid bilayers using recently developed general all-atom force fields", *Journal of Computational Chemistry*, Vol. 29, pp. 24–37

Rovere, M. (2004), "Water in confined geometries", *Journal of Physics: Condensed Matter*, Vol. 16

Roy, S., Gruenbaum, S. M., and Skinner, J. L. (2014), "Theoretical vibrational sum-frequency generation spectroscopy of water near lipid and surfactant monolayer interfaces. II. Two-dimensional spectra", *The Journal of Chemical Physics*, Vol. 141, p. 22D505

Russo, D., Murarka, R. K., Copley, J. R. D., and Head-Gordon, T. (2005), "Molecular View of Water Dynamics near Model Peptides", *The Journal of Physical Chemistry B*, Vol. 109, pp. 12966–12975

Russo, J. and Tanaka, H. (2015), "Assessing the role of static length scales behind glassy dynamics in polydisperse hard disks", *Proceedings of the National Academy of Sciences*, Vol. 112, pp. 6920–6924

Sapir, L. and Harries, D. (2017), "Revisiting Hydrogen Bond Thermodynamics in Molecular Simulations", *Journal of Chemical Theory and Computation*, Vol. 13, pp. 2851–2857

Sarangi, N. K., Ayappa, K. G., and Basu, J. K. (2017), "Complex dynamics at the nanoscale in simple biomembranes", *Scientific Reports*, Vol. 7, p. 11173

Schiró, G., Fichou, Y., Gallat, F.-X., Moulin, M., Härtlein, M., Heyden, M., Colletier, J.-P., Orecchini, A., Paciaroni, A., Wuttke, J., Tobias, D. J., and Weik, M. (2015), "Translational diffusion of hydration water correlates with functional motions in folded and intrinsically disordered proteins", *Nature Communications*, Vol. 6, p. 6490

Schmid, F. (2013), "Fluctuations in lipid bilayers : are they understood ?", *Biophysical Reviews*

and Letters, Vol. 08, pp. 1–20

Schmidt, J. R., Corcelli, S. A., and Skinner, J. L. (2005), "Pronounced non-Condon effects in the ultrafast infrared spectroscopy of water", *The Journal of Chemical Physics*, Vol. 123, p. 044513

Schuler, L. D., Daura, X., and van Gunsteren, W. F. (2001), "An improved GROMOS96 force field for aliphatic hydrocarbons in the condensed phase", *Journal of Computational Chemistry*, Vol. 22, pp. 1205–1218

Sciortino, F., Geiger, A., and Stanley, H. E. (1991), "Effect of defects on molecular mobility in liquid water", *Nature*, Vol. 354, pp. 218–221

Sciortino, F., Geiger, A., and Stanley, H. E. (1992), "Network defects and molecular mobility in liquid water", *The Journal of Chemical Physics*, Vol. 96, pp. 3857–3865

Sciortino, F., Gallo, P., Tartaglia, P., and Chen, S.-H. (1996), "Supercooled water and the kinetic glass transition", *Physical Review E*, Vol. 54, pp. 6331–6343

Sedlmeier, F., Horinek, D., and Netz, R. R. (2011), "Spatial Correlations of Density and Structural Fluctuations in Liquid Water: A Comparative Simulation Study", *Journal of the American Chemical Society*, Vol. 133, pp. 1391–1398

Seelig, J. and Niederberger, W. (1974), "Deuterium-labeled lipids as structural probes in liquid crystalline bilayers. Deuterium magnetic resonance study", *Journal of the American Chemical Society*, Vol. 96, pp. 2069–2072

Sengupta, S. and Karmakar, S. (2014), "Distribution of diffusion constants and Stokes-Einstein violation in supercooled liquids", *The Journal of Chemical Physics*, Vol. 140, p. 224505

Shafique, N., Kennedy, K. E., Douglas, J. F., and Starr, F. W. (2016), "Quantifying the Heterogeneous Dynamics of a Simulated Dipalmitoylphosphatidylcholine (DPPC) Membrane", *The Journal of Physical Chemistry B*, Vol. 120, pp. 5172–5182

Shell, M. S., Debenedetti, P. G., and Stillinger, F. H. (2005), "Dynamic heterogeneity and non-Gaussian behaviour in a model supercooled liquid", *Journal of Physics: Condensed Matter*, Vol. 17, pp. S4035–S4046

Sillescu, H. (1999), "Heterogeneity at the glass transition: a review", *Journal of Non-Crystalline Solids*, Vol. 243, pp. 81–108

Sinha, S. K. and Bandyopadhyay, S. (2011), "Dynamic properties of water around a protein-DNA complex from molecular dynamics simulations", *The Journal of Chemical Physics*, Vol. 135, p. 135101

Siu, S. W., Vácha, R., Jungwirth, P., and Böckmann, R. A. (2008), "Biomolecular simulations of membranes: Physical properties from different force fields", *The Journal of Chemical Physics*, Vol. 128, p. 125103

Skinner, L. B., Huang, C., Schlesinger, D., Pettersson, L. G. M., Nilsson, A., and Benmore, C. J. (2013), "Benchmark oxygen-oxygen pair-distribution function of ambient water from x-ray diffraction measurements with a wide Q-range", *The Journal of Chemical Physics*, Vol. 138, p. 074506

Skinner, L. B., Galib, M., Fulton, J. L., Mundy, C. J., Parise, J. B., Pham, V.-T., Schenter, G. K., and Benmore, C. J. (2016), "The structure of liquid water up to 360 MPa from x-ray diffraction measurements using a high Q-range and from molecular simulation", *The Journal of Chemical*

Physics, Vol. 144, p. 134504

Smondyrev, A. M. and Voth, G. A. (2002a), "Molecular Dynamics Simulation of Proton Transport Near the Surface of a Phospholipid Membrane", *Biophysical Journal*, Vol. 82, pp. 1460–1468

Smondyrev, A. M. and Voth, G. A. (2002b), "Molecular Dynamics Simulation of Proton Transport through the Influenza A Virus M2 Channel", *Biophysical Journal*, Vol. 83, pp. 1987–1996

Sokolov, A. P., Hurst, J., and Quitmann, D. (1995), "Dynamics of supercooled water: Mode-coupling theory approach", *Physical Review B*, Vol. 51, pp. 12865–12868

Spiess, H. W. (2017), "50th Anniversary Perspective: The Importance of NMR Spectroscopy to Macromolecular Science", *Macromolecules*, Vol. 50, pp. 1761–1777

Spoel, D. V. D., Lindahl, E., Hess, B., Groenhof, G., Mark, A. E., and Berendsen, H. J. C. (2005), "GROMACS: Fast, flexible, and free", *Journal of Computational Chemistry*, Vol. 26, pp. 1701–1718

Srivastava, A. and Debnath, A. (2018), "Hydration dynamics of a lipid membrane : Hydrogen bond networks and lipid-lipid associations", *The Journal of Chemical Physics*, Vol. 148, p. 094901

Srivastava, A. and Voth, G. A. (2013), "Hybrid Approach for Highly Coarse-Grained Lipid Bilayer Models", *Journal of Chemical Theory and Computation*, Vol. 9, pp. 750–765

Srivastava, A., Karmakar, S., and Debnath, A. (2019a), "Quantification of spatio-temporal scales of dynamical heterogeneity of water near lipid membranes above supercooling", *Soft Matter*, Vol. 15, pp. 9805–9815

Srivastava, A., Malik, S., and Debnath, A. (2019b), "Heterogeneity in structure and dynamics of water near bilayers using TIP3P and TIP4P/2005 water models", *Chemical Physics*, Vol. 525, p. 110396

Starr, F. W., Sciortino, F., and Stanley, H. E. (1999), "Dynamics of simulated water under pressure", *Physical Review E*, Vol. 60, pp. 6757–6768

Starr, F. W., Douglas, J. F., and Sastry, S. (2013), "The relationship of dynamical heterogeneity to the Adam-Gibbs and random first-order transition theories of glass formation", *The Journal of Chemical Physics*, Vol. 138, p. 12A541

Stein, R. S. L. and Andersen, H. C. (2008), "Scaling Analysis of Dynamic Heterogeneity in a Supercooled Lennard-Jones Liquid", *Physical Review Letters*, Vol. 101, p. 267802

Stiopkin, I. V., Jayathilake, H. D., Bordenyuk, A. N., and Benderskii, A. V. (2008), "Heterodyne-Detected Vibrational Sum Frequency Generation Spectroscopy", *Journal of the American Chemical Society*, Vol. 130, pp. 2271–2275

Stirnemann, G. and Laage, D. (2012), "Communication: On the origin of the non-Arrhenius behavior in water reorientation dynamics", *The Journal of Chemical Physics*, Vol. 137, p. 031101

Stockton, G. W., Polnaszek, C. F., Tulloch, A. P., Hasan, F. B., and Smith, I. C. P. (1976), "Molecular motion and order in single-bilayer vesicles and multilamellar dispersions of egg lecithin and lecithin-cholesterol mixtures. A deuterium nuclear magnetic resonance study of specifically labeled lipids.", *Biochemistry*, Vol. 15, pp. 954–66

Swenson, J., Kargl, F., Berntsen, P., and Svanberg, C. (2008), "Solvent and lipid dynamics of hydrated lipid bilayers by incoherent quasielastic neutron scattering", *The Journal of Chemical Physics*, Vol. 129, p. 045101

Tah, I., Sengupta, S., Sastry, S., Dasgupta, C., and Karmakar, S. (2018), "Glass Transition in Supercooled Liquids with Medium-Range Crystalline Order", *Physical Review Letters*, Vol. 121, p. 085703

Tang, F., Ohto, T., Sun, S., Rouxel, J. R., Imoto, S., Backus, E. H. G., Mukamel, S., Bonn, M., and Nagata, Y. (2020), "Molecular Structure and Modeling of Water-Air and Ice-Air Interfaces Monitored by Sum-Frequency Generation", *Chemical Reviews*, Vol. 120, pp. 3633–3667

Tarek, M. and Tobias, D. J. (2000), "The Dynamics of Protein Hydration Water: A Quantitative Comparison of Molecular Dynamics Simulations and Neutron-scattering Experiments", *Biophysical Journal*, Vol. 79, pp. 3244–3257

Tarek, M. and Tobias, D. J. (2002), "Role of Protein-Water Hydrogen Bond Dynamics in the Protein Dynamical Transition", *Physical Review Letters*, Vol. 88, p. 138101

Teixeira, J., Bellissent-Funel, M.-C., Chen, S. H., and J.Dianoux, A. (1985), "Experimental determination of the nature of diffusive motions of water molecules at low temperatures", *Physical Review A*, Vol. 31, pp. 1913–1917

Tepper, H. L. and Voth, G. A. (2005), "Protons May Leak through Pure Lipid Bilayers via a Concerted Mechanism", *Biophysical Journal*, Vol. 88, pp. 3095–3108

Terzi, M. M. and Deserno, M. (2017), "Novel tilt-curvature coupling in lipid membranes", *The Journal of Chemical Physics*, Vol. 147, p. 084702

Tieleman, D. P. and Berendsen, H. J. C. (1996), "Molecular dynamics simulations of a fully hydrated dipalmitoylphosphatidylcholine bilayer with different macroscopic boundary conditions and parameters", *The Journal of Chemical Physics*, Vol. 105, pp. 4871–4880

Tobias, D. J., Sengupta, N., and Tarek, M. (2009), "Hydration dynamics of purple membranes", *Faraday Discussions*, Vol. 141, pp. 99–116

Tolonen, L. K., hle Wohlert, M. B., Sixta, H., and Wohlert, J. (2015), "Solubility of Cellulose in Supercritical Water Studied by Molecular Dynamics Simulations", *The Journal of Physical Chemistry B*, Vol. 119, pp. 4739–4748

ToolBox, E. (2009), "Density of Liquids versus change in Pressure and Temperature", `http://www.engineeringtoolbox.com/fluid-density-temperature-pressure-d_309.html` 2009

Toppozini, L., Roosen-Runge, F., Bewley, R. I., Dalgliesh, R. M., Perring, T., Seydel, T., Glyde, H. R., Sakai, V. G., and Rheinstädter, M. C. (2015), "Anomalous and anisotropic nanoscale diffusion of hydration water molecules in fluid lipid membranes", *Soft Matter*, Vol. 11, pp. 8354–8371

Tracht, U., Wilhelm, M., Heuer, A., Feng, H., Schmidt-Rohr, K., and Spiess, H. W. (1998), "Length Scale of Dynamic Heterogeneities at the Glass Transition Determined by Multidimensional Nuclear Magnetic Resonance", *Physical Review Letters*, Vol. 81, pp. 2727–2730

Trapp, M., Gutberlet, T., Juranyi, F., Unruh, T., Demé, B., Tahei, M., and Peters, J. (2010), "Hydration dependent studies of highly aligned multilayer lipid membranes by neutron scattering", *The Journal of Chemical Physics*, Vol. 133, p. 164505

Tse, J. S. and Klein, M. L. (1987), "Pressure-induced phase transformations in ice", *Physical Review Letters*, Vol. 58, pp. 1672–1675

Tuckerman, M. E., Marx, D., Klein, M. L., and Parrinello, M. (1997), "On the Quantum Nature of

the Shared Proton in Hydrogen Bonds", *Science*, Vol. 275, pp. 817–820

Ueda, I. and Yoshida, T. (1999), "Hydration of lipid membranes and the action mechanisms of anesthetics and alcohols", *Chemistry and Physics of Lipids*, Vol. 101, pp. 65–79

Ulrich, A. and Watts, A. (1994), "Molecular response of the lipid headgroup to bilayer hydration monitored by 2H-NMR", *Biophysical Journal*, Vol. 66, pp. 1441–1449

van der Ploeg, P. and Berendsen, H. J. C. (1982), "Molecular dynamics simulation of a bilayer membrane", *The Journal of Chemical Physics*, Vol. 76, pp. 3271–3276

van der Spoel, D., van Maaren, P. J., Larsson, P., and Tîmneanu, N. (2006), "Thermodynamics of Hydrogen Bonding in Hydrophilic and Hydrophobic Media", *The Journal of Physical Chemistry B*, Vol. 110, pp. 4393–4398

Veatch, S. L. and Keller, S. L. (2005), "Seeing spots: Complex phase behavior in simple membranes", *Biochimica et Biophysica Acta (BBA) - Molecular Cell Research*, Vol. 1746, pp. 172–185

Vega, C., Abascal, J. L. F., Conde, M. M., and Aragones, J. L. (2009), "What ice can teach us about water interactions: a critical comparison of the performance of different water models", *Faraday Discussions*, Vol. 141, pp. 251–276

Volke, F. and Pampel, A. (1995), "Membrane hydration and structure on a subnanometer scale as seen by high resolution solid state nuclear magnetic resonance: POPC and POPC/C12EO4 model membranes.", *Biophysical Journal*, Vol. 68, pp. 1960–1965

Volke, F., Eisenblätter, S., Galle, J., and Klose, G. (1994), "Dynamic properties of water at phosphatidylcholine lipid-bilayer surfaces as seen by deuterium and pulsed field gradient proton NMR", *Chemistry and Physics of Lipids*, Vol. 70, pp. 121–131

Volkhard, H. (2006), "Protein Dynamics Tightly Connected to the Dynamics of Surrounding and Internal Water Molecules", *ChemPhysChem*, Vol. 8, pp. 23–33

von Hansen, Y., Gekle, S., and Netz, R. R. (2013), "Anomalous Anisotropic Diffusion Dynamics of Hydration Water at Lipid Membranes", *Physical Review Letters*, Vol. 111, p. 118103

Vorselaars, B., Lyulin, A. V., Karatasos, K., and Michels, M. A. J. (2007), "Non-Gaussian nature of glassy dynamics by cage to cage motion", *Physical Review E*, Vol. 75, p. 011504

Wassenaar, T. A., Ingólfsson, H. I., Prie, M., Marrink, S. J., and Schäfer, L. V. (2013), "Mixing MARTINI: Electrostatic Coupling in Hybrid AtomisticCoarse-Grained Biomolecular Simulations", *The Journal of Physical Chemistry B*, Vol. 117, pp. 3516–3530

Watson, M. C., Brandt, E. G., Welch, P. M., and Brown, F. L. H. (2012), "Determining Biomembrane Bending Rigidities from Simulations of Modest Size", *Physical Review Letters*, Vol. 109, p. 028102

Williams, G. and Watts, D. C. (1970), "Non-symmetrical dielectric relaxation behaviour arising from a simple empirical decay function", *Transactions of the Faraday Society*, Vol. 66, pp. 80–85

Wohlfromm, T. and Vogel, M. (2019), "On the coupling of protein and water dynamics in confinement: Spatially resolved molecular dynamics simulation studies", *The Journal of Chemical Physics*, Vol. 150, p. 245101

Wolfe, J. and Bryant, G. (1999), "Freezing, Drying, and/or Vitrification of Membrane-Solute-Water Systems", *Cryobiology*, Vol. 39, pp. 103–129

Wong, B. Y. and Faller, R. (2007), "Phase behavior and dynamic heterogeneities in lipids: A coarse-grained simulation study of DPPC-DPPE mixtures", *Biochimica et Biophysica Acta (BBA) - Biomembranes*, Vol. 1768, pp. 620–627

Wood, K., Plazanet, M., Gabel, F., Kessler, B., Oesterhelt, D., Tobias, D. J., Zaccai, G., and Weik, M. (2007), "Coupling of protein and hydration-water dynamics in biological membranes", *Proceedings of the National Academy of Sciences*, Vol. 104, pp. 18049–18054

Woutersen, S. and Bakker, H. J. (1999), "Resonant intermolecular transfer of vibrational energy in liquid water", *Nature*, Vol. 402, pp. 507–509

Woutersen, S., Emmerichs, U., and Bakker, H. J. (1997), "Femtosecond Mid-IR Pump-Probe Spectroscopy of Liquid Water: Evidence for a Two-Component Structure", *Science*, Vol. 278, pp. 658–660

Xu, L., Kumar, P., Buldyrev, S. V., Chen, S.-H., Poole, P. H., Sciortino, F., and Stanley, H. E. (2005), "Relation between the Widom line and the dynamic crossover in systems with a liquid–liquid phase transition", *Proceedings of the National Academy of Sciences*, Vol. 102, pp. 16558–16562

Xue, C., Zheng, X., Chen, K., Tian, Y., and Hu, G. (2016), "Probing Non-Gaussianity in Confined Diffusion of Nanoparticles", *The Journal of Physical Chemistry Letters*, Vol. 7, pp. 514–519

Yamada, S. A., Thompson, W. H., and Fayer, M. D. (2017), "Water-anion hydrogen bonding dynamics: Ultrafast IR experiments and simulations", *The Journal of Chemical Physics*, Vol. 146, p. 234501

Yamamoto, E., Kalli, A. C., Akimoto, T., Yasuoka, K., and Sansom, M. S. P. (2015), "Anomalous Dynamics of a Lipid Recognition Protein on a Membrane Surface", *Scientific Reports*, Vol. 5, p. 18245

Yan, Z., Buldyrev, S. V., Kumar, P., Giovambattista, N., Debenedetti, P. G., and Stanley, H. E. (2007), "Structure of the first- and second-neighbor shells of simulated water: Quantitative relation to translational and orientational order", *Physical Review E*, Vol. 76, p. 051201

Yang, N. J. and Hinner, M. J., *Getting Across the Cell Membrane: An Overview for Small Molecules, Peptides, and Proteins*, pp. 29–53 2015

Youssef, M., Pellenq, R. J.-M., and Yildiz, B. (2011), "Glassy Nature of Water in an Ultraconfining Disordered Material: The Case of CalciumSilicateHydrate", *Journal of the American Chemical Society*, Vol. 133, pp. 2499–2510

Zhang, B. and Cheng, X. (2016), "Structures and Dynamics of Glass-Forming Colloidal Liquids under Spherical Confinement", *Physical Review Letters*, Vol. 116, p. 098302

Zhang, Z. and Berkowitz, M. L. (2009), "Orientational Dynamics of Water in Phospholipid Bilayers with Different Hydration Levels", *The Journal of Physical Chemistry B*, Vol. 113, pp. 7676–7680

Zhao, W., Moilanen, D. E., Fenn, E. E., and Fayer, M. D. (2008), "Water at the Surfaces of Aligned Phospholipid Multibilayer Model Membranes Probed with Ultrafast Vibrational Spectroscopy", *Journal of the American Chemical Society*, Vol. 130, No. 42, pp. 13927–13937

Zhuang, X., Makover, J. R., Im, W., and Klauda, J. B. (2014), "A systematic molecular dynamics simulation study of temperature dependent bilayer structural properties", *Biochimica et biophysica acta*, Vol. 1838, pp. 2520–2529

List of publications

- Abhinav Srivastava and Ananya Debnath, *Hydration Dynamics of a Lipid Membrane : Hydrogen Bond Networks and Lipid-Lipid Associations*, Journal of Chemical Physics, **148**, 094901, 2018.

- Abhinav Srivastava, Sheeba Malik and Ananya Debnath, *Heterogeneity in Structure and Dynamics of Water near Bilayers using TIP3P and TIP4P/2005 Water Models*, Chemical Physics, **525**, 110396, 2019.

- Abhinav Srivastava, Smarajit Karmakar and Ananya Debnath, *Quantification of Spatio-Temporal Scales of Dynamical Heterogeneity of Water near Lipid Membranes above Supercooling*, Soft Matter, **15**, 9805, 2019.

- Abhinav Srivastava, Sheeba Malik, Smarajit Karmakar and Ananya Debnath, *Dynamic coupling of hydration layer to a fluid phospholipid membrane: Intermittency and multiple time-scale relaxations*, (accepted in Physical Chemistry Chemical Physics, 2020).